High Density Lipoprotein Metabolism in the Kidney

Dalibor Breznan

Thesis submitted in partial fulfillment of the requirement for the degree of Masters of Science

Department of Biochemistry, Microbiology and Immunology
University of Ottawa
Ottawa Heart Institute

Abstract

The kidney is believed to play a major role in the clearance and re-absorption of high density lipoprotein (HDL) particles from the blood. Experiments were undertaken to explore the specific sites of renal HDL metabolism *in vivo* and to investigate *in vitro* the factors that regulate the renal re-absorption of HDL by HKC-8 human proximal tubule (PT) cells.

Perfusion of a rabbit renal artery with [^{3}H]cholesteryl ester (CE) and ^{125}I-protein labeled HDL particles showed that the kidneys are capable of filtering both apolipoprotein A-I (apoA-I) and whole HDL. An electron microscopic, immunochemical analysis of the kidneys perfused with reconstituted HDL (rHDL) particles or lipid-free apoA-I utilizing two different anti-apoA-I monoclonal antibodies (mAb) 5F6 and 4H1 revealed different labeling patterns. The ligands were localized throughout the PT cells, with the 5F6 mAb, and within the PT basal lamina only, with the 4H1 mAb.

A fluorescent microscopic study with the HKC-8 cells showed that the PT cells can bind and take up HDL particles. Binding studies showed that the ^{125}I-HDL binding to the HKC-8 cell surface is saturable and specific. The cells did not considerably degrade ^{125}I-HDL, as observed by a TCA precipitation of the cell media. The specific binding of HDL was higher than that of the apoA-I. In contrast, more apoA-I than HDL was retained in the extracellular matrix of the HKC-8 cells. Reconstituted HDL prepared from apoA-I and the lipids extracted from native HDL (rHDL-lipid) bound to the HKC-8 cells similarly to native HDL. However, addition of phospholipids to the rHDL particle decreased its binding to the cells substantially. In contrast, inclusion of cholesteryl ester in the lipoprotein (rHDL-CE) enhanced its binding to the cells.

To study the transcytotic transport of HDL through polarized HKC-8 cells, the cells were cultured on fibronectin-coated transwell filters. Incubations of ^{125}I-HDL in the apical or basolateral compartments of the HKC-8 cells showed a higher HDL association with the basolateral, than with the apical cell surface. The effects of varied HDL composition on its metabolism in polarized HKC-8 cells were examined by evaluating the transport and degradation of ^{125}I-apoA-I and different ^{125}I-labeled HDL particles. Basolateral to apical HDL transport was higher than that in the opposite direction. ^{125}I-apoA-I transport from the apical surface was lower than ^{125}I-HDL transport. Also, rHDL-CE and rHDL-lipid particles displayed an enhanced apical to basolateral transport comparable to that of native HDL. CE enrichment had less effect on HDL transport from the basolateral surface. Thus, HDL-CE content directly affects the transport of HDL through the PT cells.

In contrast to the conventionally cultured HKC-8 cells, polarized cells degraded considerable amounts of HDL. Most of the transported ^{125}I-HDL and about ~50% of the transported ^{125}I-apoA-I were detected in the degraded form. While CE and HDL lipid inclusion affected rHDL transport, it had little effect on particle degradation. In addition, a higher amount of degraded ^{125}I-apoA-I and ^{125}I-rHDL was detected after basolateral to apical transport compared to that detected after transport in the opposite direction. Thus, while the lipid composition affects the transport of HDL through HKC-8 cells, HDL apolipoprotein composition appears to govern the degradation of HDL in these cells.

In summary, the results show that the kidneys are capable of taking up and processing both apoA-I and small HDL particles, and that the HDL lipid composition can dramatically affect the metabolism of this lipoprotein in the kidney.

Dedication

This work is dedicated to my family.

Acknowledgements

First, I would like to thank my supervisor Dr. Daniel Sparks for providing me the opportunity to take on this project, and for providing me with outstanding guidance throughout my studies in his laboratory. Also I would like to acknowledge everyone who has contributed to this project, has offered their friendship and contributed to a good team spirit, all crucial to the successful completion of this project. Namely, Tracey Neville, Chris Stamler, Tanya Ramsamy, France Viau, Bobby Chauhan, Claudine Gourgue-Jeannot, Jonathan Boucher, Patricia Rouillard and Vasanthi Veereswaran. I would like to thank France and Tracey for their great work in the early HDL-binding studies, and also would like to thank Tracey for expertly teaching me numerous biochemical laboratory techniques and providing me with lots of great advice, and Dr. Jim Burgess for his useful advice on the establishment of the transwell cell culture system.

Table of Contents

List of Tables

List of Figures

Abbreviations

A	**apical**
Apo	**apolipoprotein**
ABCA1	**adenosine tri-phosphate binding cassette protein 1**
B	**basolateral**
BB	**brush border**
BCA	**bicinchoninic acid**
BL	**basal lamina**
BSA	**bovine serum albumin**
CE	**cholesteryl ester**
CETP	**cholesteryl ester transfer protein**
CUB	**c1r/c1s uegf bmp1**
Cy3	**indocarbocyanine 3**
DG	**diglyceride**
DMEM	**dulbecco's modified eagle medium**
ECM	**extracellular matrix**
EDTA	**ethylenediaminetetraacetic acid**
EGF	**epidermal growth factor**
EM	**electron microscopy**
FBS	**fetal bovine serum**
FC	**free cholesterol**
FCR	**fractional catabolic rate**
HBP	**high density lipoprotein binding protein**

HDL	**high density lipoprotein**
HDL-C	**high density lipoprotein cholesterol**
HKC-8	**human kidney cells clone 8**
HL	**hepatic lipase**
HRP	**horseradish peroxidase**
IDL	**intermediate-density lipoprotein**
IF	**intrinsic factor**
Ig	**immunoglobulin**
kDa	**kilodalton**
LCAT	**lecithin-cholesterol acyl transferase**
LDL	**low density lipoprotein**
LDLr	**low density lipoprotein receptor**
Lp	**lipoprotein**
LPL	**lipoprotein lipase**
LRP	**low density lipoprotein receptor-related protein**
mAb	**monoclonal antibody**
MDCK	**madine-darby canine kidney**
N	**nucleus**
OK	**opossum kidney**
PBS	**phosphate buffered saline**
PCT	**proximal convoluted tubule**
PI	**phosphatidylinositol**
PL	**phospholipid**

PLTP	**phospholipid-transfer protein**
POPC	**phosphatidylcholine**
RCT	**reverse cholesterol transport**
rHDL	**reconstituted high density lipoprotein**
RT	**room temperature**
SD	**standard deviation**
SM	**sphingomyelin**
SR-B1	**scavenger receptor class B1**
TCA	**trichloroacetic acid**
TD	**tangier disease**
TG	**triacylglyceride**
TJ	**tight junction**
TLC	**thin-layer chromatography**
VHDL	**very high density lipoprotein**
VLDL	**very low density lipoprotein**
VLDLr	**very low density lipoprotein receptor**

Chapter 1: Introduction

Atherosclerosis

Atherosclerotic cardiovascular disease is the leading cause of death in Western countries. It is characterized by the accumulation of lipids and fibrous materials in the large arteries (Breslow, 2000; Lusis, 2000; Glass and Witztum, 2001). It is a form of chronic inflammation resulting from interaction between modified lipoproteins and T cells, monocyte-derived macrophages and normal cellular arterial elements (Ross, 1999; Glass and Witztum, 2001). The early lesions of atherosclerosis typically form in the branch points of arteries, which are areas of turbulent blood flow. They consist of subendothelial accumulations of lipid-laden macrophages, called foam cells. Foam cells derive from monocytes, which attach to the endothelium in response to endothelial adhesion signals and which subsequently transmigrate into the subendothelial space to take up the accumulated modified lipids (Breslow, 2000; Lusis, 2000; Glass and Witztum, 2001). T-cells also accumulate in such lesions and activate in response to endothelial chemotactic signals and growth factors. Subsequently, such early fatty streaks progress into more complex lesions characterized by the immigration of smooth muscle cells from the medial layer into subendothelial space, where they synthesize extracellular matrix proteins. This, along with the accumulation of foam cells results in a formation of a characteristic fibrous cap lesion (Lusis, 2000; Glass and Witztum, 2001). In the final stage, advanced lesions occur, characterized by the presence of a necrotic core and extracellular cholesterol, that come from the extensive necrosis of macrophage and smooth muscle cell-derived foam cells (Glass and Witztum, 2001). Such plaques are unstable due to the thinning of their fibrous caps, caused by neovascularization and

macrophage secretion of matrix metalloproteinases. Subsequently, the unstable plaques rupture in their shoulder regions and release tissue factors into the bloodstream, leading to the initiation of coagulation, platelet recruitment and thrombus formation (Lusis, 2000; Glass and Witztum, 2001). Plaque rupture and thrombosis can then cause coronary or carotid occlusions which result in the acute clinical complications of myocardial infarction or stroke (Ross, 1999; Breslow, 2000).

Epidemiological studies over the past 50 years have proven atherosclerosis to be a complex multifactorial disease and have revealed a large number of genetic and environmental risk factors for the disease. The genetic risk factors include elevated levels of LDL/VLDL, reduced levels of HDL, hypertension, elevated levels of Lp(a) and homocysteine, family history, obesity and diabetes, elevated levels of haemostatic factors, metabolic syndrome, insulin resistance, gender (male), depression and systemic inflammation. The environmental risk factors include high-fat diet, smoking, lack of exercise, infectious agents and low antioxidant levels (Lusis, 2000; Glass and Witztum, 2001). Among these well known risk factors, dyslipidaemia is the major contributing factor for the development of atherosclerosis, in particular, high levels of low density lipoprotein (LDL) and low levels of high density lipoprotein (HDL). While the majority of current therapies for atherosclerosis are aimed at the reduction of plasma cholesterol by exploiting the well-established pathways of receptor-mediated LDL metabolism, the mechanisms involved in cellular HDL metabolism remain mostly unknown (Acton *et al.*, 1999; Rader and Maugeais, 2000)

The strong inverse relationship between atherosclerosis and plasma levels of HDL-cholesterol (HDL-C), established by numerous clinical and epidemiological

studies, clearly demonstrates the consequences of low levels of HDL (Gordon and Rifkind, 1989; Brinton *et al.*, 1991; von Eckardstein and Assmann, 2000). This has resulted in much interest in elucidating the mechanisms that modulate the concentration of this lipoprotein *in vivo*. While HDL cholesterol content is used predominantly to reflect plasma HDL levels, previous studies have established that accelerated apolipoprotein A-I (apoA-I) catabolism is also an important metabolic predictor of HDL levels (Brinton *et al.*, 1991). Furthermore, the protective effects of increasing HDL cholesterol levels are at least in part mediated by apoA-I, the plasma levels of which appear to be determined by the rate of its catabolism rather than production (Brinton *et al.*, 1991; Plump *et al.*, 1994; Paszty *et al.*, 1994; Tangirala *et al.*, 1999). This emphasizes the importance of understanding how the HDL lipid and apolipoprotein components influence the synthesis, modification and catabolism of HDL, if we are to clarify the role of this lipoprotein in atherosclerosis.

Lipoproteins

The major neutral lipids, cholesteryl esters (CE) and triglycerides (TG), that circulate in the body are insoluble in aqueous solutions and therefore are coated with amphipathic molecules, which enables their transport through the vascular system. Such spherical macromolecular complexes are termed lipoproteins. They comprise a neutral core of hydrophobic CE and TG enveloped by a surface monolayer of amphipathic lipids (free cholesterol and phospholipids) and specific apolipoproteins, important lipid transport regulators (Ginsberg, 1998). Lipoproteins can be classified into relatively distinct subclasses that can be isolated by various physical methods (see Table 1).

Table 1: Subclasses of lipoproteins (Lp) and their properties

Lp Class	Buoyant Density (g/ml)	Diameter (nm)	Apolipoproteins
Chylomicron	<0.95	100-500	ApoA-I, II, IV, ApoB-48, ApoC-I, II, III, ApoE
VLDL	0.95-1.006	30-80	ApoB-100, ApoC-I, II, III, ApoE
IDL	1.006-1.019	25-50	ApoB-100, ApoC-I, II, III, ApoE
LDL	1.019-1.063	18-28	ApoB-100
HDL	1.063-1.21	5-12	ApoA-I, II, IV, ApoC-I, II, III, ApoD, ApoE

Adapted from Brown, M., and Goldstein, J., 1987. *In* Garrett, R.H., and Grisham, C.M., eds., 1995. *Biochemistry*, Orlando, FL: Saunders College Publishing

Chylomicrons, the least dense lipoproteins, are produced by the cells of the intestinal mucosa and secreted into the lymph ducts and carry exogenous, dietary TG and cholesterol from the intestines to other tissues. Very low density lipoproteins (VLDL), intermediate density lipoproteins (IDL) and low density lipoproteins (LDL) transport endogenous TG and cholesterol from the liver to the extrahepatic tissues. The TG of the chylomicrons and VLDL are then hydrolyzed by lipoprotein lipase (LPL) into free fatty acids, making them available for peripheral tissues. LPL is a lipolytic enzyme bound to the vascular surface of capillary endothelium of muscle and adipose cells. Hepatic lipase (HL), a liver-localized enzyme, homologous to LPL, hydrolyzes TG from chylomicrons and VLDL remnants as well as phospholipids (PL) from the VLDL remnants and HDL. The remnant cholesterol-rich chylomicron particles are cleared rapidly through a receptor-mediated process by hepatocytes. The VLDL remnants appear in circulation initially in the form of IDL, which can be taken up by the liver or subsequently catabolized into LDL by LPL or HL. (Garrett and Grisham, 1995; Davis and Vance, 1996; Ginsberg, 1998). The CE-enriched LDL particles are then either returned to the

liver or directed to adrenal glands or adipose tissues through an LDL-receptor (LDLr) mediated endocytosis. The mammalian LDLr family comprises a considerable number of receptors characterized by distinct functional domains (Willnow *et al.*, 1999). Besides LDLr, other members of the family include the LDLr-related protein (LRP), megalin, the VLDL receptor (VLDLr) and others. These receptors are expressed in various tissues including intestine, liver, lung, brain, muscle, skin, with the highest expression in the liver (Gliemann, 1998; Willnow *et al.*, 1999). The hepatic LDLr-mediated uptake of LDL is an important process for the removal of cholesterol from circulation (Brown and Goldstein, 1986). In the catabolism of chylomicrons and the conversion of VLDL to LDL, all the proteins with the exception of apoB-48, are transferred to HDL. FC is esterified by the HDL-associated enzyme, lecithin-cholesterol acyl transferase (LCAT). Another HDL-associated protein, cholesteryl ester transfer protein (CETP), transfers some of the CE to VLDL and LDL, the majority of which are then taken up by the liver via the LDLr (Fielding and Fielding, 1996). Additionally, CE in HDL and LDL is selectively taken-up by the scavenger receptor class B1 (SR-B1) on the surface of hepatocytes (von Eckardstein and Assmann, 2001).

Hence HDL transports endogenous cholesterol from the peripheral tissues into the liver, a process termed reverse cholesterol transport (RCT). The sterols taken up by the liver are then eliminated into the bile either directly or through conversion to bile acids. The ability of HDL to facilitate RCT is thought to explain the correlation between high HDL levels and reduced risk of cardiovascular disease (Garrett and Grisham, 1995; Davis and Vance, 1996). RCT pathways are described in more detail in context of HDL metabolism below.

HDL metabolism

HDL Maturation

HDL is a dense, protein rich particle, with a small apolar core surrounded by a surface layer of apoA-I and amphiphilic lipid molecules (Fig. 1). HDL represents a complex lipoprotein class with subclasses varying in density, size and composition upon isolation by various physical-chemical methods (Table 1,2). The major HDL apolipoprotein is apoA-I, which, while present in all HDL subclasses may vary in number of protein molecules per HDL particle. ApoA-I is synthesized by the liver and intestines (Davis and Vance, 1996). HDL also acts as a circulating store of apoC and apoE and can also contain apoA-II and apoA-IV. HDL exists as three subclasses, HDL_2, the largest and least dense HDL particle, HDL_3 and VHDL, the smallest and most dense particles. HDL_2 and HDL_3 are further subdivided into further subclasses, HDL_{2b}, HDL_{2a}, HDL_{3a}, HDL_{3b} and HDL_{3c} (Shepherd, 1994). Nascent HDL precursors are lipid-poor, contain apoA-I and are synthesized by the liver and intestines. They display a characteristic preβ1 electrophoretic mobility on an agarose gel, which distinguishes them from the bulk of α-migrating HDL. The preβ1 HDL particles may also be discoidal in shape (Fielding and Fielding, 1996; Ginsberg, 1998). Furthermore, nascent HDL particles form by dissociation from chylomicrons and VLDL during LPL-mediated TG hydrolysis and by the interconversion of HDL_2 to HDL_3, described later in more detail (von Eckardstein *et al.*, 2001). Nascent HDL interact with peripheral cells to acquire excess unesterified cholesterol and phospholipid through an ATP-binding cassette protein 1 (ABCA1) mediated lipid efflux process. The ABCA1 protein was discovered in studies of patients with Tangier disease (TD), suffering from an almost complete lack of circulating HDL

Table 2: Composition of HDL subclasses

HDL subclass	Composition (% w/w)				
	Protein	PL	FC	CE	TG
Preβ1 HDL	70	25	5	nd	nd
HDL_3	55	25	3	16	1
HDL_2	43	30	5	20	2

PL, phospholipid; FC, free cholesterol; CE, cholesteryl ester; TG, triacylglycerol; nd, not detectable.

Adapted from Fielding , P.E. and C.J. Fielding, 1996. *In* Vance, D.E. and J.E. Vance, eds., 1996. *Biochemistry of Lipids, Lipoproteins and Membranes*, New York, New York: Elsevier

and from the accumulation of FC in several tissues. It was shown that patients with TD and familial HDL deficiency have a defect in the gene encoding ABCA1 (Bodzioch *et al.*, 1999; Hobbs and Rader; 1999). The ABCA1-mediated lipidation of preβ1 HDL particles leads to their conversion into spherical α-migrating HDL. The conversion is facilitated by the LCAT, which catalyzes the conversion of unesterified FC into CE and lysolecithin and is activated by apoA-I. The newly formed CE moves to the lipid core of the HDL (Rader and Mauegais, 2000; Santamarina-Fojo *et al.*, 2000; von Eckardstein *et al.*, 2001). Such newly formed HDL_3 particles continue to adsorb FC, which results in their enlargement and progressive FC esterification. Additionally, HDL_3 particles also continue to acquire more phospholipids from apoB containing lipoproteins through the action of the phospholipid transfer protein (PLTP) and may undergo a PLTP-mediated fusion with other HDL_3 particles (Tall *et al.*, 2000; von Eckardstein *et al.*, 2001). Such enlarged HDL_3 particles can now accommodate apoCII and III also derived from apoB-containing lipoproteins catabolized by LPL. ApoE can also transfer to HDL at this time.

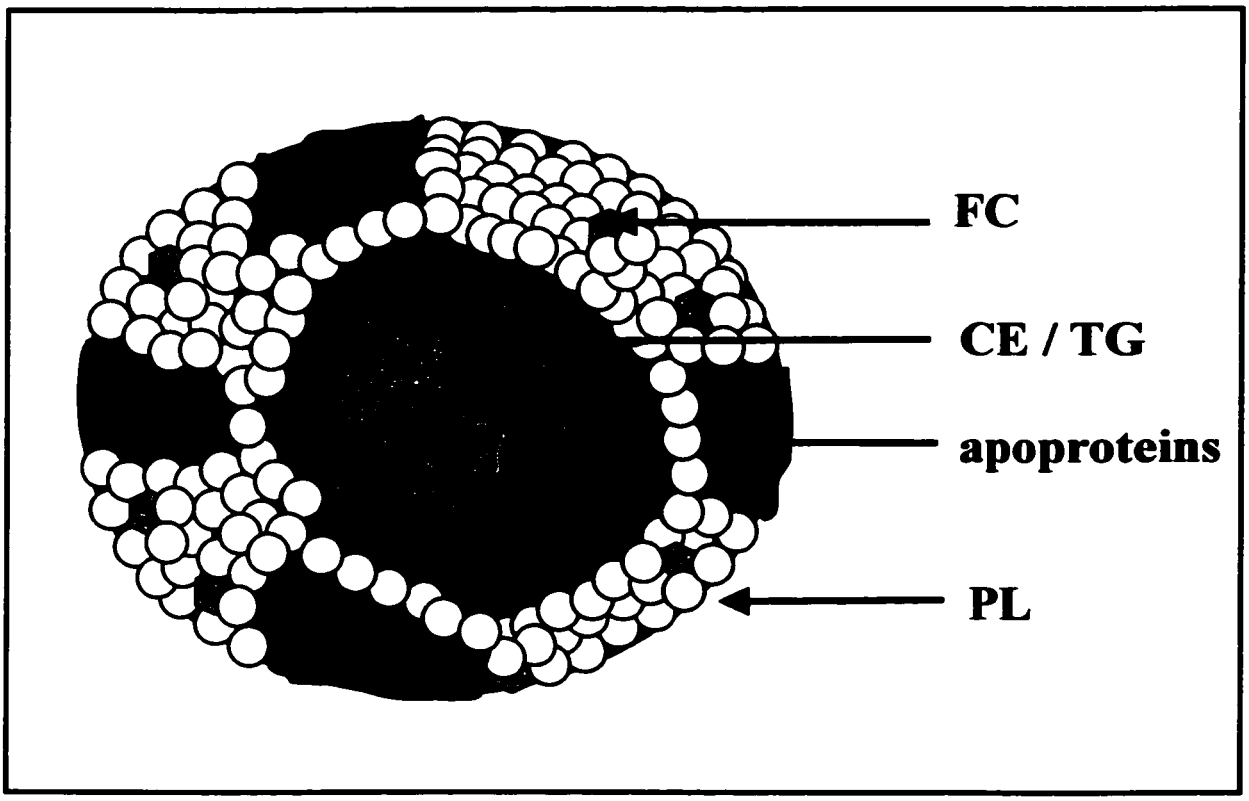
FC
CE / TG
apoproteins
PL

Figure 1: Schematic representation of HDL

The high density lipoprotein (HDL) is a dense, protein rich particle with a small apolar core comprised mainly of cholesteryl ester (CE) and triacylglycerol (TG), surrounded by a surface layer of apoproteins (mainly apoA-I), amphiphilic phospholipids (PL) and free cholesterol (FC). HDL circulates in the bloodstream, extracting cholesterol from body tissues and transporting it to the liver for excretion or recycling.

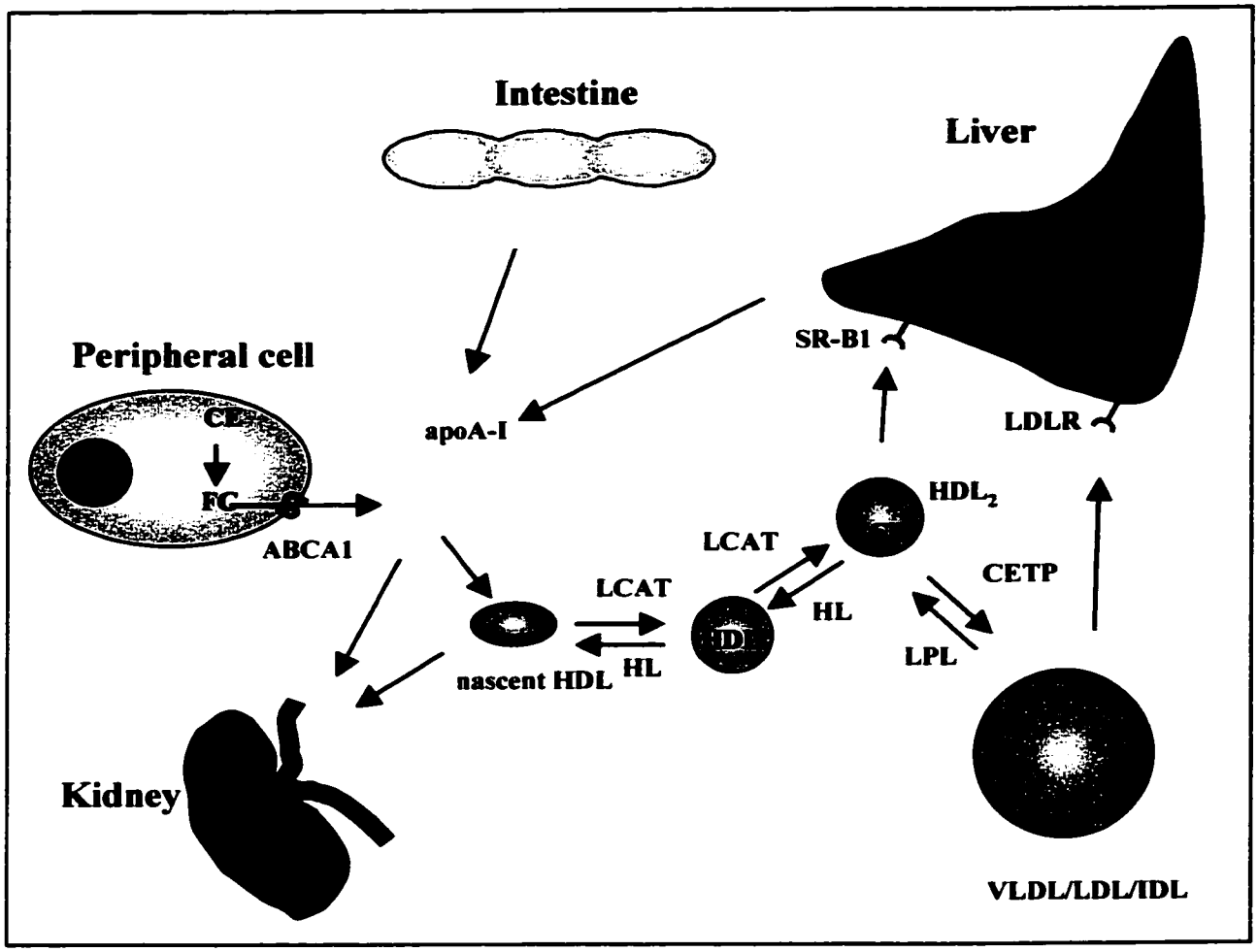
Intestine
Liver
Peripheral cell
CE
FC
ABCA1
apoA-I
SR-B1
LDLR
HDL2
LCAT
HL
CETP
LPL
LCAT
HL
nascent HDL
ID
Kidney
VLDL/LDL/IDL

Figure 2: Brief overview of the HDL metabolism

Mature HDL particles are generated from lipid-free apoA-I or lipid-poor nascent HDL precursors. These precursors are synthesized by the liver and intestine. Nascent HDL particles then acquire excess FC and PL from peripheral cells through a lipid efflux mediated by ABCA1. The surface FC is then esterified by the enzyme LCAT to form CE, which then moves to the core of the HDL. Through the action of LCAT, HDL is progressively enlarged, taking the form of HDL_3 and eventually HDL_2 particles. Through the action of CETP, CE can be transferred from HDL to apoB-containing lipoproteins in exchange for TG, or selectively removed by the SR-B1 receptor in the liver. Hydrolysis of TG-rich lipoproteins leads to the transfer of lipids and apolipoproteins to HDL. Mature HDL_2 is progressively degraded into HDL_3 and nascent HDL. Nascent HDL and lipid-free apoA-I can then be metabolized by the kidneys and undergo a glomerular filtration and tubular reabsorption.

Through these processes, mature HDL_2 are formed (Ginsberg, 1998). For a brief overview of HDL metabolism see Figure 2.

HDL catabolism

The clearance of HDL from the blood can occur through the selective transfer of cholesterol to other lipoproteins and to cells, and then by the selective metabolism of HDL apolipoproteins and the direct uptake of whole HDL particles.

In an indirect sterol-eliminating pathway, CETP exchanges the CE from HDL_2 with TG from VLDL, IDL and LDL. The CE derived from HDL are then removed from the circulation via the LDLr pathway, and the TG in HDL are hydrolyzed by HL. The enrichment of LDL with CE from HDL may be seen as a potentially proatherogenic process. However, the result of the concerted action of HL and CETP leads to the enhancement of RCT through the progressive conversion of HDL_2 into HDL_3 and into preβ1 HDL or lipid-free apoA-I. The re-generated preβ1 HDL or lipid-free apoA-I are now available for further sterol removal from peripheral tissues by RCT (Tall *et al.*, 2000; von Eckardstein *et al.*, 2001).

The CE can also be removed from HDL through a direct pathway. This CE-selective pathway was first elucidated by Pittman and coworkers (Glass *et al.*, 1983) and was shown by Krieger and coworkers (Acton *et al.*, 1996) to be mediated by the SR-B1 receptor. The CE is transferred into the hepatocytes and the cells of steroidogenic tissues. While HDL binding appears to be a necessary step for the selective uptake by SR-B1, the presence of cofactors may also be necessary. HL is one such cofactor. HL hydrolyzes PL and TG and it is the HL-mediated hydrolysis of HDL-surface phospholipids that appears to be necessary for enabling the CE transport from the HDL core to the plasma

membrane (Lambert *et al.*, 1999). As a TG hydrolase, HL can hydrolyze TG in HDL. As mentioned previously, the action of HL along with CETP leads to the formation of smaller HDL, as well as the lipid-free apoA-I and preβ1 HDL. Since apoA-II inhibits HL, HDL devoid of apoA-II is preferred substrate for HL (von Eckardstein *et al.*, 2001).

The clearance of HDL apolipoproteins from the blood is less well understood than the removal of HDL-lipids. Potential mechanisms of the catabolism of HDL apolipoproteins and whole HDL particles are thought to be through endocytosis in liver and kidney cells, placenta and yolk sac (Moestrup and Kozyraki, 2000). Early studies of apoA-I metabolism, by Glass *et al.* have shown the kidney cortex to be an important tissue for the uptake of this principal protein component of HDL. Their studies also suggested that the uptake of HDL-dissociated apoA-I was the result of glomerular filtration and a tubular reabsorption of free apoA-I (Glass *et al.*, 1983). The importance of the kidney in apoA-I metabolism was further highlighted by observations obtained from studies of the metabolic turnover of serum HDL apolipoproteins in rats (van Tol, 1984). The studies indicated that while a partial hepatectomy decreased the fractional turnover rate (FCR) of HDL-derived CE, it had no effect on the FCR of HDL apolipoproteins, which remained unchanged from that of the sham operated animal. The accumulation of apoA-I HDL-derived radioactivity was the highest in the kidneys and the kidneys were also most active per gram tissue in degradation of apoA and C. Therefore, renal degradation of apolipoproteins appears to be the rate-limiting step in overall HDL apolipoprotein catabolism (van Tol, 1984).

HDL Receptors

While a number of HDL binding proteins have been identified and cloned, their role in HDL metabolism, in particular their importance in HDL catabolism, still remains unclear. In the early 90s, McKnight and colleagues isolated a cDNA clone encoding a 110 kDa cell surface protein which they named high-density lipoprotein binding protein (HBP). The expression of HBP mRNA in cultured endothelial cells increased in response to cholesterol loading (McKnight *et al.*, 1992). HBP was later found to be homologous to vigilin (Chiu *et al.*, 1997). The receptor was capable of binding both HDL and lipid-free apoA-I on ligand blots (Graham and Oram, 1987). Structurally, HBP was dissimilar to typical cell surface receptors, as it did not show the presence of a classic hydrophobic transmembrane spanning sequence or clearly defined extracellular or cytoplasmic domains, characteristic of known receptors. The receptor was thought to anchor to the cell surface at some later stage, after which it was capable of interacting with HDL. However, the mechanism has still not been clearly elucidated and while the receptor has been found to play a role in cell signaling, its function in HDL metabolism is still unclear. (Fidge, 1999).

By expression cloning in CHO cells, Acton *et al.* have isolated the cDNA of SR-B1, an 82 kDa protein, a member of the CD36 family of membrane receptors (Acton *et al.*, 1996). SR-B1 belongs to the class B scavenger receptor family of proteins, characterized by the presence of an immunodominant ligand binding domain (Fidge, 1999) and the absence of polyanionic ligand binding sites. These sites are found in class A type I and II macrophage scavenger receptors. SR-B1 is characterized by two transmembrane domains, with the bulk of the protein, between the two domains, being

extracellular and the NH_2- and COOH- termini both localized within the cells. It is also glycosylated and acylated, and co-localizes with plasma membrane caveolae (Babitt *et al.*, 1997; Fidge, 1999). SR-B1 is highly expressed in liver, ovary and adrenal glands (Acton *et al.*, 1996). While murine SR-B1-transfected cells were capable of taking up 20% of HDL cholesterol added, less than 0.5% of the apolipoprotein was internalized, indicating, that a selective uptake of cholesteryl ester had occurred, rather than whole HDL particle endocytosis (Acton *et al.*, 1996). Besides its important function in RCT as a facilitator of HDL-CE selective uptake, SR-B1 can also stimulate free cholesterol efflux from cells to HDL, suggesting that it might also play a role in cholesterol clearance (Acton *et al.*, 1999).

Another putative HDL-binding protein, named HB_2 has also been cloned (Matsumoto *et al.*, 1997). HB_2 has a molecular mass of 100 kDa and was originally isolated and purified from rat liver. (Hidaka and Fidge, 1992). HB_2 is highly expressed in the lungs, liver, intestine and is present in smaller amounts in the kidneys, ovaries and testis. The deduced amino acid sequence of HB_2 predicted a cell-surface transmembrane protein, structurally resembling the activated-leukocyte cell adhesion molecule (ALCAM) and a surface glycoprotein of bursal epithelia and neurons (BEN), of the immunoglobulin superfamily. When HB_2-encoding cDNA was transfected into HepG2 or COS cells, protein expression increased specific HDL_3 binding by 80-100% (Matsumoto *et al.*, 1997). Furthermore, HB_2 expression was inversely related to the cell cholesterol content, suggesting that it is linked with cholesterol metabolism (Fidge, 1999). However, a clear role of HB_2 in HDL metabolism and cholesterol homeostasis is yet to be determined. While HBP, SR-B1 and HB_2 seem to have important cellular functions, there

is little evidence that these receptors are important in the clearance and degradation of apoA-I.

In contrast, a newly identified receptor in the kidney has been reported, which unlike SR-B1 mediates a non-selective endocytosis of whole HDL particles and apoA-I (Hammad *et al.*, 1999; Kozyraki *et al.*, 1999). The novel receptor, named cubilin is expressed in the apical membranes of various absorptive epithelia including those of the kidney, intestine, the yolk sac and placenta (Sahali *et al.*, 1992; Seetharam *et al.*, 1997). Cubilin has been previously known to function in the uptake of the IF/B_{12} complex in the intestine (Seetharam, *et al.*, 1999). Previously known as gp280, cubilin is a 460 kDa peripheral membrane protein characterized by the presence of a large cluster of 27 C1r/C1s Uegf Bmp1 (CUB) domains, following the amino terminus and eight epidermal growth factor(EGF) repeats, and the absence of a transmembrane domain and cytoplasmic tail. While the amino terminus, with its alpha-helical characteristics has been shown to be important for the association of the receptor with the cell membrane, the CUB cluster appears to be important for the ligand binding. No specific function has yet been assigned to the EGF repeats (Kristiansen *et al.*, 1999). Cubilin is a multiligand receptor capable of binding a variety of ligands, in addition to apoA-I, HDL and intrinsic factor/vitamin B_{12}, such as immunoglobulin light chains (Batuman *et al.*, 1998), receptor-associated protein (Birn *et al.*, 1997), megalin (Moestrup *et al.*, 1998) and albumin (Birn *et al.*, 2000). In the kidney, cubilin is concentrated in the intermicrovillar areas of the apical brush border of proximal tubule cells (PCT), and can be detected in clathrin-coated pits, small and large endosomes, dense apical tubules and to a lesser extent lysosomes (Verroust and Kozyraki, 2001). In these areas of the apical endocytic apparatus, cubilin

co-localizes with megalin, a multiligand endocytic receptor, a member of the LDLr family. The two receptors, while belonging to distinct protein families have in common the presence of CUB domains and EGF repeats, though in a differing structural arrangement (Verroust and Kozyraki, 2001). The co-localization and strong binding of purified cubilin to megalin supports the hypothesis of a functional relationship of the two receptors, where megalin acts as a vehicle for cubilin to traverse the cell membrane and mediate ligand endocytosis. In agreement with a co-receptor function, anti-megalin antibodies partly inhibit the uptake of apoE-depleted HDL (Hammad *et al.*, 2000; Kozyraki *et al.*, 1999; Moestrup *et al.*, 1998). Binding of apoA-I and HDL to cubilin is of high affinity, and is calcium dependent, as demonstrated by affinity chromatography of serum on a cubilin column and a characterization of binding by surface plasmon resonance. In yolk sac epithelial cells, following binding to cubilin, HDL was internalized and underwent endocytic processing similar to that of LDL by the LDL receptor (Kozyraki *et al.*, 1999). The inhibition of HDL uptake by polyclonal anti-cubilin and anti-apoA-I antibodies emphasized the importance of the binding of apoA-I to cubilin in HDL uptake (Hammad *et al.*, 1999). The role of cubilin in the renal catabolism of apoA-I is evident from the increased urinary excretion of apoA-I in some cases of functional cubilin deficiency (Kozyraki *et al.*, 1999). In contrast with these studies, Shamburek *et al.* provided evidence against a significant role of cubilin in renal HDL metabolism (Shamburek *et al.*, 2000). Their study shows no significant difference in the catabolism of apoA-I on HDL between the controls and the canine cubilin dysfunctional animal model. In addition, no intact apoA-I is detected in the urine of the cubilin

deficient canines. The authors conclude that a receptor other than cubilin may be responsible for HDL catabolism in the kidney (Shamburek *et al.*, 2000).

In addition to the above discussed receptors, there is also evidence for the existence of other HDL-binding capable proteins (Fidge, 1986; Lutton and Fidge, 1994; van Tol *et al.*, 1986). Alternatively, apoE-containing whole HDL particles, a small minority of HDL can be internalized by hepatic apoE receptors (LDLr and LRP), and there is also some evidence for hepatic receptors for apoE-free HDL capable of taking up and re-secreting the lipoprotein (Delamatre *et al.*, 1990; von Eckardstein *et al.*, 2001).

Renal physiology

The Nephron

The basic functional unit of the kidney is the nephron. Each kidney is composed of 1-4 million nephrons within its cortex. Each nephron constitutes a renal corpuscle (glomerulus), the proximal convoluted tubule (PCT), the thin and thick limbs of Henle's loop and the distal convoluted tubule. The collecting tubules and ducts which collect urine produced by nephrons do not constitute the nephron, as they are of a different embryological origin (Junqueira *et al.*, 1998). See Figure 3 for a schematic depiction of the nephron. The glomeruli comprise of a bed of capillaries, surrounded by a protective Bowman's capsule. The glomerulus has an internal layer of visceral epithelial cells and their basement membranes and the outer parietal layer with its basement membrane. Between the two layers is the urinary space, which receives filtrate from the capillary wall and the visceral layer. At the vascular pole of the glomerulus, the afferent arteriole enters and the efferent arteriole leaves. The PCT origin is at the urinary pole. The incoming afferent arteriole divides into several branches, which then subdivide into

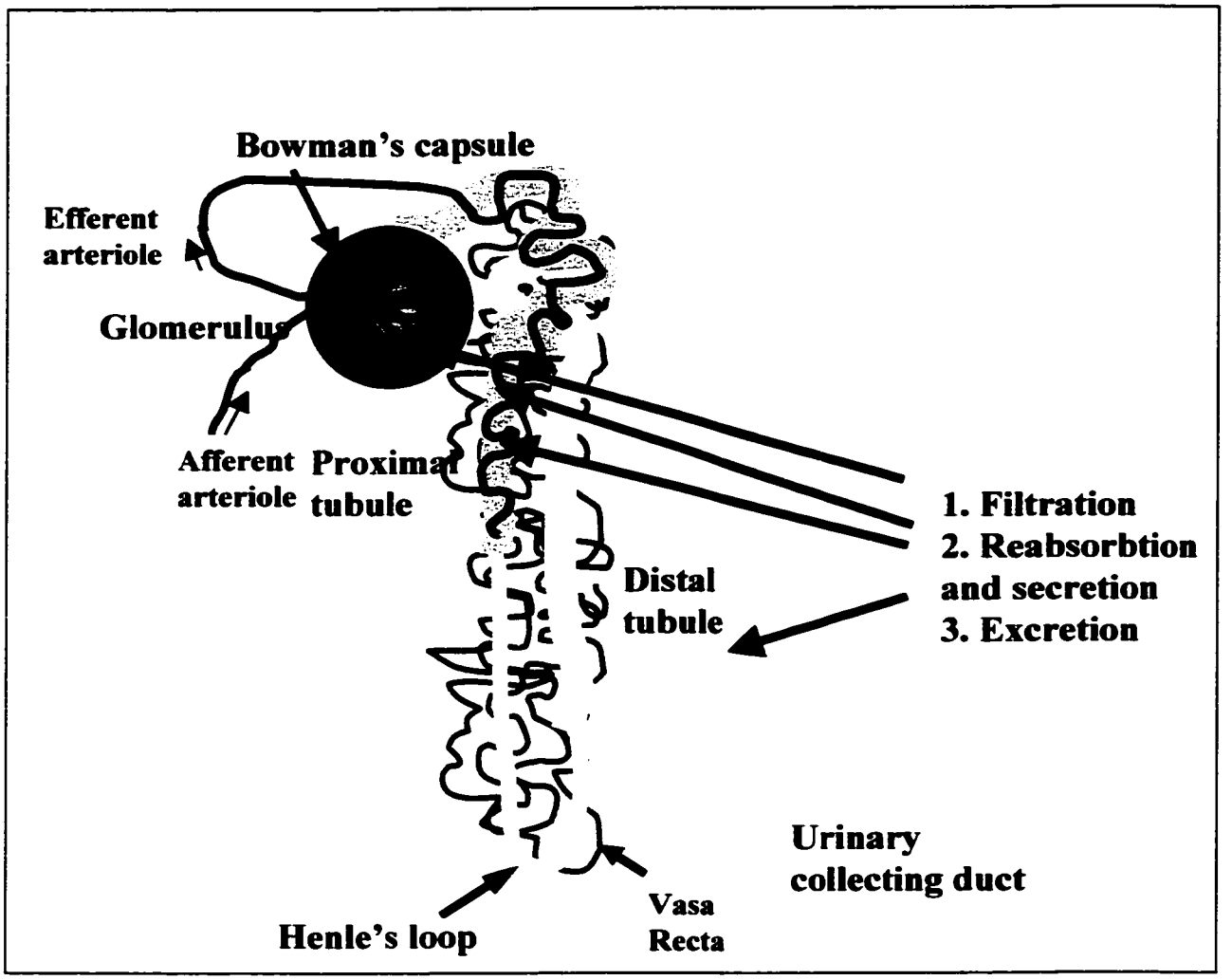
Bowman's capsule
Efferent arteriole
Glomerulus
Afferent arteriole
Proximal tubule
1. Filtration
2. Reabsorbtion and secretion
3. Excretion
Distal tubule
Urinary collecting duct
Vasa Recta
Henle's loop

Figure 3: Schematic representation of a nephron

The afferent arteriole which brings the systemic blood into the glomerulus gives rise to a glomerular capillary bed in which the blood is filtered. The filtration of the blood plasma components across the filtration barrier between the capillaries and the urinary space of the glomerulus is complex and is governed by the size, charge and shape -selective properties of the filtration barrier. From the glomerular capillaries the blood exits the glomerulus through the efferent arteriole to nourish the tubular network of the nephron and to eventually leave the kidney via the venous system. The collected plasma ultrafiltrate exits the lumen of the Bowman's capsule to enter the proximal tubule, the Henle's loop, the distal tubule and the collecting duct, which are involved the reabsorption, processing and secretion of useful components of the ultrafiltrate leaving behind the collected urine which is then excreted from the kidneys via the ureter.

the glomerular capillaries (Junqueira *et al.*, 1998). The outgoing efferent arteriole is formed by the abrupt convergence of the glomerular capillary pathways (Dworkin *et al.*, 2000). The efferent arteriole branches into the peritubular (postglomerular) capillary network which nourishes the proximal and distant tubules of the nephron. The efferent arteriole carries away larger plasma components that are unable to penetrate the glomerular filtration barrier. Some of these components can still be taken-up from the peritubular circulation if capable of traversing across the tubular basement membrane to encounter the basolateral cell surface of the renal tubule cells.

The glomerular filtrate forms in response to the hydrostatic pressure of blood (45 mm Hg), opposed to the osmotic pressure of the plasma colloids (20 mm Hg) and the hydrostatic pressure of the fluids in the Bowman's capsule (10 mm Hg). This results in the net filtration pressure of 15 mm Hg at the afferent end of the glomerular capillaries (Junqueira *et al.*, 1998). The glomerular capillaries are lined by a thin layer of endothelial cells. The endothelium is fenestrated, with pores 70-100nm in diameter. These pores form the initial barrier to the passage of plasma constituents from the capillary lumen of the glomerulus to the urinary space of the Bowman's capsule. The surface of the endothelial cells contains polyanionic surface glycoproteins and other negatively charged molecules, thereby contributing to the charge-selective property of the glomerular capillary wall (Tisher and Madsen, 2000). Specialized cells, termed podocytes exist within the visceral layer of the glomerulus. Podocytes have long cytoplasmic processes, trabeculae which extend from the cell body and divide into foot processes, pedicels, which intedigitate and come in contact with the external layer of the glomerular basement membrane. The distance between the adjacent pedicels on the glomerular basement

membrane is 25-60 nm. This gap, or a filtration slit is bridged by a 6 nm thick diaphragm. Besides their function in the formation of the filtration slits, the podocytes provide mechanical support to the glomerular basement membrane. The glomerular basement membrane is formed from the fusion of the capillary and podocyte-produced basal laminae. The basement membrane contains fibronectin, collagen IV and laminin, in a matrix containing the negatively charged heparan sulfate proteoglycans (HSPG). Thus the glomerular basement membrane forms the main filtration barrier between the blood in the capillaries and the urinary space, with both physical and charge selective barrier properties. Specialized cells, called mesangial cells also exist in the vicinity of the glomerular filtration barrier. These cells are though to act as macrophages by mediating the uptake of unfiltered particulate material that accumulates in the basal lamina during filtration. In light of its size and charge selectivity, the filtration barrier is effective at preventing the entry of the majority of particles greater than 10 nm in diameter (Junqueira *et al.*, 1998; Tisher and Madsen, 2000). The least known aspect of the filtration barrier properties of the glomerular basement membrane is its shape selectivity. While spherical molecules with a mean radius greater than 50 Å, will hardly penetrate the glomerular filtration barrier, molecules which display asphericity under shear could present smaller effective radii to the filtration barrier, which could enable their filtration. Molecules that have been shown to display such properties are dextrans (Myers, 1989) and bikunin, a chondroitin-sulfate containing serum protein (Lindstrom *et al.*, 1997) among others. Several structural investigations show that HDL may also exhibit an elongated, flexible configuration (Scanu, 1971; Marcel *et al.*, 1991; Segrest *et al.*, 1992; Sparks *et al.*, 1999). In diseases such as glomerulonephritis or diabetes melittus, the

glomerular filtration barrier is altered, becoming more permeable to larger proteins otherwise excluded from the filtrate; a condition termed proteinuria. Such proteins can then be detected in the urine (Junqueira *et al.*, 1998). Cytochemical studies have revealed that proteinuria is often associated with the depletion of the anionic HSPG components of the glomerular capillary wall, or the fusion of the podocyte foot processes into a continuous cytoplasmic band along the glomerular basement membrane (Tisher and Madsen, 2000).

The plasma ultrafiltrate that forms in the glomerulus passes into the PCT. The PCT has an initial convoluted section (pars convoluta) which starts at the urinary pole of the glomerulus and a straight section, the pars recta which extends into the medulla. The PCT is lined with simple cuboidal or columnar epithelium. The epithelial cells are enriched in mitochondria, thus have a strongly acidophilic cytoplasm. Three to five nuclei are present in the centre of each epithelial cell. The PCT cells also contain large quantities of smooth and rough endoplasmic reticulum and free ribosomes and have a well-developed Golgi aparatus located above and lateral to the nuclei (Tisher and Madsen, 2000). The PCT cells are polarized, with distinct apical and basolateral poles. While the apical regions of the PCT cells face the tubular lumen, the basolateral regions rest on the tubular basement membrane, which separates the cells from the underlying peritubular capillaries. In the apical region, the PCT cells display a prominent microvillar brush border. The apical brush border increases the apical cell surface area 40-fold. The brush border is coated with a glycoprotein rich coat for maximizing peptide and glucose absorption. Also enzymes such as ATPase and alkaline phosphatase are present. At the base of the individual microvilli, small canaliculi form and are involved

in rounding up vesicles and fusing them together into larger vacuoles. The vacuoles represent the initial elements of the well-developed endocytic apparatus of the PCT. In their proximity are vesicles such as lysosomes and dense bodies (Zamboni, 1989; Junqueira *et al.*, 1998). The lateral and basal portions of the cells are characterized by the presence of large plasma membrane processes, often interdigitating with adjacent cells. The membrane also contains sodium pumps for active ion transport. The adjacent PCT cells are separated by an intercellular compartment which contains regions at which the adjacent cells are bound together through junctions. These include the tight junction (zonula occludens) in the apical region, the intermediate junction (zonula adherens) and the desmosome (macula adherens) in the basal regions of the cell (Zamboni, 1989). While intermediate junctions and desmosomes provide mechanical link between adjacent cells, tight junctions are responsible for intercellular sealing and regulation of paracellular transport of specific solutes, ions and water (Gumbiner, 1993). As the intercellular space is completely obliterated at tight junctions, paracellular diffusion of proteins and lipids is restricted (Nelson, 1992). For a schematic depiction of the PCT cells see Figure 4.

Protein Handling in the Proximal Tubule

After glomerular filtration, the macromolecular components of the plasma ultrafiltrate are reabsorbed by the cells of the PCT. While the PCT is active in reabsorption and processing of a variety of components of the ultrafiltrate, including proteins, amino acids, vitamins and NaCl, the handling of components other than proteins is beyond the scope of this overview. The apical brush border is covered by a glycoprotein-rich coat that maximizes the absorption of peptides and glucose. In addition, the apical membrane of the pit formations at the base of individual microvilli is coated

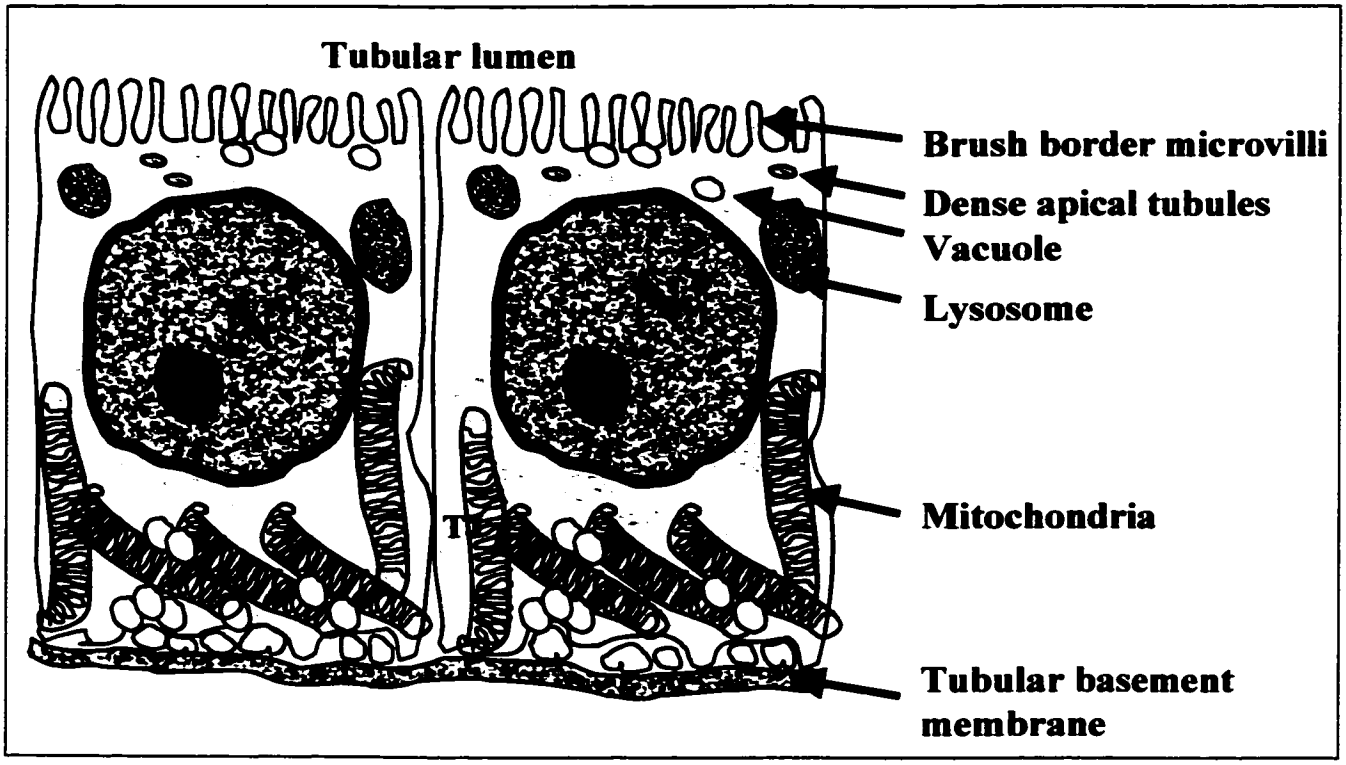
Tubular lumen
Brush border microvilli
Dense apical tubules
Vacuole
Lysosome
Mitochondria
Tubular basement membrane

Figure 4: Schematic representation of proximal tubule cells (PCT)

The apical surfaces of the cuboidal epithelial PCT cells face the renal tubular lumen. They have an extensive microvillar brush border which greatly increases the absorptive surface area of the apical membrane. The PCT cells are enriched in mitochondria and are multinucleated (N). They also possess a well-developed endocytic apparatus comprising of clathrin coated pits, vacuoles, dense apical bodies and lysosomes. The basolateral surfaces of the PCT cells are characterized by long interdigitating membrane processes which contact the tubular basement membrane. The basement membrane represents a selective barrier that separates the PCT cells from the peritubular capillaries. The adjacent PCT cells are separated by intercellular spaces, with junctional areas at which the paracellular diffusion is tightly regulated via structures such as tight junctions (TJ).

with clathrin (Rodman *et al.*, 1984). Such pits eventually give rise to clathrin-coated endocytic vesicles, which will transport their cargo into the cell interior. The vesicles, or vacuoles (upon fusion) can be subdivided into early and late endosomes, which mainly differ by their size and external coating (Cui and Christensen, 1993). The brush border membrane also contains enzymes such as peptidases and hydrolases capable of directly degrading small peptides into their amino acid constituents. However, studies show that such degradation is mainly limited to small linear peptides, such as glucagon (Peterson *et al.*, 1982), whereas larger peptides and proteins are reabsorbed by endocytosis (Christensen and Nielsen, 1991). The initial event of endocytosis is the binding of the proteins to their binding sites on the luminal membrane, where they may migrate laterally in the plane of the membrane into the coated pit formations (Christensen and Nielsen, 1991). Many receptors capable of facilitating the endocytosis of components of the ultrafiltrate have been discovered. Both, megalin and cubilin for example have been detected associated with the clathrin-coated membrane areas, with cubilin extending to the microvilli as well (Sahali *et al.*, 1988; Christensen *et al.*, 1995). Both receptors are known for facilitating the endocytosis of a multitude of ligands at the apical lumen of the PCT cells. Furthermore, in light of the studies showing the functional relationship of megalin and cubilin in mediating endocytosis of some of their ligands (Moestrup *et al.*, 1998; Hammad *et al.*, 2000), the two receptors have been shown to colocalize in numerous organelles of the endocytic apparatus (Sahali *et al.*, 1988; Seetharam *et al.*, 1997). After the proteins bind to the extracellular coat of the membrane pit formations, the membrane is pinched off to form small vesicles, which later fuse to form large endocytic vacuoles (late endosomes) (Christensen and Nielsen, 1991). Dense apical

tubules are often seen connected to the endosomes. These organelles are though to be involved in recycling membrane proteins back to the plasma membrane (Christensen, 1982). The protein ligands are delivered to the lysosomes for degradation. The lysosomes contain a variety of acid hydrolases capable of degrading a multitude of ligands (Maunsbach, 1966).While a majority of ligands that undergo endocytosis are lysosomally degraded, a small amount can escape degradation. For example, small amounts of cationized peroxidase have been localized in the Golgi apparatus after internalization in the proximal tubule (Coudrier *et al.*, 1988).

It has been demonstrated that proteins such as peroxidase (Nielsen and Christensen, 1985), lysozyme (Ottosen, 1978) or albumin (Tisher and Kokko, 1974) can diffuse retrograde from the peritubular space through the tubular basement membrane into the intercellular space. Such macromolecules may then be reabsorbed by receptors present on the basolateral membrane of the PCT cells (Christensen and Nielsen, 1991). Indeed, basolateral receptors capable of binding insulin, epidermal growth factor (Nielsen *et al.*, 1989), HDL (Senault *et al.*, 1994) and other macromolecules have already been demonstrated. As insulin has been demonstrated to undergo both apical and basolateral processing, the processing of ^{125}I-insulin at the two cells surfaces in isolated, perfused, rabbit proximal tubules has been compared by Nielsen *et al.* They have found that the basolateral binding and uptake constituted 15% of the total tubular extraction of insulin (Nielsen *et al.*, 1987). In contrast, a similar study using cultured opossum kidney (OK) cells showed that the basolateral endocytosis of ^{125}I-insulin was about two times higher than the luminal (Rabkin *et al.*, 1996).

In their study, Nielsen *et al.* have also shown that a small amount of intact ^{125}I-insulin was also transferred from the peritubular space to the apical vesicles of the luminal compartment, suggesting a basal to apical transcytosis (Nielsen *et al.*, 1987). Similar observations were also made for the epidermal growth factor (Nielsen *et al.*, 1989). In addition, ^{125}I-insulin was also able to undergo transcytosis in the opposite, apical to basal direction. The transport represented about 5% of the total tubular extraction of insulin (Nielsen *et al.*, 1987; Nielsen *et al.*, 1989). Experiments with isolated, HRP-perfused rabbit kidneys have revealed that the transcytosis occurred via vacuoles (Nielsen *et al.*, 1985). Studies of transcytosis in cultured renal tubule cells revealed that cultured cells can facilitate significant transcytosis of the internalized ligands (Goligorsky and Hruska, 1986).

Rationale and Aims

It is well established that apoA-I catabolism is a metabolic predictor of plasma HDL levels (Brinton *et al.*, 1991; Ikewaki *et al.*, 1995) and that apoA-I catabolism, rather than its production, determine the levels of this apolipoprotein in the plasma (Ikewaki *et al.*, 1995). Furthermore, with the increasing amount of evidence pointing towards the importance of the kidney in the catabolism of both apoA-I and HDL (Rader and Ikewaki, 1996; Hammad *et al.*, 1999; Kozyraki *et al.*, 1999), it remains clear that the mechanisms of renal handling of HDL need to be established if we want to gain more insight into HDL metabolism *in vivo*.

Previous work in our laboratory and by others has shown that the lipid composition-dependent biophysical properties of HDL may affect the catabolism of HDL and apoA-I (Horowitz *et al.*, 1993; Brinton *et al.*, 1994; Braschi *et al.*, 1999). In

addition, the lipid composition of HDL has also been shown to exert marked effects on its association with endocytic receptors by strongly influencing the conformation of apoA-I, an important ligand for HDL receptors (Sviridov *et al.*, 1988; Fidge, 1999). However, the mechanisms for these interactions remain to be elucidated. The discovery of cubilin, an endocytic receptor important in the renal clearance of apoA-I and small HDL particles (Hammad *et al.*, 1999; Kozyraki *et al.*, 1999), as well as of other potential HDL-binding renal receptors (Senault *et al.*, 1994), adds more emphasis towards the potentially important role of the kidney in HDL metabolism.

This work will attempt to address the role of the kidney in HDL metabolism by first, exploring the specific cellular sites of HDL metabolism in the kidney and re-evaluating the transport of HDL particles through this organ *in vivo*, and second, by characterising the parameters that regulate the renal handling of HDL particles by evaluating the binding, uptake and degradation of HDL particles by the proximal tubule cells of the renal cortex *in vitro*.

Chapter 2: Experimental Procedures

Materials

FluoroLink™ Cy3™ Monofunctional Dye and [1α,2α(n)-^{3}H]cholesteryl-oleate were purchased from Amersham Pharmacia Biotech (Baie d'Urfé, PQ). Egg PC, brain SM, liver PI, FC and POPC were purchased from Avanti Polar Lipids (Birmingham, AL). CE and TG were obtained from Sigma Chemical Co. (ST. Louis, MO), while DG was obtained from Nuchek Prep, Inc. (Elysian, MN). Bovine Fibronectin was purchased from Sigma-Aldrich Canada Ltd. (Oakville,ON). Iodobeads were from Pierce (Rockford, IL). Falcon Transwell Tissue-culture Inserts (3 μm, HD, PET) were obtained from VWR-Canlab (Ville Mont-Royal, Quebec). Monoclonal antibodies 5F6 and 4H1 against human apoA-I were a generous gift from Dr. Yves Marcel (The Heart Institute Lipoprotein Research Group, University of Ottawa, Ontario). All other reagents were analytical grade. The HKC-8 kidney proximal tubule cell line was obtained from the laboratory of Dr. Lorraine Racusen (John Hopkins School of Medicine, Baltimore, MD).

Methods

I. Preparation of the Ligands

Purification of ApoA-I

Human HDL (ρ =1.063-1.210 g/mL) was isolated from fresh plasma by sequential density gradient ultracentrifugation according to the procedure of (Havel *et al.*, 1955). HDL was delipidated in chloroform:methanol as previously described (Scanu and Edelstein,1971). Purified apoA-I was isolated by size-exclusion chromatography on a

Sephacryl S-200 HR column (Brewer *et al.*, 1986). ApoA-I was stored in lyophilized form at –80 °C. Prior to use, it was resolubilized in 6M guanidine hydrochloride and 10 mM Tris, pH 7.2, and dialyzed extensively against PBS. Protein concentrations were determined using the Lowry method as modified by Markwell (Markwell *et al.*, 1978).

Iodination of ApoA-I

Purified apoA-I was iodinated with $Na^{125}I$ using the IODO-BEAD Iodination reagent (Pierce; Rockford, IL) and manufacturer-recommended protocols. The efficiency of labeling was 52%, and the resultant specific activity of apoA-I was 1 μCi/μg of protein.

Preparation of Reconstituted Spherical HDL Particles

Reconstituted HDL particles were prepared by co-sonication of a fixed ratio of lipid:apoA-I. Briefly, specific amounts of lipids in chloroform (see Table 3 for molar ratios) were dried under nitrogen in a 12 x 75 mm glass tube, and 800 μl of PBS was added. The lipid-buffer mixture was successively sonicated with a Branson Sonifier 450 (Branson Ultrasonics, Danbury, CT) under nitrogen for 1 min at constant output, incubated at 37 °C for 30 min and sonicated again for 5 min at 95% duty cycle under nitrogen. 0.5 mg of ^{125}I-labeled apoA-I and unlabeled apoA-I (diluted to 1.4 mg/mL solution in PBS) were added to the lipid mixture and co-sonicated for 4 x 1 min at 90% duty cycle under nitrogen, with 1 min cooling periods between sonications. The particles were then filter sterilized. The size and homogeneity of the particles were estimated by non-denaturing gradient gel electrophoresis (Pharmacia, Phast System). Particle charge was calculated from electrophoretic mobility in 0.5 % agarose gels containing BSA (Beckman, Paragon Lipo kit).

In addition, following a chloroform:methanol extraction (Scanu and Edelstein, 1971), both lipids and proteins from HDL particles were recovered and used to make reconstituted particles.

Table 3: rHDL complex composition

Lipid [a]	POPC:lipid:apoA-I [b] (mol:mol:mol)	Surface potential [c] (-mV)
DG	120:40:2	10.0
TG	120:40:2	9.5
SM	140:40:2	9.7
PI	120:40:2	12.7
CE	120:60:2	9.7
FC	120:40:2	9.7
POPC	120:0:2	8.5

[a] Spherical rHDL particles containing the listed lipids were prepared by sonication as described in the text.
[b] Composition determined as described of phosphatidylcholine (POPC), phosphatidylinositol (PI), sphingomyelin (SM), free cholesterol (FC), cholesteryl ester (CE), diglyceride (DG), triglyceride (TG) and apoA-I.
[c] Charge potential at the particle surface ± 0.2 mV (SD).

Preparation of the Double-labeled HDL

One hundred µl (100µCi) of [^{3}H]cholesteryl-oleate was dried under N_2 and dissolved in 50µl of ethanol. 1.5 ml of LPDS (ρ > 1.21 g/ml) and a 0.01% protease inhibitor-glutathione cocktail were added to 5 mg of HDL followed by a rapid addition of 50 µl of [^{3}H]cholesteryl-oleate. The mixture was incubated at 37°C for 32 hours under N_2. HDL is then re-isolated ultracentrifugally (ρ > 1.21 g/ml). [^{3}H]-labeled HDL was iodinated as described above. The double-labeled HDL was dialyzed extensively against PBS to remove any non-protein associated ^{125}I.

II. *In vivo* Experiments

Kidney perfusion with the Lp2A-I and ApoA-I Ligands

The animal protocols were reviewed and approved by the animal ethics committee of the University of Ottawa, Heart Institute. Two male New Zealand White rabbits were anaesthetized and the renal arteries were perfused with 800 µl of rHDL (Lp2AI), human apoA-I particles (1 mg protein /ml) or sterile saline control, followed by a saline wash (1ml for 30 sec). The kidneys were immediately excised from the animal.

Immunoelectron Microscopy

Following excision from the animal, the perfused rabbit kidneys were fixed in 1.6% glutaraldehyde in 0.1M Na Cacodylate buffer, followed by a 0.1M Na Cacodylate buffer wash. To reduce non-specific binding, tissue was washed in 0.15M glycine in PBS for 1 hour at 4°C. The tissues were dehydrated in a series of graded methanols (60%, 80%, 95%) for 15 min each at 4°C. Next they were transferred to a 2:1 mixture of LR white resin and 95% methanol for 60 minutes at RT. Tissues were infiltrated overnight in pure LR white resin at 4°C, followed by 1 hour at RT. Tissues are then embedded in fresh LR white in gelatin capsules. The blocks are then polymerized for 24 hrs in a 50°C oven and sectioned. Non-specific binding was further prevented by incubating the grids in a few drops of 1% BSA for 30 minutes. The grids were transferred to drops of 5F6 and 4H1, mouse anti-human apoA-I IgGs (diluted in 1% BSA) at a 1:100 dilution, or 1% BSA controls and incubated overnight at 4°C in a humid chamber. Grids are washed in PBS and placed onto drops of PBS 3 x 15 min. Grids are next floated onto drops of gold-conjugated goat anti-mouse IgG (15 nm) (E-Y Laboratories, San Mateo, CA) and incubated for 1 hour. The grids were next washed in double distilled H_2O and blot dried. A counterstain with saturated aquaeous uranyl acetate (20 sec)

and Reynold's lead citrate (45 seconds) followed. Thin sections of the embedded material were viewed using a Hitachi H-7100 electron microscope (EM) operating at 75 keV.

Kidney perfusion with the double-labeled HDL

A male New Zealand White rabbit was anaesthetized and the renal arteries were perfused with 800 µl of double-labeled HDL (0.4 mg protein /ml), followed by a sterile saline wash (1ml for 30 sec). The kidneys were immediately excised from the animal.

Lipid Extraction of the Rabbit Kidneys

The kidneys were extracted by a modification of the method of Kates (Kates, 1972). Briefly, the kidneys were extracted in 3 g sections. To each, 2 ml of water and 15 ml of methanol-chloroform (2:1, v/v) was added, followed by blending in a Cyclone Virtishear IQ homogenizer (Canberra Packard Canada, Mississauga, ON) for 2 min at room temperature. The homogenate was centrifuged, the supernatant was decanted and the residue was re-extracted with 19 ml of methanol-chloroform-water (2:1:0.8, v/v/v) with homogenization for 2 min. After centrifugation, the combined supernatants were diluted with 10 ml each of chloroform and water and the phases separated by centrifugation. The lower chloroform phase was withdrawn and concentrated by evaporation under N_2. The residue was then dissolved in a suitable volume of chloroform.

Lipid Separation by Thin-layer Chromatography

The amount of lipid-associated [^{3}H] in extracts was determined by thin-layer chromatography on ITLC-SG (Gelman, Ann Arbor, MI) plates using a solvent system composed of hexane:diethyl ether:acetic acid (90:10:1, v/v/v). The lipids were resolved into CE, FC and POPC subfractions. The lipids were further visualized with iodine and quantified by counting on a Tri-Carb 2100TR Liquid Scintillation Analyzer (Canberra Packard Canada,

Mississauga, ON). Protein associated ^{125}I was measured in Cobra II Auto-Gamma counter (Canberra Packard Canada, Mississauga, ON).

III. *In vitro* Experiments

Ligand Binding and Degradation Assays

HKC-8 cells were seeded into 24-well Falcon plates (Fisher Scientific, Nepean. ON) and grown to confluency in a CO_2 incubator at 37°C. Cells were maintained in DMEM-Ham's F-12 (DMEM/F12) medium (Life Technologies, Burlington, ON) supplemented with 10% fetal bovine serum (FBS), 100 U/ml penicillin and 100 μg/ml streptomycin. The cells were washed twice with media and 1 ml of ^{125}I-ligand (100 nM) in media (6 mg/ml BSA, 0.1% $CaCl_2$) was added either alone (total binding) or in the presence of an excess (1 mg/ml) of unlabelled HDL (non-specific binding). Specific binding was calculated by subtracting the non-specific from the total binding. Plates were incubated at 37°C for various times to allow cell association. At the end of the incubation period, the cells were put on ice, washed two times with cold PBS (6 mg/ml BSA, 0.1% $CaCl_2$) and twice again with cold PBS alone. One ml of 0.2 M NaOH was added to each well and incubated overnight at 23°C with gentle rocking. Lysates were removed and radioactivity was measured with a Cobra II Auto-Gamma counter (Canberra Packard Canada, Mississauga, ON). Cell protein was determined using the BCA protein assay (Pierce, Rockford, IL). For degradation analysis, an aliquot of media post incubation was added to an equal volume of 25% for precipitation. The samples were incubated at 37 °C for 30 min, followed by a centrifugation at 12,000rpm for 10 minutes. The pellet represented insoluble, intact, radiolabeled protein, and the supernatant contained radioactivity freed upon the TCA solubilization of the degraded protein products. The

radioactivity of the soluble products was measured and expressed as the percentage of total radioactivity.

Immunofluorescence

The FluoroLink™ Cy3™ Monofunctional Dye was conjugated with HDL by adding 1 mg of dye to 68 µl of HDL and 932 µl of 0.1M sodium carbonate buffer at pH 9.3 for a total volume of 1 ml. The 1 mg/mL solution was mixed and incubated at room temperature for 30 minutes with additional mixing (Amersham, Baie d'Urfé, PQ). The un-conjugated dye was removed from the HDL preparation by gel permeation chromatography. HKC-8 cells grown to confluence on microscopy wells were washed with media containing HEPES buffer and 2 mg/ml BSA. For cell surface labeling, the cells were incubated 1 hour on ice with the labeled HDL in the media at 10 µg/ml. For cell uptake, the cells were incubated at 37°C up to 60 minutes after the labeled ligand was added. In both cases, cells were washed twice with cold PBS, fixed in 500 µl of cold paraformaldehyde and washed again twice with cold PBS. The cells were viewed with Olympus IX50 inverted fluorescent microscope and photographed with a Micromax Camera equipped with Win View software (Princeton Instruments, Whitley, ON).

Extracellular Matrix Association Assay

HKC-8 cells were seeded into 24-well Falcon plates and grown to confluency in a CO_2 incubator at 37°C. The cells were cultured in DMEM/F12 supplemented with 10% FBS, 100 U/ml penicillin and 100 µg/ml streptomycin. Next, they were washed twice with serum-free DMEM/F12. One ml of ^{125}I-ligand (100 nM) in media (6 mg/ml BSA, 0.1% $CaCl_2$) was added per well and the cells were incubated for 4 hr at 37°C. Following incubation, the cells were washed twice with PBS (Ca^{2+}/Mg^{2+} -free) and treated with

3mM EDTA in PBS for 5 min at 37°C to lift the cells of their extracellular matrices (ECM). The cells were then collected from the wells for counting and protein determination. The ECM were treated with 1ml of 0.2M NaOH per well and incubated overnight in a humid chamber on a rocking platform. The ECM-lysates were then collected from the wells for counting and protein determination.

IV. *In vitro* Experiments with Polarized Cells

Cell Culture

HKC-8 cells were seeded into 24-well Falcon plates and grown to confluence in a CO_2 incubator at 37°C. The cells were cultured in DMEM/F12 supplemented with 10% FBS, 100 U/ml penicillin and 100 μg/ml streptomycin. The transwell tissue-culture inserts were pre-coated with 30 μg/ml fibronectin in DMEM to a final coating concentration of 3 $\mu g/cm^2$ according to manufacturer-recommended protocols. The cells were then plated onto fibronectin-coated tissue-culture inserts and allowed to grow for 4 days in DMEM/F12 supplemented with 2% FBS, 100 U/ml penicillin and 100 μg/ml streptomycin.

Ligand Processing and Degradation Assays

Growth medium was removed and cells were washed twice with serum-free DMEM/F12. ^{125}I-labeled ligand in DMEM/F12 media (6 mg/ml BSA, 0.1% $CaCl_2$) was then added either to the top or the bottom compartment of each transwell chamber (0.5 ml to the top compartment (apical) or 1.5 ml to the bottom compartment (basolateral), with each opposing chamber containing a corresponding amount of ligand-free media) at a final concentration of 300 μg/ml per well. The cells were then incubated at 37°C for various times. At the end of each time-point, medium was collected at 4°C from both

chambers for counting and protein determination. The cells were washed twice with PBS containing 0.1% $CaCl_2$, 2mg/ml BSA and twice with PBS (0.1% $CaCl_2$, no BSA). The cells were then lysed in 0.2 M NaOH , overnight at room temperature, with gentle rocking. Following the incubation, lysates were removed for counting and cell protein determination. For degradation analysis, an aliquot of media post incubation was added to an equal volume of 25% TCA for precipitation. The radioactivity of the soluble products was measured and expressed as the percentage of total radioactivity.

In order to monitor the integrity of the confluent monolayers throughout the experiment, [^{14}C]inulin (0.1μCi) was added to apical compartments of a separate set of wells for each time point. The presence of [^{14}C]inulin in the apical and basolateral compartments was then monitored by scintillation counting. Fibronectin-coated transwells without cells were used as controls at each timepoint.

Statistical Analysis

Using SigmaStat version 2 software, a multivariate ANOVA analysis with a post-hoc Tukey multiple comparisons test was performed on the data sets to obtain significance levels (p-values) to compare the means.

Chapter 3: RESULTS

I. *In vivo* Experiments

Rationale

Numerous tissue uptake studies have shown that HDL can be filtered by the kidneys and that radioactively labelled HDL components can be found in the kidney cortex (Glass *et al.*, 1983; Glass *et al.*, 1985; Goldberg *et al.*, 1988, Kaysen *et al.*, 1995; Woollett and Spady, 1997; Spady *et al.*, 1998; Wang *et al.*, 1998). While the general consensus was that it is lipid poor apoA-I that is fitered by the kidney, some studies suggest that the kidney is capable of both the filtration and re-absorption of apoA-I and small-sized HDL particles (Segal *et al.*, 1979; Glass *et al.*, 1983; Peterson *et al.*, 1984). The goal of this work was to explore the specific cellular sites of HDL metabolism in the kidney and to re-evaluate the transport of HDL particles through this organ *in vivo*.

Kidney Perfusion with Double-labeled HDL

In order to determine whether rabbit kidneys can take-up whole HDL particles, a rabbit renal artery was perfused with [^{3}H]CE and ^{125}I protein –labeled HDL ligand. Immediately after perfusion, the kidneys were excised and homogenized. The ^{125}I-proteins and [^{3}H]CE were extracted from the homogenates, with the lipids subsequently resolved into CE, FC and POPC subfractions by TLC to determine the lipid associated radioactivity. The results indicate that both [^{3}H] lipid and ^{125}I protein are retained in the rabbit renal cortex with a 12.9% and 31.6% recovery respectively (Fig. 5). This result shows that about 2.4 times more protein than CE is taken up by the kidneys. A comparison of the ratios of neutral lipid to protein in the ligand prior to injection and in the kidney post injection differed considerably. The ratio in stock ligand was 1 : 2.1

versus 1 : 5.1 in the kidney (Table 4). This similarly suggests that both HDL holoparticle uptake and a selective protein uptake component occur in the kidney.

Table 4: Kidney perfusion with a [^{3}H]CE and ^{125}I-protein labeled HDL ligand

neutral lipid : protein in stock[a]	neutral lipid : protein in kidney[b]
1 : 2.1	1 : 5.1

[a][^{3}H] lipid and ^{125}I-protein cpm in HDL ligand prior to injection
[b][^{3}H] lipid and ^{125}I-protein cpm in renal extract post analysis

Kidney Perfusion with the rHDL and ApoA-I Ligands

Renal arteries of anaesthesized New Zealand rabbit were perfused with purified human apoA-I or rHDL particles and the kidneys were harvested and processed immediately for immunoelectron microscopy. The rHDL particles used were composed of POPC and apoA-I (Table 3). The perfused ligands were immuno-localized in the kidney cortex using a primary mouse anti-human apoA-I monoclonal antibodies (mAb) 5F6 and 4H1 and a secondary goat anti-mouse gold-conjugated IgG. The electron micrograph tracking the immunoreactivity of mAb 5F6 showed profuse specific labeling of rHDL particles throughout the apical regions of proximal tubule epithelial cells of the renal cortex with some label localized at the brush border (Fig. 7). A comparable labeling pattern was observed with the apoA-I perfusate localized with the 5F6 mAb (not shown). Similarly, Glass and coworkers have shown the presence of the perfused ^{125}I-TC-apoA-I in the rat PCT cells by immunofluorescence microscopy (Glass, *et al.*, 1983).

A different labeling pattern was observed when the perfused apoA-I protein was immunolocalized in the kidney tissues with mAb 4H1. Distinct labeling of apoA-I

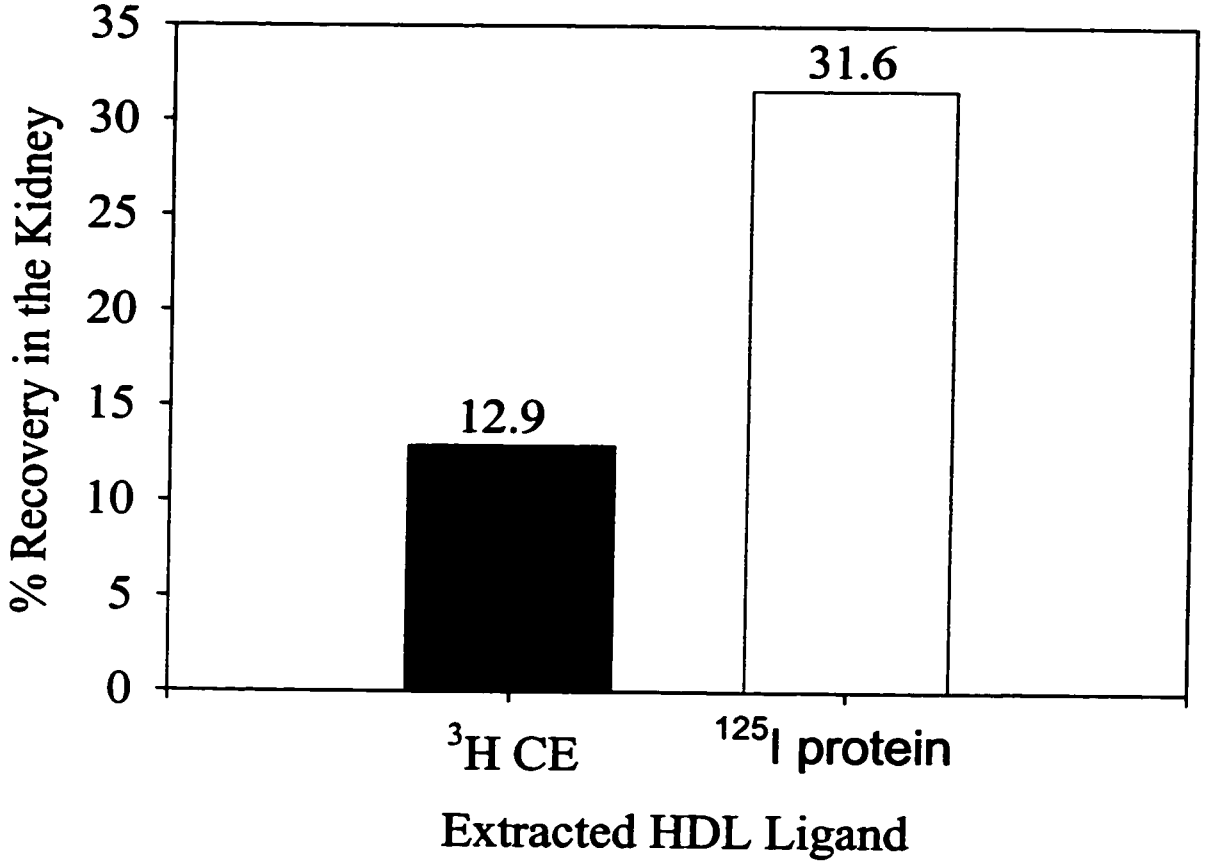
35
30
25
20
15
10
5
0
% Recovery in the Kidney
31.6
12.9
^{3}H CE
^{125}I protein
Extracted HDL Ligand

Figure 5: Both [^{3}H] lipid and ^{125}I protein are retained in the rabbit kidney

HDL isolated from human plasma was labeled with [^{3}H]CE and then with ^{125}I protein. The renal arteries of an anesthesized rabbit were perfused with 0.4 mg protein/ml of the ligand. The kidneys were then excised, homogenized and analyzed for protein associated ^{125}I radioactivity. The lipids were extracted, separated by TLC and analyzed for lipid-associated [^{3}H] radioactivity. The figure represents a determination from duplicate experiments. (n=2)

Figure 6: The basal lamina of rabbit proximal tubule cells is enriched with the apoA-I perfusate

To visualize the localization of apoA-I in the rabbit kidney cortex, after perfusion of the renal artery, the cortex was fixed in glutaraldehyde, sectioned and treated with 4H1 mouse anti-human apoA-I IgG and gold-conjugated goat anti-mouse secondary IgG. The sections were then analyzed by EM. A distinct labeling of the basal lamina (**BL**) is observed. Bar = 2 μm


BB

Figure 7: Localization of perfused rHDL particles in the proximal tubule cells of a rabbit kidney

To visualize the localization of rHDL particles in the rabbit kidney cortex, after perfusion of the renal artery, the cortex was fixed in glutaraldehyde, sectioned and treated with 5F6 mouse anti-human apoA-I IgG and gold-conjugated goat anti-mouse secondary IgG. The secions were analyzed by EM. The rHDL particle was composed of POPC and apoA-I (Table 3). The electron micrograph shows profuse staining of rHDL particles within proximal tubule cells, with some label localized at the brush border (**BB**). Bar = 1 μm

within the basal lamina of proximal tubule cells was observed (Fig. 6). Similar labeling pattern was observed with the rHDL perfusate (not shown) localized with the 4H1 mAb. No significant amount of apoA-I was identified within glomerular structures using either monoclonal antibody. No labelling was observed in controls, with the primary mAb absent (not shown).

II. *In vitro* Experiments

Rationale

The aim of this project was to characterise the factors that regulate the renal processing of HDL particles by characterising the binding, uptake and degradation of HDL particles by the proximal tubule cells of the renal cortex. To corroborate the findings of the *in vivo* studies, we have chosen to utilize a cell culture system, using HKC-8 cells, an immortalized human renal tubule epithelial cell line. The cell line has been shown to maintain normal expression of tubule markers such as alkaline phosphatase, γ-glutamyl traspeptidase or glutathione-S-transferase, maintain normal biochemical properties and display a normal epithelial monolayer morphology with a well developed brush border for prolonged periods. The HKC-8 cell line is comparable to established cell lines such as OK, HK-2, and LLC-RK1 (Racusen *et al.*, 1997).

Immunofluorescence

Confluent HKC-8 cells were incubated with fluorescently labelled HDL to follow binding and uptake of the HDL particles. Cell surface binding was estimated after removal of the cell media by incubation of labelled HDL with the live cells on ice. Figure 9A shows that the Cy3-HDL readily binds to the cell surface of HKC-8 cells, as evidenced by the intense peripheral labelling, highlighting the cell membrane. To

determine if this cell surface bound HDL can be taken up, HKC-8 cells were incubated with media containing Cy3-HDL at 37 °C up to 60 minutes. Microscopic evaluation of the HKC-8 cells showed a progressive internalization of the labelled lipoprotein over time. After 60 minutes, most of the surface-bound HDL particles were internalized, as evidenced by label appearance in vesicles in the perinuclear region within the HKC-8 cells (Fig. 9B). Similar observations were made by Glass and colleagues who have immunolocalized fluorescently labelled apoA-I to the brush border and to densely staining granules in the apical regions of the proximal tubule in frozen sections of rat kidney (Glass *et al.*, 1983).

Ligand Binding and Degradation Assays

In order to evaluate the effect of structural components of HDL on its association with human proximal tubule cells, we have performed a series of time-course experiments in HKC-8 cells using ^{125}I-labeled HDL, rHDL and apoA-I. Cells were incubated with 100nM of radiolabeled lipoproteins for up to two hours either alone, or in the presence of an excess of unlabeled HDL, to measure the specific binding component. The cells were washed in buffer on ice and lysed in O.2M NaOH. The cell lysates were then evaluated for radioactivity by gamma counting. Figure 10 shows the time course of native ^{125}I-labeled HDL binding to human proximal tubule cells. The amount of cell-associated particles reached a plateau at 2 hours, after a rapid increase to 30 minutes and a gradual levelling off thereafter. Specific binding component represented about 58% of the total binding ($p<0.05$). Several laboratories have demonstrated comparable ^{125}I-HDL binding to the membranes of the renal cortex of various species, including those of

human, porcine and rat origin (van Tol *et al.*, 1986; Senault *et al.*, 1994; Kozyraki *et al.*, 1999).

Figure 11 represents a comparison of the interaction of various lipoprotein particles with HKC-8 cells over time. The lipid-free apoA-I was obtained by purifying delipidated HDL and the reconstituted HDL (rHDL) was prepared by co-sonication of POPC and apoA-I (Table 3). The figure further shows saturable cell association for all three particles evaluated, with ^{125}I-rHDL and ^{125}I-apoA-I reaching a plateau more rapidly than ^{125}I-HDL. 78% and 65% of total binding was represented by the specific binding component for ^{125}I-apoA-I ($p<0.05$) and ^{125}I-rHDL respectively. In addition, ^{125}I-apoA-I specific binding was 2-fold higher than that of the ^{125}I-rHDL ($p<0.05$). Furthermore, both particles showed noticeably lower levels of association than ^{125}I-native HDL (Fig. 11). Pure ^{125}I-apoA-I has also been shown to compete less effectively for HDL binding sites than ^{125}I-HDL$_3$ in human enterocytes (Sviridov *et al.*, 1988).

Evaluating the fate of the HDL particles upon their internalization by HKC-8 cells, it appears that ^{125}I-HDL, ^{125}I-apoA-I and ^{125}I-rHDL undergo minimal degradation over the incubation period. Less than 2% of protein degradation in cell media was measured as TCA soluble radioactivity over the two hour incubation period (not shown).

A chloroform-methanol organic extraction was performed to separate native HDL into its lipid and apoprotein constituents. The obtained HDL lipids and HDL apoproteins were then used to reconstitute rHDL particles by adding apoA-I and POPC, respectively by co-sonication. The cell association of the two reconstituted particles was assessed following their incubation with HKC-8 cells at 37 °C for up to 2 hours and was compared to that of ^{125}I- native HDL. As seen in Figure 12, compared to ^{125}I- native

HDL, a 5-fold decrease in specific cell association was observed with the ^{125}I-rHDL reconstitued with HDL apoproteins ($p<0.05$). In contrast, specific cell association comparable to that of ^{125}I- native HDL was observed with ^{125}I-rHDL reconstituted with native HDL lipids (Fig. 12).

To elucidate the enhancing effect of HDL lipids on rHDL particle association with HKC-8 cells, new particles were reconstituted by co-sonication method with specific lipids; sphingomyelin (SM), diglyceride (DG), triglyceride (TG), phosphatidyl inositol (PI), cholesteryl linoleate (CE) and free cholesterol (FC). Particles reconstituted with SM, DG, TG, PI and FC showed specific binding equivalent to that of ^{125}I-rHDL containing POPC and pure apoA-I (data not shown). ^{125}I-rHDL reconstituted with cholesteryl linoleate showed a 2-fold increase in specific cell association when compared to that of ^{125}I-rHDL containing no cholesteryl esters, and was about half as effective as ^{125}I- native HDL in associating with HKC-8 cells ($p<0.05$) (Fig. 13). Previous studies have also demonstrated an effect of CE on HDL particles and showed an increase in the negative surface charge and stability of the lipoprotein complexes and an increase in the content of α-helical structures in apoA-I (Braschi *et al.*, 1999). A ^{125}I-rHDL reconstituted with a core containing both cholesteryl linoleate and free cholesterol showed comparable levels of specific cell association to that of ^{125}I-rHDL containing cholesteryl linoleate only, suggesting that free cholesterol had no effect on cell association (not shown).

Extracellular Matrix Association Assay

The *in vivo* EM experiment described previously showed a substantial apoA-I and rHDL enrichment in the basal lamina of renal proximal tubule cells, when localized with a 4H1 anti-apoA-I mAb. This prompted us to analyze the interaction of the ECM with

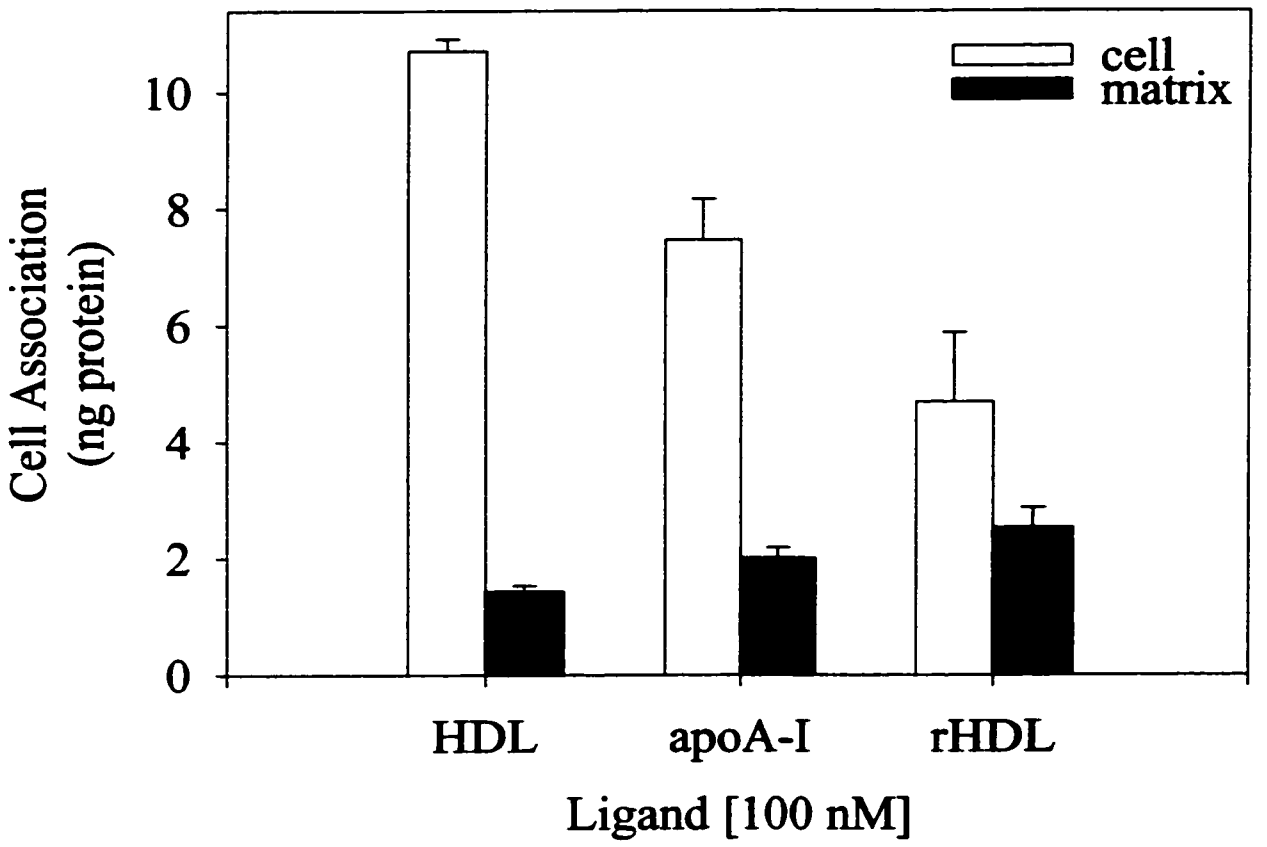
cell
matrix
Cell Association
(ng protein)
10
8
6
4
2
0
HDL
apoA-I
rHDL
Ligand [100 nM]

Figure 8: Association of ^{125}I-ligands with Extracellular matrices (ECM) of HKC-8 cells

HKC-8 cells were cultured in 24-well Falcon plates to confluency in DMEM/F12 supplemented with 10% FBS. Cells were rinsed with serum-free DMEM/F12 prior to the addition of ^{125}I-ligands (100 nM) to the wells. After a 4hr incubation at 37°C, the cells were washed with Ca^{2+}/Mg^{2+} -free PBS and treated with 3mM EDTA for 5 min at 37°C. The cells were removed and the remaining ECM were lysed with 1ml of 0.2M NaOH per well. The lysates were analyzed for associated radioactivity and protein content. The ligands used were ^{125}I-HDL, ^{125}I-apoA-I and ^{125}I-rHDL (POPC). The ^{125}I-rHDL was prepared by co-sonication. See Table 3 for its composition. The data are presented as the mean ± SD of triplicate determinations. (n=1)

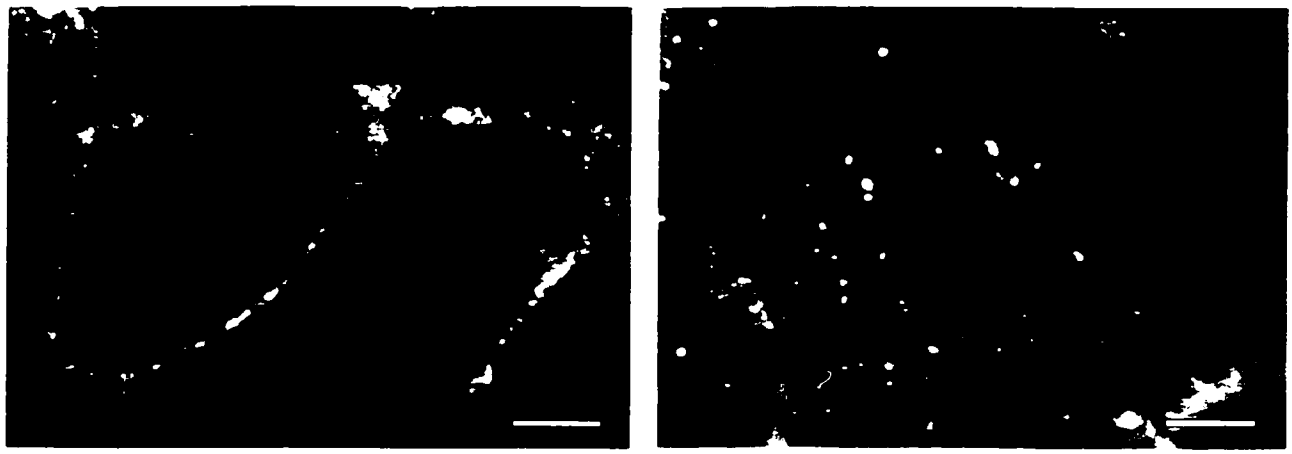

(A) Surface-bound HDL

(B) Internalized HDL

Figure 9: Cy3-HDL is bound and internalized by the HKC-8 cells

(A) HKC-8 cells were incubated with Cy3-labelled HDL particles for 1 hour at 4°C, washed, fixed and viewed on a fluorescent microscope. The labeled lipoprotein was seen associated with the proximal tubule cell surface. Bar = 5 μm
(B) HKC-8 cells were treated as in **(A)**, except for 1 hour at 37°C. Internalization of the labeled lipoprotein was observed, with label seen in vesicles in the perinuclear regions of the cells. Nucleus (**N**). Bar = 5 μm

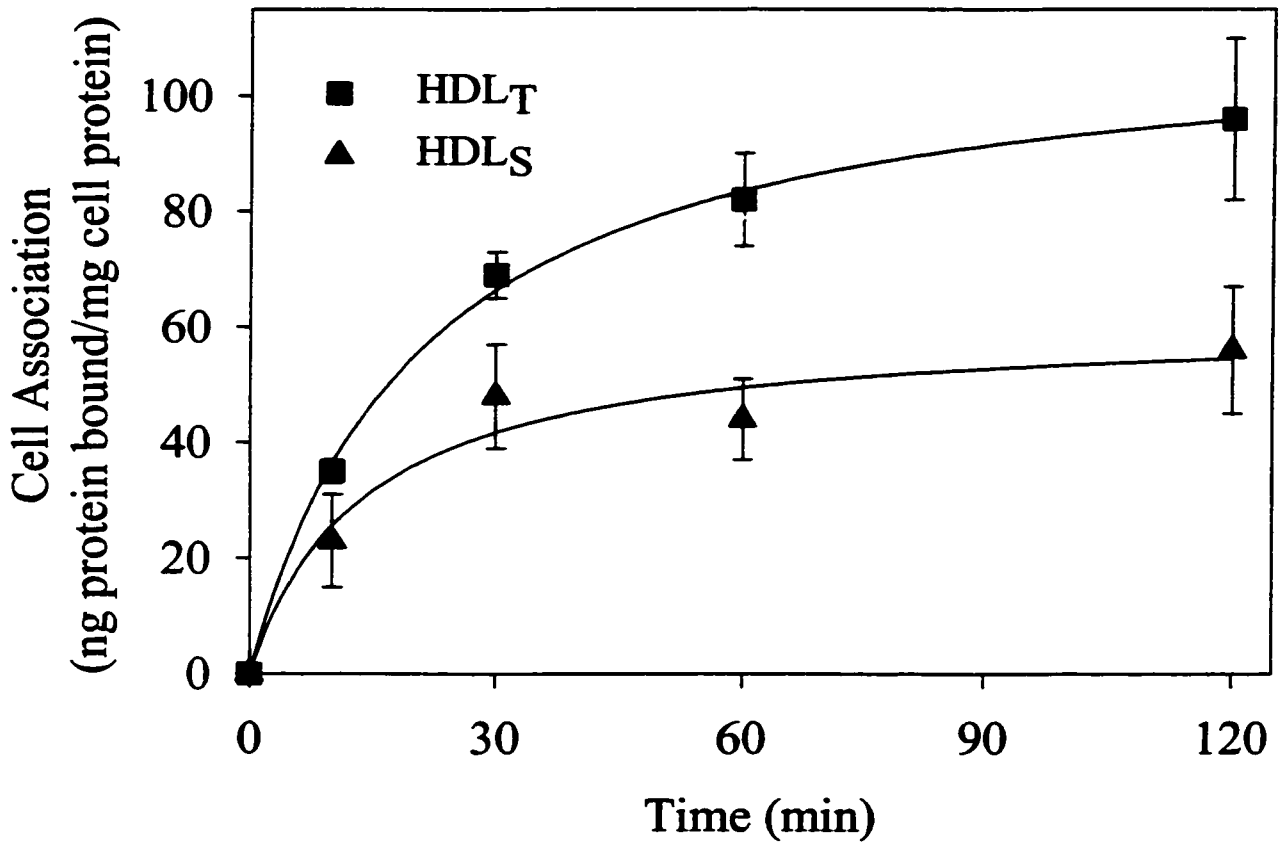
Cell Association
(ng protein bound/mg cell protein)
100
80
60
40
20
0
HDL$_T$
HDL$_S$
0
30
60
90
120
Time (min)

Figure 10: ^{125}I-HDL association increases over time to saturating levels in HKC-8 cells

Total and specific binding of ^{125}I-HDL to HKC-8 cells are derived from cell-associated radioactivity. HKC-8 cells were incubated with 100 nM of ^{125}I-HDL, either alone or in the presence of an excess of unlabelled HDL, at 37°C for various times. Specific association was calculated by subtracting the nonspecific from the total binding. The data are presented as the mean ± SD of triplicate determinations. (n=3)

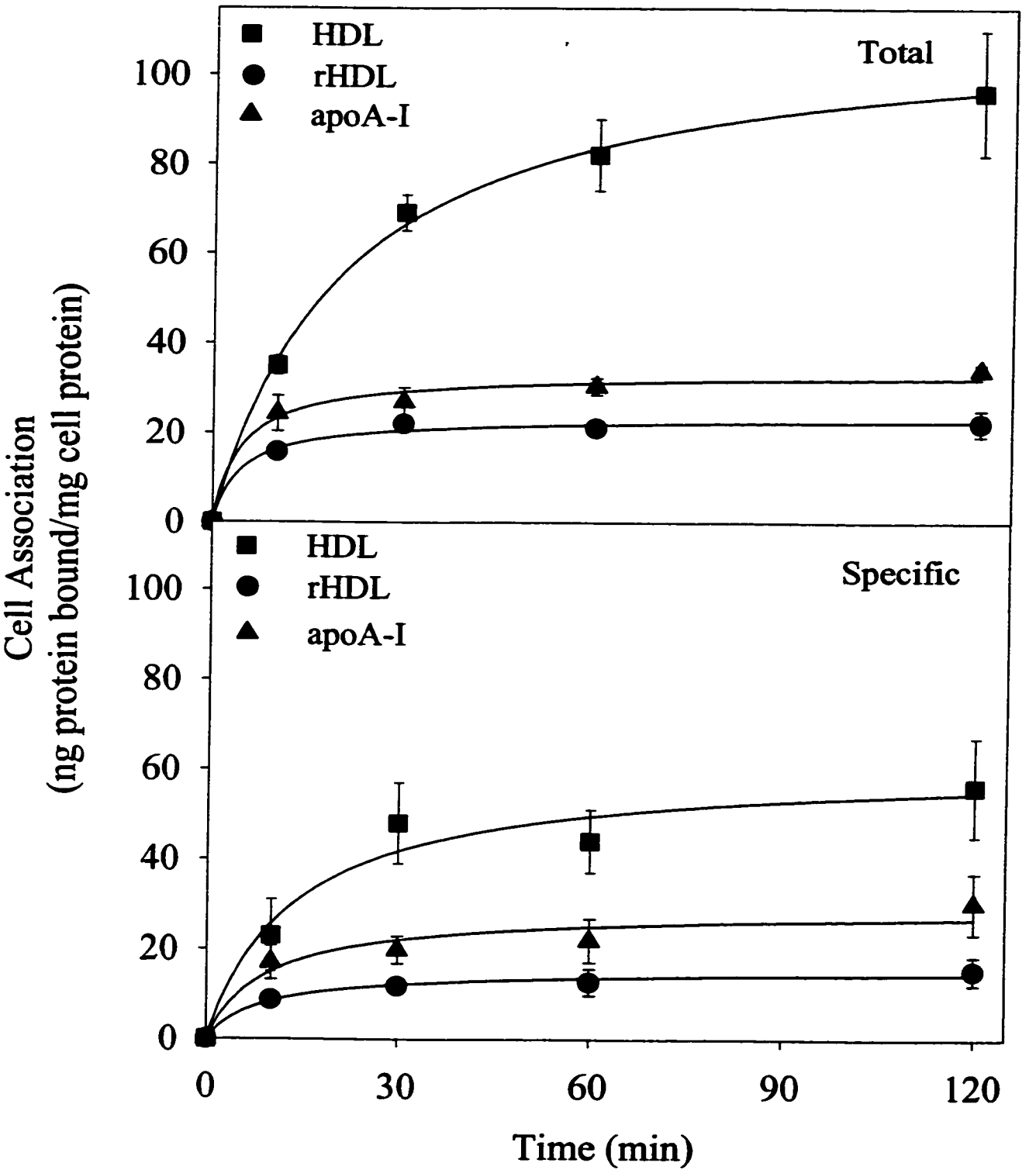
HDL
rHDL
apoA-I
Total
Specific
Cell Association
(ng protein bound/mg cell protein)
Time (min)
0
20
40
60
80
100
0
30
60
90
120

Figure 11: Comparative association of ^{125}I-apoA-I and reconstituted ^{125}I-HDL with HKC-8 cells

Total and specific binding are derived from cell-associated radioactivity. HKC-8 cells were incubated with 100 nM of ^{125}I-apoA-I or ^{125}I-reconstituted HDL particles (rHDL), either alone or in the presence of an excess of unlabelled HDL, at 37°C for various times. Specific association was calculated by subtracting the nonspecific from the total binding. The rHDL particle was prepared by co-sonification of POPC and apoA-I. See Table 3 for particle composition. The data are presented as the mean ± SD of triplicate determinations. (n=3)

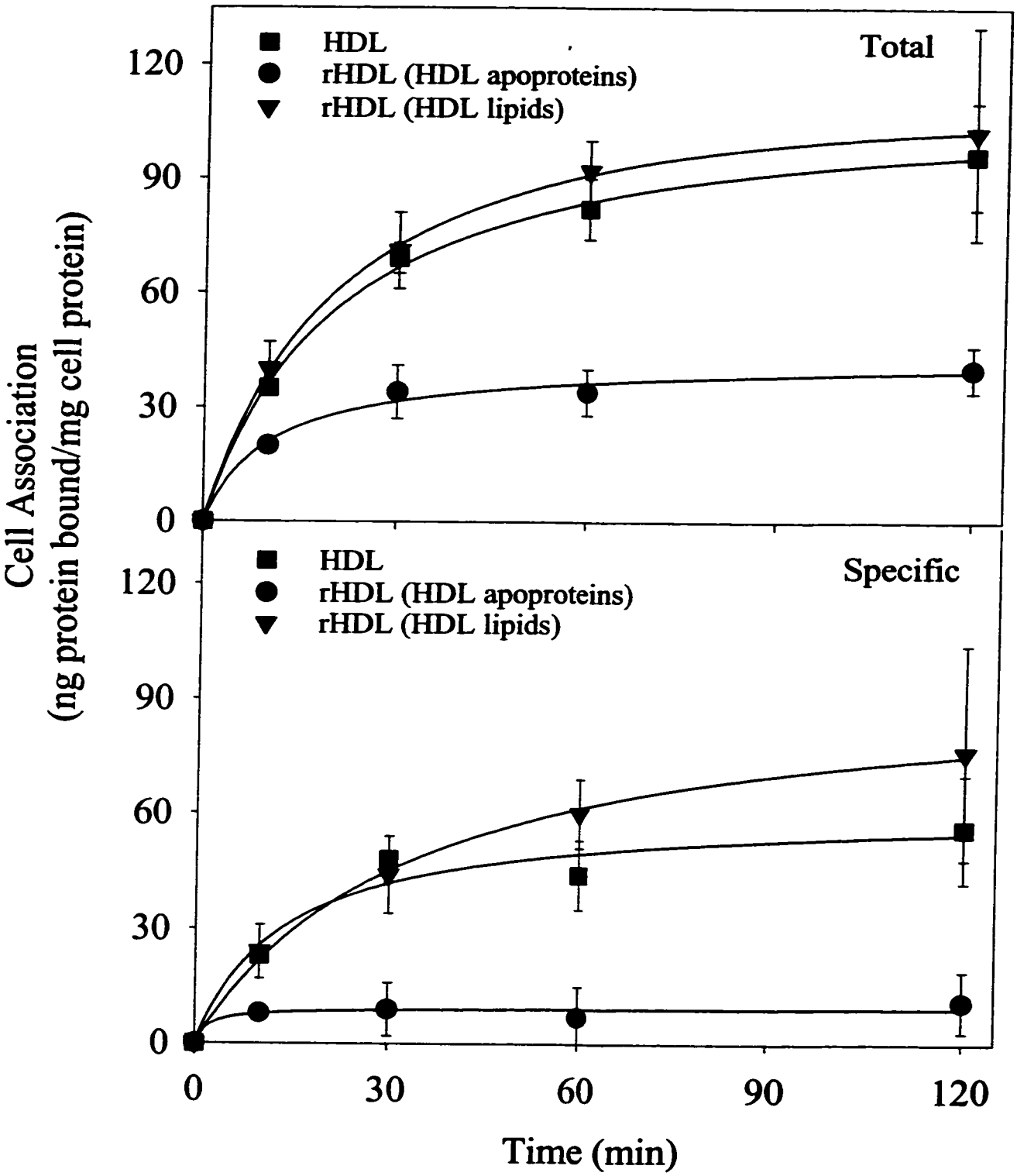
HDL
rHDL (HDL apoproteins)
rHDL (HDL lipids)
Total
Specific
Cell Association
(ng protein bound/mg cell protein)
Time (min)
0
30
60
90
120

Figure 12: HDL lipids, but not apoproteins can rescue cell association with HKC-8 cells to levels comparable to native HDL

Total and specific binding are derived from cell-associated radioactivity. HKC-8 cells were incubated with 100 nM of ^{125}I- native HDL particles or ^{125}I-rHDL particles containing either native HDL apoproteins or native HDL lipids, at 37°C for various times, with or without an excess of unlabelled HDL particles added to the media. Specific binding was calculated by subtracting the nonspecific from the total binding. The rHDL particles (Table 3) were prepared by co-sonification. The data are presented as the mean ± SD of triplicate determinations. (n=3)

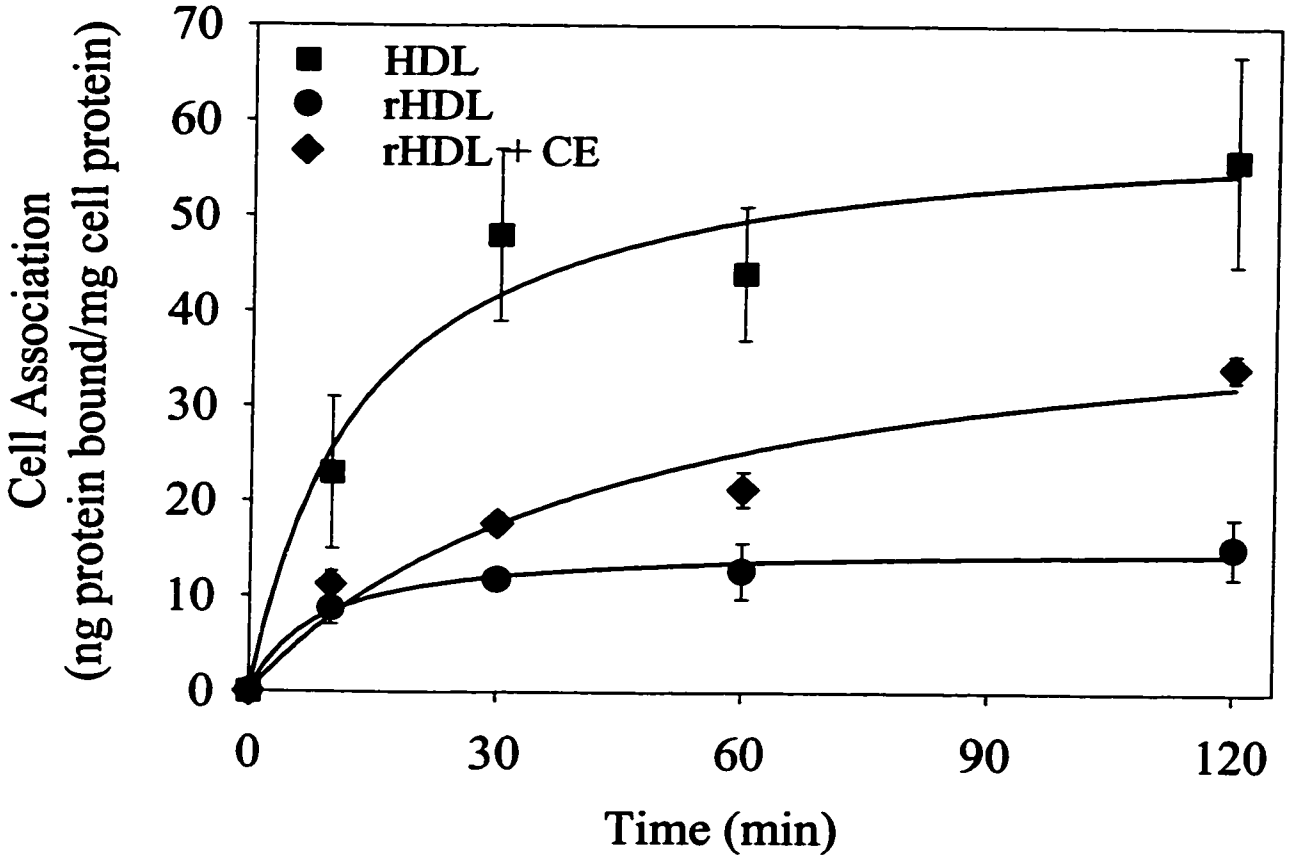
Cell Association
(ng protein bound/mg cell protein)
70
60
50
40
30
20
10
0
HDL
rHDL
rHDL + CE
0
30
60
90
120
Time (min)

Figure 13: Cholesteryl ester enrichment of ^{125}I-rHDL enhances association of these particles with HKC-8 cells

The specific binding is derived from cell-associated radioactivity. HKC-8 cells were incubated with 100 nM of ^{125}I-HDL or ^{125}I-rHDL with or without cholesteryl ester at 37°C up to 2 hours. Specific binding was calculated by subtracting the nonspecific from the total binding. The rHDL particles were prepared by co-sonification. For particle composition see Table 3. The data are presented as the mean ± SD of triplicate determinations. (n=3)

lipoproteins in more detail by performing an *in vitro* analysis of the HKC-8 cell association with ^{125}I-HDL, ^{125}I-apoA-I and ^{125}I-rHDL (POPC). After the HKC-8 cells were incubated for 4 hr at 37°C with the different ^{125}I-ligands, they were washed with Ca^{2+}/Mg^{2+}-free PBS and treated with 3mM EDTA for 5 min at 37°C to isolate the ECM. The cells were then removed and the remaining ECM were solubilized with 0.2M NaOH. The ECM lysates were analyzed for associated radioactivity. From the three ligands studied, ^{125}I-rHDL displayed highest ECM association followed by ^{125}I-apoA-I and ^{125}I-HDL (Fig. 8). An opposite trend was observed for cell association of the ligands, with highest amount of bound ^{125}I-HDL, followed by ^{125}I-apoA-I and ^{125}I-rHDL ($p<0.05$) (Fig. 8). Similar cell association trend was observed in the *in vitro* ligand binding assay done previously (Fig. 11). Differences were observed between the cell- and ECM-associated amounts of each particular ligand. The cell-bound ^{125}I-HDL was 7.5 fold higher than ECM-bound ^{125}I-HDL ($p<0.05$), while the cell-bound ^{125}I-apoA-I was 3.7 fold higher than the ECM-bound ^{125}I-apoA-I ($p<0.05$), and the cell-bound ^{125}I-rHDL was only 1.9 fold higher than that of the ECM-bound ^{125}I-rHDL ($p<0.05$).

III. *In vitro* Experiments with Polarized Cells

Rationale

Epithelial cells protect the underlying vascularized tissues and regulate the macro-molecular and ionic transport into and out of these tissues (Shaw, 1996). The cells are supported on a basement membrane and are attached to each other laterally by cell junctions. An essential feature of these cells is their polarity. In case of absorptive epithelia such as of the intestine or the renal tubule, their luminal (apical) surface is exposed to a fluid filled space while their basal surface is attached to the basement

membrane, above the underlying vascular tissues. The two membranes differ morphologically, functionally and biochemically. While a lot of valuable information may be obtained from studying epithelial cells cultured with conventional (solid surface) *in vitro* techniques, such differences emphasize the importance of studying these cells in a polarized environment, as this would more closely resemble the *in vivo* situation. The focus of this work was to study the processing of HDL by polarized HKC-8 cells grown *in vitro* on transwell tissue-culture inserts.

As previously stated, polarized epithelial cells *in vivo* rest on a basement membrane. This can be recreated *in vitro* by culturing epithelial cells on porous polycarbonate transwell filters. Pre-coating these filters with ECM components such as fibronectin or collagen and establishing the proper media conditions can dramatically alter the morphology of epithelial cells, enabling them to display polarity and reach a well-differentiated state (Shaw, 1996).

Ligand Processing and Degradation Assays

HKC-8 cells were cultured on fibronectin-coated transwell filters as described in the Materials and Methods. To ensure that the trafficking of the HDL ligands can be attributed to active processing by the cells, rather than a passive paracellular movement, [^{14}C]inulin diffusion across the cell monolayer was assessed. Inulin is a small polysaccharide (~ 5 kDa) isolated from dahlia tubers. It is routinely used as a measure of monolayer integrity. Data in Table 5 show that HKC-8 cells cultured on a fibronectin-coated cell culture inserts form a considerable barrier to [^{14}C]inulin diffusion, when compared to inserts without cells ($p<0.05$). The monolayer integrity of the HKC-8 cells is consistent over the 9 hour time course ($p<0.05$) (Fig. 14).

Table 5: [^{14}C]inulin diffusion across a fibronectin-coated transwell in 1 hr

Control[a] (% cpm diffused)	HKC-8 cells (% cpm diffused)
15.8 ± 1.4	1.2 ± 0.08

[a]fibronectin-coated transwell without cells

The results of the ^{125}I-HDL cell association time course at 37°C indicate that ^{125}I-HDL associates with both apical and basolateral cell surfaces. The cell association appears to increase over the first four hours of the time course and gradually levels off thereafter. The ^{125}I-HDL association with the basolateral cell surface is about 2.5 fold higher than with the apical surface of HKC-8 cells ($p<0.05$) (Fig. 15). Similarly, Remaley and colleagues have shown a 3-fold increased association of ^{125}I-HDL with basolateral membranes compared to the apical membranes of MDCK, canine renal cells of a distal tubule / collecting duct origin (Remaley *et al.*, 1998). For ^{125}I-HDL processing studies, 300 μg/ml ^{125}I-HDL was added to one compartment and its appearance was monitored in the opposite compartment over a 9 hour time period. When ^{125}I-HDL was added apically, the highest amount of ^{125}I-HDL on the basolateral side was detected after 6 hours, while somewhat less ligand was detected basolaterally after 9 hours ($p<0.05$) (Fig. 16). In contrast to the non-polarized HKC-8 cells cultured by conventional solid surface techniques, considerable ^{125}I-HDL degradation was detected in polarized cells. A gradually increasing amount of degraded ^{125}I-HDL was seen over time. Maximal degradation was detected after 9 hours of incubation, when all of the apically-added ligand detected on the opposite side was in a degraded form ($p<0.05$) (Fig. 16). When the ^{125}I-HDL (300 μg/ml) was added to the basolateral side, the appearance of the ligand

was monitored apically. The results show a distinct and parallel increase in both, transport and degradation over time ($p<0.05$). All of the ligand processed by the cells appears to be degraded at each time point (Fig. 17). Comparison of ^{125}I-HDL transport at the apical and basolateral membranes indicates that the basolateral membrane can process about 2.5 fold more ^{125}I-HDL than the apical membrane ($p<0.05$) (Figs. 16, 17).

To determine the effects of HDL composition on its processing by polarized HKC-8 cells, ^{125}I-HDL, ^{125}I-apoA-I, ^{125}I-rHDL enriched in CE (rHDL–CE) and ^{125}I-rHDL reconstituted with HDL lipid and pure apoA-I (rHDL-lipid) were compared in a ligand processing and degradation assay over a 9 hour time period. At 9 hours after the apical addition of the various ligands, ^{125}I-apoA-I transport is about 3 fold lower than the transport of ^{125}I-HDL ($p<0.05$). The CE enrichment of ^{125}I-rHDL as well as ^{125}I-rHDL reconstitution with HDL lipid both appear to enhance the transport of the these ligands to that comparable with ^{125}I-HDL (Fig. 18). Similar, although less striking results were seen at all time points (not shown). As seen previously, all of the ^{125}I-HDL transported appears to be degraded. In comparison, the levels of degradation of the other particles are considerably lower than that of ^{125}I-HDL ($p<0.05$). ^{125}I-apoA-I, ^{125}I-rHDL CE and ^{125}I-rHDL-lipid, displaying 33%, 28% and 21% degradation of the transported ligands, respectively (Fig. 18). Overall, the degradation of the apically added ^{125}I-HDL detected after its transport to basolateral compartment, is considerably lower than that of the basolaterally added ^{125}I-HDL ($p<0.05$).

An analysis of processing of different basolaterally added ligands shows that the ^{125}I-apoA-I, ^{125}I-rHDL-CE and ^{125}I-rHDL-lipid transports are 1.5, 1.7 and 2.8 fold lower respectively, than the transport of ^{125}I-HDL (Fig. 19). Since the transport of ^{125}I-apoA-I is

comparable to that of ^{125}I-rHDL-CE, CE enrichment does not appear to have an appreciable effect on HDL transport at the basolateral membrane. Interestingly, the transport of ^{125}I-rHDL-lipid is several fold lower than that of the other particles ($p<0.05$). As seen previously, all of the basolaterally added ^{125}I-HDL appeared to be in a degraded form, when detected on the opposite side. Comparing the other particles, 41%, 67% and 55% of the transported ^{125}I-apoA-I, ^{125}I-rHDL-CE and ^{125}I-rHDL-lipid respectively, were degraded ($p<0.05$) (Fig. 19).

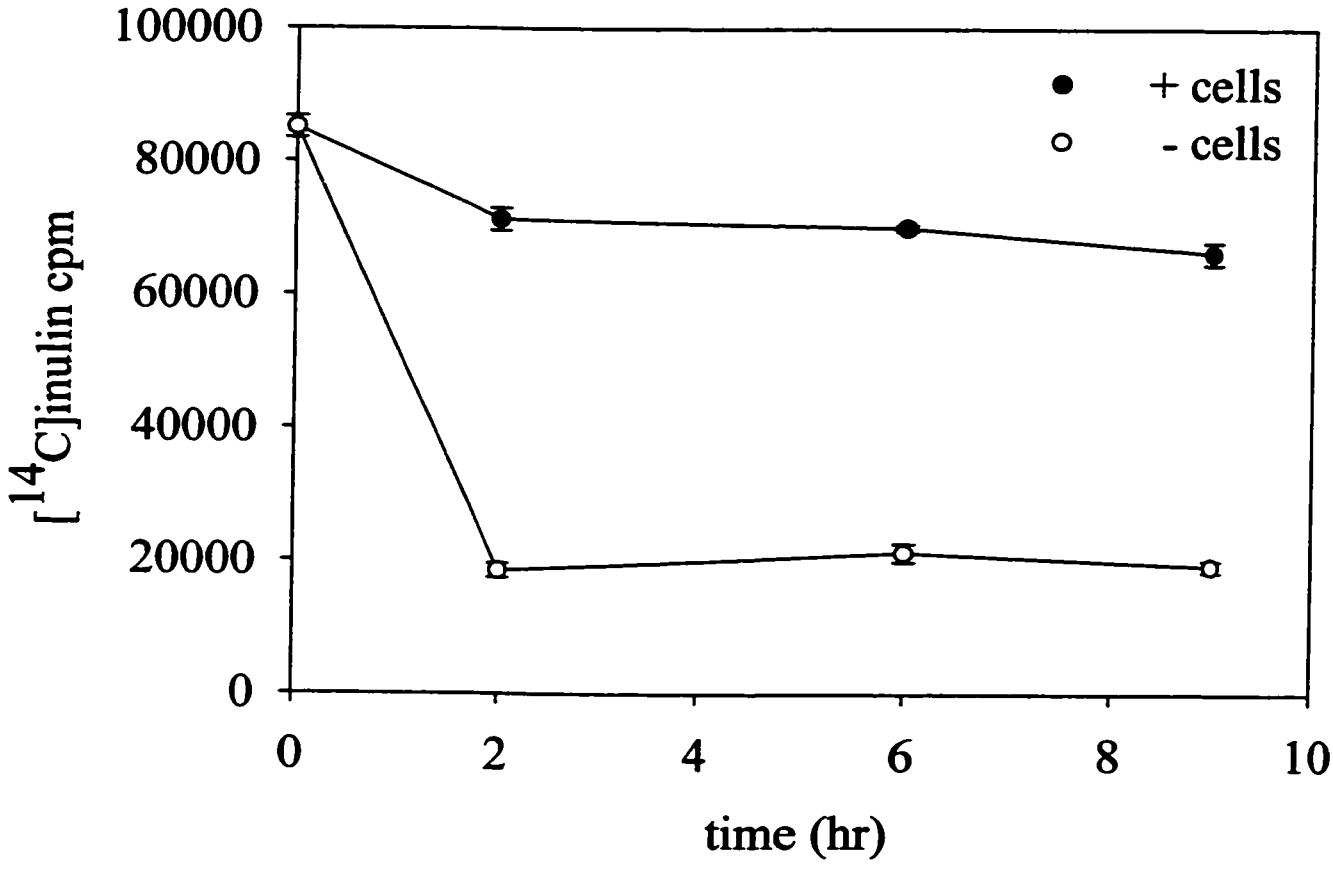
100000
80000
60000
40000
20000
0
[14C]inulin cpm
0
2
4
6
8
10
time (hr)
+ cells
- cells

Figure 14: An Assessment of permeability of polarized HKC-8 cells to [^{14}C]inulin

HKC-8 cells cultured on fibronectin-coated cell culture inserts were incubated with [^{14}C]-inulin in serum-free DMEM/F12 media at 37°C for various times. The [^{14}C]-inulin remaining in the apical compartment at each timepoint was detected in the media by scintillation counting. Fibronectin-coated inserts without cells served as controls at each timepoint. The data are presented as the mean ± SD of triplicate determinations. (n=2)

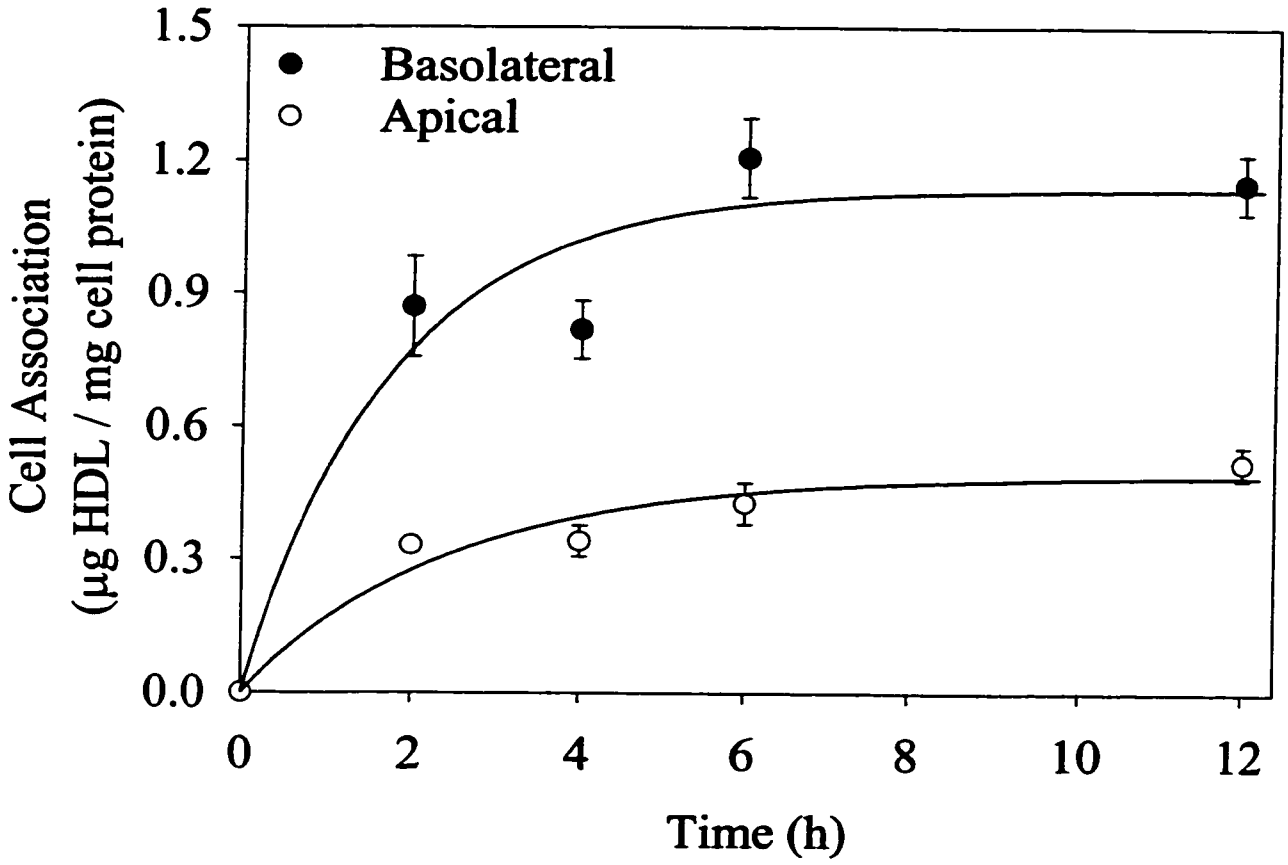
Basolateral
Apical
Cell Association
(µg HDL / mg cell protein)
1.5
1.2
0.9
0.6
0.3
0.0
0
2
4
6
8
10
12
Time (h)

Figure 15: ^{125}I-HDL association with polarized HKC-8 cells

HKC-8 cells cultured on fibronectin-coated transwell tissue-culture inserts were incubated with ^{125}I-HDL in serum-free DMEM/F12 media at 37°C for various times. ^{125}I-HDL was added either to the apical or the basolateral compartment. The total HDL concentration per well was 300 μg/ml. Following incubations, the medium was removed and cells were rinsed with PBS-BSA and PBS prior to lysis in 0.2M NaOH. The lysates were counted to determine total cell associated radioactivity and assessed for protein content by a BCA assay. The data are presented as the mean ± SD of triplicate determinations. (n=2)

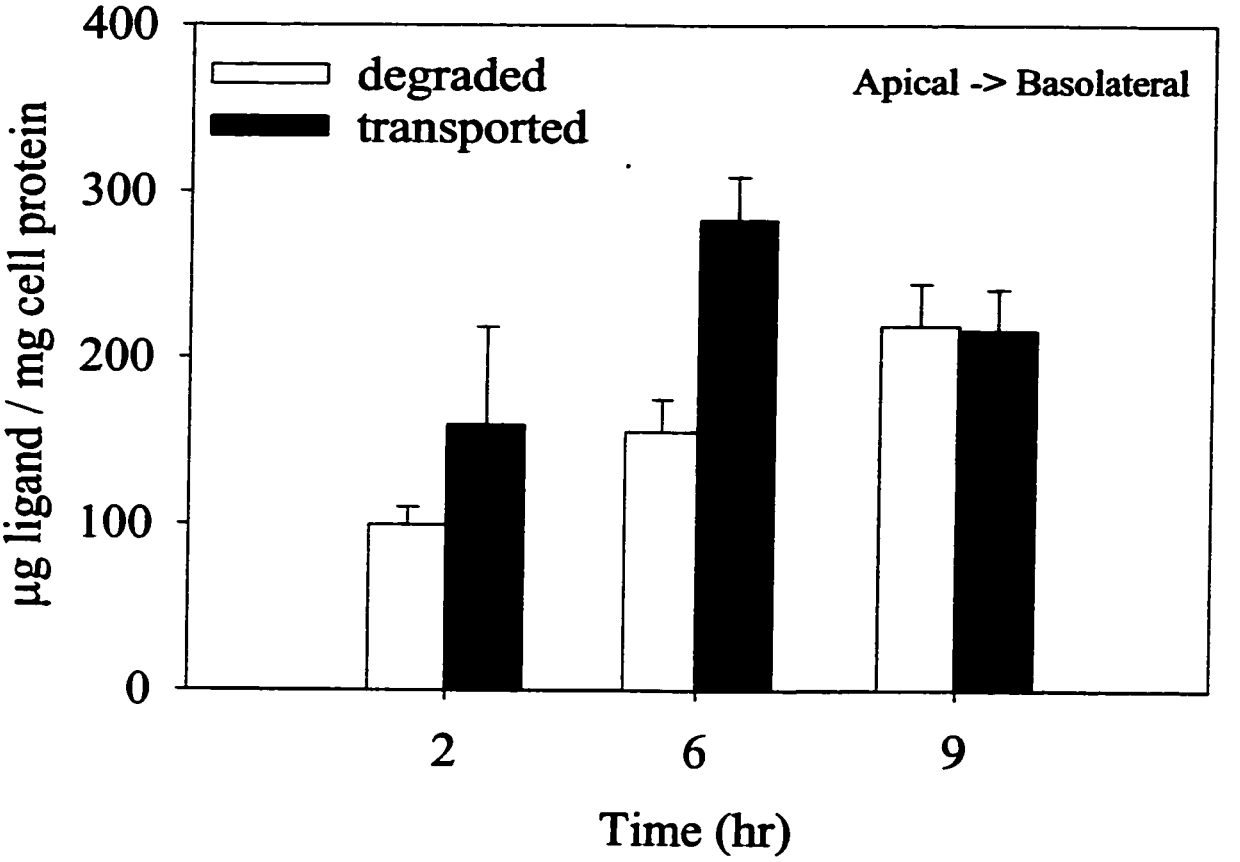
400
300
200
100
0
µg ligand / mg cell protein
degraded
transported
Apical -> Basolateral
2
6
9
Time (hr)

Figure 16: Apical to basolateral (A -> B) transport and degradation of ^{125}I-HDL in polarized HKC-8 cells

HKC-8 cells cultured on fibronectin-coated transwell tissue-culture inserts were incubated with ^{125}I-HDL in serum-free DMEM/F12 media at 37°C in a time-course up to 9 hr. 0.5 ml ^{125}I-HDL was added to the apical transwell compartment and 1.5 ml ligand-free media were added to the opposite basolateral compartment. The total HDL concentration per well was 300 μg/ml. Following incubations, the medium was removed from both compartments and counted to determine total radioactivity per compartment. An aliquot of the media at each timepoint was analyzed for degradation products by precipitation in 25% TCA. The data are presented as the mean ± SD of triplicate determinations. (n=1)

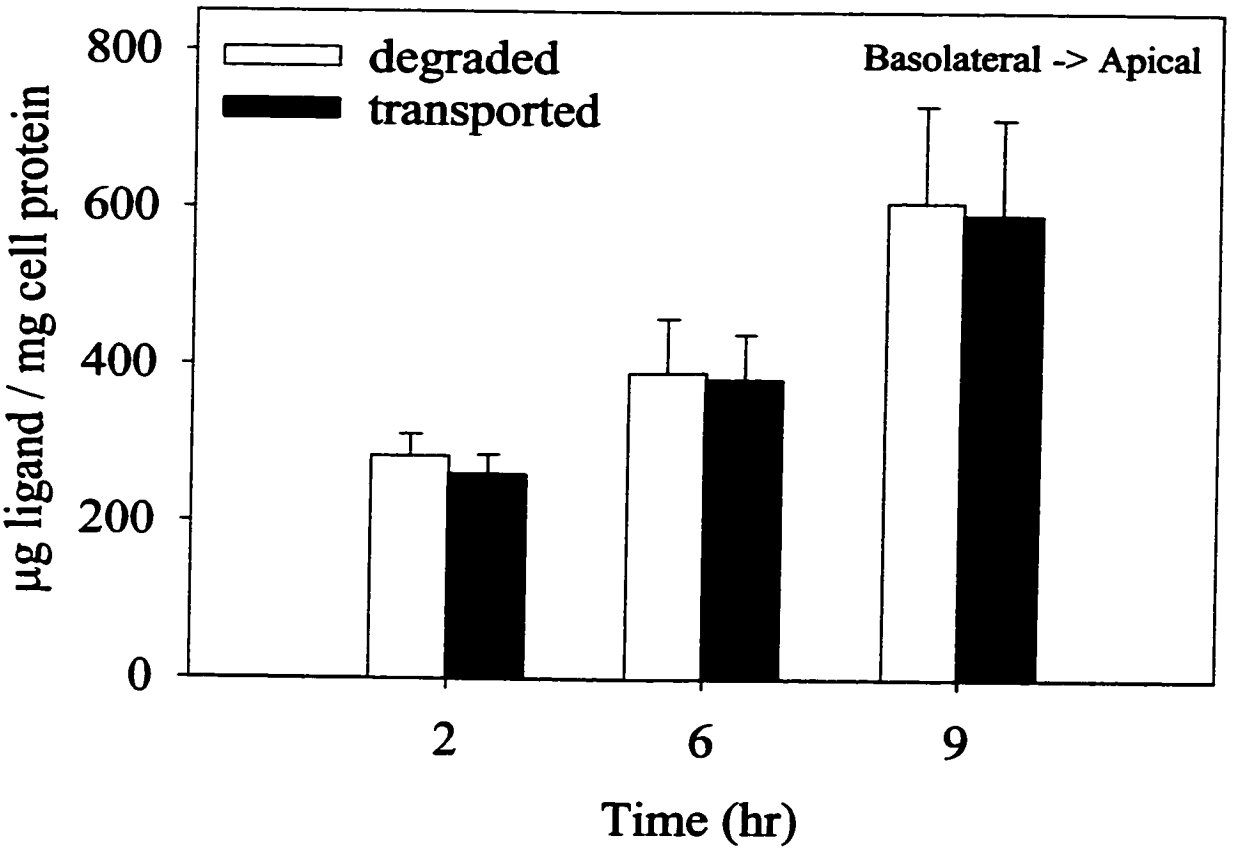
800
600
400
200
0
degraded
transported
Basolateral -> Apical
µg ligand / mg cell protein
2
6
9
Time (hr)

Figure 17: Basolateral to apical (B -> A) transport and degradation of ^{125}I-HDL in polarized HKC-8 cells

HKC-8 cells cultured on fibronectin-coated transwell tissue-culture inserts were incubated with ^{125}I-HDL in serum-free DMEM/F12 media at 37°C in a time-course up to 9 hr. 1.5 ml ^{125}I-HDL was added to the basolateral transwell compartment and 0.5 ml ligand-free media were added to the opposite apical compartment. The total HDL concentration per well was 300 μg/ml. Following incubations, the medium was removed from both compartments and counted to determine total radioactivity per compartment. An aliquot of the media per each timepoint was analyzed for degradation products by precipitation in 25% TCA. The data are presented as the mean ± SD of triplicate determinations. (n=1)

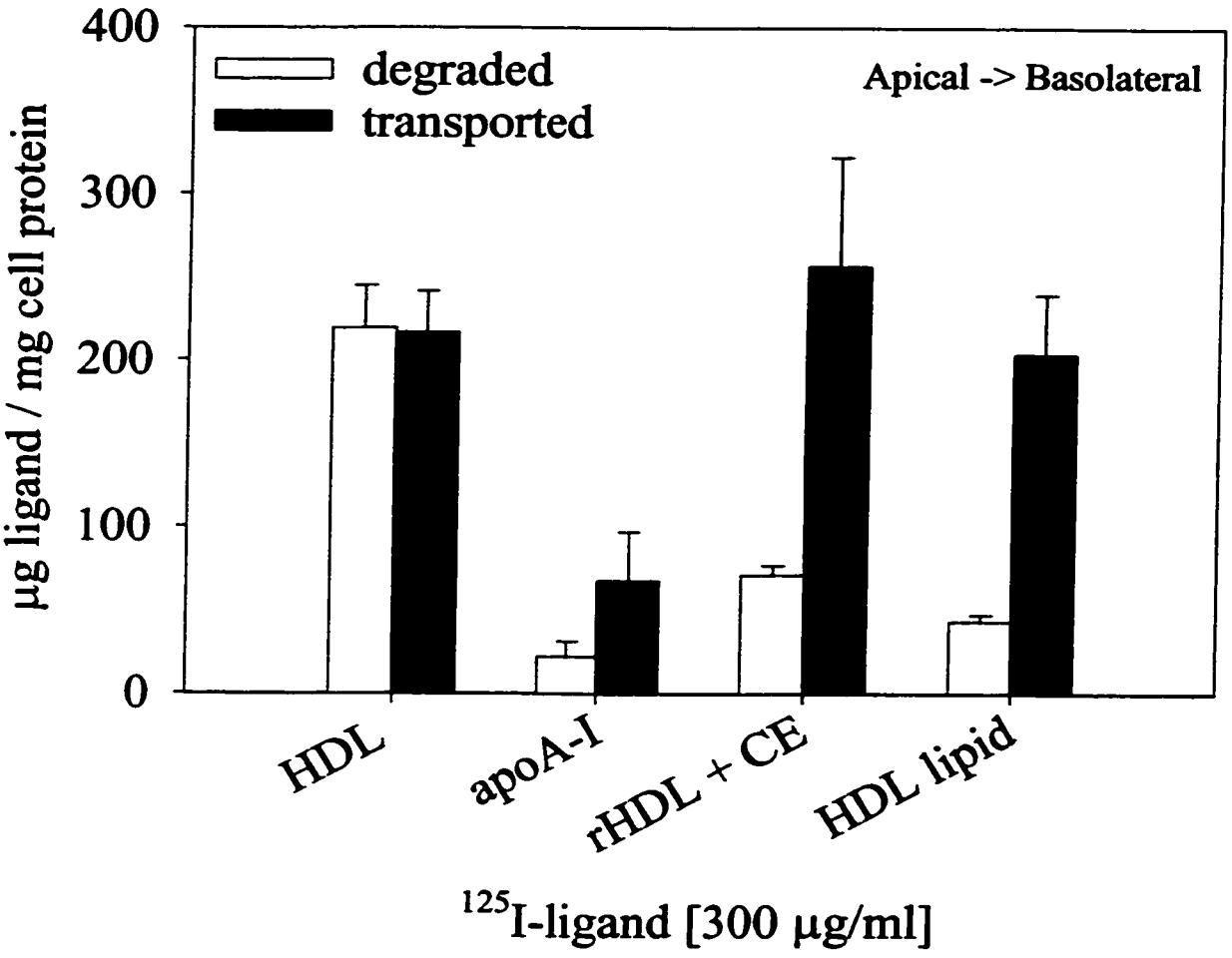
400
300
200
100
0
µg ligand / mg cell protein
degraded
transported
Apical -> Basolateral
HDL
apoA-I
rHDL + CE
HDL lipid
125I-ligand [300 µg/ml]

Figure 18: Comparative analysis of apical to basolateral (A -> B) transport and degradation of various ^{125}I-ligands in polarized HKC-8 cells

HKC-8 cells cultured on fibronectin-coated transwell tissue-culture inserts were incubated with ^{125}I-ligands in serum-free DMEM/F12 media at 37°C in a time-course up to 9 hr. 0.5 ml ^{125}I-ligands were added to the apical transwell compartment and 1.5 ml ligand-free media were added to the opposite basolateral compartment. The total ligand concentration per well was 300 μg/ml. Following incubations, the medium was removed from both compartments and counted to determine total radioactivity per compartment. An aliquot of the media at each timepoint was analyzed for degradation products by precipitation in 25% TCA. The data are presented as the mean ± SD of triplicate determinations. The ligands added were ^{125}I-HDL, ^{125}I-apoA-I, ^{125}I-rHDL-CE and ^{125}I-rHDL-lipid. (n=1)

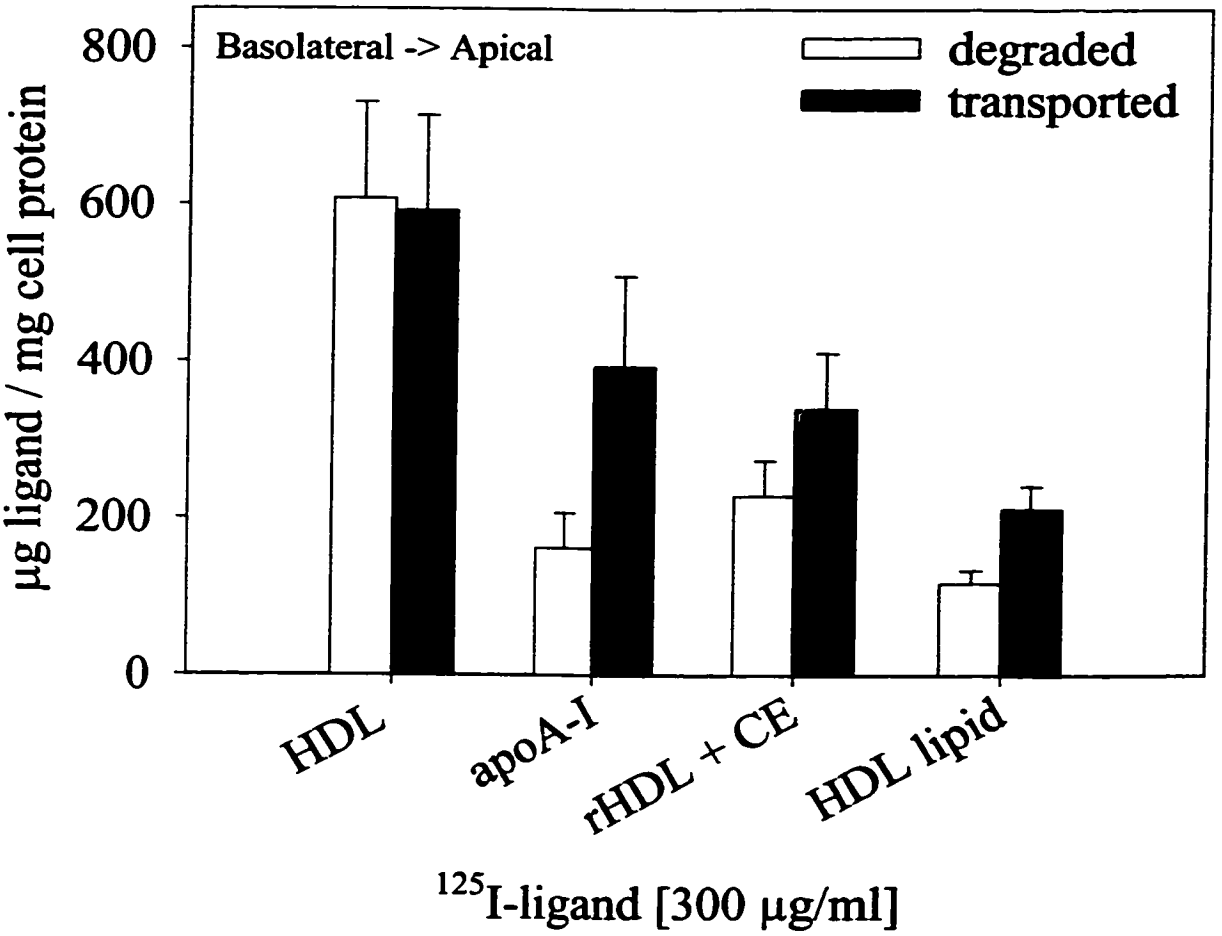
Basolateral -> Apical
degraded
transported
800
600
400
200
0
µg ligand / mg cell protein
HDL
apoA-I
rHDL + CE
HDL lipid
125I-ligand [300 µg/ml]

Figure 19: Comparative analysis of basolateral to apical (B -> A) transport and degradation of various ^{125}I-ligands in polarized HKC-8 cells

HKC-8 cells cultured on fibronectin-coated transwell tissue-culture inserts were incubated with ^{125}I-ligands in serum-free DMEM/F12 media at 37°C in a time-course up to 9 hr. 1.5 ml ^{125}I-ligands were added to the basolateral transwell compartment and 0.5 ml ligand-free media were added to the opposite apical compartment. The total ligand concentration per well was 300 μg/ml. Following incubations, the medium was removed from both compartments and counted to determine total radioactivity per compartment. An aliquot of the media per each timepoint was analyzed for degradation products by precipitation in 25% TCA. The data are presented as the mean ± SD of triplicate determinations. The ligands added were ^{125}I-HDL, ^{125}I-apoA-I, ^{125}I-rHDL-CE and ^{125}I-rHDL-lipid. (n=1)

Chapter 4: Discussion

The objective of this investigation was to attempt to evaluate the role of the kidney in HDL metabolism. First, we explored the specific cellular sites of HDL metabolism in the kidney and re-evaluated the transport of HDL particles through this organ *in vivo*. Then we characterised the parameters that regulate the renal processing of HDL particles by measuring the binding, uptake and degradation of HDL particles by the proximal tubule cells of the renal cortex *in vitro*.

I. *In vivo* Studies

While a number of studies support the view that labeled HDL apolipoproteins can be filtered by the kidney glomerulus and can be found in the kidney cortex, some work suggests that besides filtration and reabsorption of apoA-I, the kidneys are capable of processing small HDL molecules as well (Segal *et al.*, 1979; Peterson *et al.*, 1984). The amount of lipid following the apolipoprotein into the glomerular filtrate remains elusive. Our results from the rabbit kidney perfusion with the double-labeled HDL ligand suggest that while the majority of the ligand recovered in the renal cortex represents ^{125}I protein (31.6%), the rabbit kidneys are capable of processing HDL holoparticles, as 12.9% of the total [^{3}H]CE content of the ligand was also recovered in the renal cortex. The neutral lipid (CE) is the core constituent of the HDL particles, while apoA-I represents the principal protein constituent of HDL (Ginsberg, 1998). Therefore, the data of ^{125}I-protein recovery in the kidneys in the current study appear to be in agreement with the literature, showing that the kidneys are responsible for a significant uptake of ^{125}I-apoA-I from the blood (Glass *et al.*, 1983; Glass *et al.*, 1985; Woollett and Spady,

1997; Spady *et al.*, 1998; Wang *et al.*, 1998). However, Glass and coworkers also demonstrated that while the kidneys accounted for 39% of the total ^{125}I-HDL-apoA-I uptake, only 1% of the total HDL-derived [^{3}H]CE was taken up by the kidneys (Glass *et al.*, 1983). Our findings show a more substantial renal uptake of 12.9% of the total [^{3}H]CE content of the perfused HDL. A possible explanation for this finding may come from the difference in the ligand perfusion. While Glass and colleagues have used an intra-venous perfusion of their HDL ligand to study the tissue-specific uptake of HDL constituents, in our study the renal arteries were directly perfused to study specifically the renal uptake of HDL. The capacity of the kidneys to process whole HDL particles may be obscured in experiments using intra-venous perfusions, as the ligand may undergo extensive remodelling in the blood before it reaches the renal circulation. For example, lipolysis of TG-rich HDL holoparticles destabilizes the particles and promotes the dissociation of the apoA-I from such particles (Horowitz *et al.*, 1993). Thus a direct perfusion of the renal arteries may be more indicative of the capacity of the kidneys to process HDL holoparticles. In addition, to minimize the possibility that the higher renal uptake of the HDL-derived neutral lipid could be attributed to the ligand left behind in the renal vasculature after the perfusion, the renal arteries were flushed with sterile saline (1ml for 30 sec) immediately following the perfused ligand.

In consideration of the permselectivity properties of the kidney glomerulus, the filtration of smaller HDL holoparticles may theoretically take place. Glomerular permselectivity to macromolecules is a function of the charge, size and shape properties of the macromolecule (Luke, 1984). Based on these selective properties, in normal conditions the glomerular filtration barrier could hinder the passage of molecules larger

than 10nm in diameter, anionic-charged and of a rigid-sphere conformation (Myers, 1989; Junqueira *et al.*, 1998; Tisher and Madsen, 2000). Other factors, such as hemodynamic influences have also been shown to play a role as a determinant of macromolecule filtration. Increases in blood pressure, blood flow or volume may increase the filtration fraction and result in a higher sieving coefficient for macromolecules with usually lower filtration rates (Myers, 1989). It is the interplay of these factors however, that ultimately determines glomerular permselectivity of a particular macromolecule. For example, while apoA-I, the major protein constituent of HDL displays a surface potential of -8.3mV as determined from its electrophoretic mobility on agarose (Braschi *et al.*, 1999), it also undergoes glomerular filtration (Saku *et al.*, 1984) and is found in the rat renal cortex (Glass *et al.*, 1983) as well as in the urine of normo-lipidemic human subjects (Segal *et al.*, 1979; Gomo and Henderson, 1988). While the anionic surface potential of apoA-I does not appear to make it an ideal candidate for renal filtration, it is of a small size of 28 kDa (Ginsberg *et al.*, 1998). In addition, plasma apoA-I is rarely found in a completely lipid-free state (Scanu *et al.*, 1980), and is more often seen as a part of a small discoidal complex with phospholipid (Swaney, 1980), which theoretically conforms to the shape selectivity of the glomerular filtration barrier. Moreover, previous experiments in our laboratory have shown that discoidal HDL has an increased rate of clearance from rabbit plasma (Braschi *et al.*, 1999). While all reconstituted apoA-I/HDL particles were negatively charged, a decrease in the particle negative surface charge correlated with an increased rate of clearance of the particles (Braschi *et al.*, 1999). In another study, Braschi and coworkers have characterized the clearance of apoA-I and reconstituted HDL particles in rabbits after a unilateral nephrectomy and have shown that

the kidney was responsible for much of HDL clearance in the rabbits (Braschi *et al.*, 2000). Taken together, the findings suggest that the glomerular filtration barrier may be more lenient to anionic macromolecules than was previously thought possible, and that it is capable of clearing less electronegatively charged HDL particles if they conform to the size- and shape-selective properties of the barrier.

The results of the immunoelectron microscopic study of the kidney cortex tissues after perfusion of the rabbit renal artery with apoA-I or rHDL particles show that upon filtration, the filtered ligand is re-absorbed from the tubular lumen by the PCT cells of the renal cortex. Both perfused apoA-I and rHDL particles were immunolocalized throughout the apical regions of the proximal tubule epithelial cells with the 5F6 mAb, with some labeling also observed at the apical brush border. The epitope for this mAb resides in the central domain (residues 118-121) of apoA-I (Collet *et al.*, 1991). Our findings confirm the observations of Glass and colleagues who have similarly demonstrated the presence of the perfused ^{125}I-TC-apoA-I in the frozen sections of rat kidney in the apical regions of the PCT cells by immunofluorescence microscopy (Glass, *et al.*, 1983). In contrast, using the 4H1 mAb, both perfused ligands were localized only within the basolateral, tubular membrane. The epitope for mAb 4H1 is located in the N-terminus (residues 2-8) of apoA-I (Collet *et al.*, 1991). Previous studies have shown that the immunoreactivity of this mAb is greatly increased when apoA-I is fragmented or partly degraded (unpublished observation). Thus the finding suggests that apoA-I fragments may preferentially accumulate within the basement membrane of the PCT cells following degradation. Catabolism of apoA-I and HDL has been shown to be the consequence of renal clearance in nephron microperfusion studies (Peterson *et al.*, 1984).

Such degradation products could then be delivered back into the circulation. The tubular basement membrane separates the PCT cells from the underlying peritubular capillaries (Zamboni, 1989) and also represents a transport interface between the PCT cells and the underlying blood vessels (Shaw, 1996).

The finding that no significant amount of apoA-I was identified within glomerular structures suggests that the filtered ligands do not accumulate in the glomerulus and are rapidly delivered into the tubular lumen for reabsorbtion by the PCT cells. Experiments show that some molecules such as cationic immunoglobulin G can penetrate into but not beyond the glomerular basement membrane, resulting in its accumulation in this subepithelial area, ultimately leading to the formation of immune complexes characteristic of membranous glomerulopathy (Myers, 1989).

In summary, the *in vivo* data clearly demonstrate the delivery of both protein and lipid components of HDL particles into the rabbit renal cortex, suggesting that the rabbit kidneys are involved in the filtration of lipid-free apoA-I and of small, whole HDL particles. Furthermore, the cells of the renal cortex appear to be capable of luminal uptake of the ligands, and of a subsequent delivery of the ligands to the basement membrane where they could be available for re-entry into the circulation.

II. *In vitro* Studies

While our *in vivo* data provide evidence for processing of HDL by the kidneys, they do not provide details about the mechanisms involved in such processing. For this purpose, *in vitro* experiments utilizing the HKC-8 human proximal tubule cell line were performed. The fluorescent study of binding and uptake of HDL to HKC-8 cells showed

that at 4°C, HDL associated with the HKC-8 cell surface but was not internalized. The exact nature of this association was unknown, as it may have represented both, specific binding to receptors or non-specific cell surface association. After the incubation with the fluorescently-labeled HDL, the cells were washed with a BSA-containing buffer to minimize non-specific binding. An incubation of HKC-8 cells at 37°C led to the internalization of the HDL ligand. It was localized in vesicles in the perinuclear regions of the cells. In their studies, Peterson *et al.* have interpreted the vesicles that accumulated ^{125}I-HDL upon perfusion as apical endocytic vesicles, vacuoles and lysosome-like dense bodies, clearly all components of the endocytic apparatus of the proximal tubule cells (Peterson *et al.*, 1984). The HKC-8 cells, which display a number of features characteristic of the PCT cells *in vivo* (Racusen *et al.*, 1997), were shown to be ideal for our studies as they were of human origin and were capable of both, binding and internalization of HDL.

The data obtained from the competitive binding assays of ^{125}I-HDL to HKC-8 cells showed that the cells can efficiently associate with ^{125}I-HDL, as witnessed by the saturable and high specific binding component of the total ^{125}I-HDL cell association. Several laboratories have demonstrated ^{125}I-HDL binding to the membranes of the renal cortex in various species, including those of rat, porcine and human origin (van Tol *et al.*, 1986; Senault *et al.*, 1994; Kozyraki *et al.*, 1999). The findings in these studies differ enough to suggest that more than one HDL-binding receptor may be present in the kidneys. Van Tol and colleagues have identified a low-affinity non-saturating and a high-affinity saturating rat HDL binding to partially purified rat kidney membranes or kidney homogenates. They have further shown that these associations did not require apoE and

were pronase and EDTA insensitive. Therefore, their binding did not require Ca^{2+} ions, differed from the LDL binding to the apoB-E receptor on hepatocytes and involved both HDL_2 and HDL_3 binding to the same site. Furthermore, the inability of unlabeled LDL to compete with the binding of ^{125}I-HDL suggested that the interaction was not of a lipid-lipid type. Finally, the binding appeared to be species specific, as unlabeled human HDL presented a poor competitor for the observed association (van Tol *et al.*, 1986). Senault and coworkers have in their studies described a two-component association of porcine ^{125}I-HDL to basolateral membranes of the porcine renal cortex; a high-affinity, lower capacity and a low-affinity, higher capacity interaction. By ligand blotting, they have isolated a 95 kDa membrane protein which was responsible for the high-affinity, low capacity interaction with ^{125}I-HDL. The interaction had a high degree of specificity to apoA-I and was apoE independent. Furthermore, the authors have suggested that their low-affinity, higher capacity binding component involved a non-specific lipid-lipid interaction with the membrane, as the interaction was not species specific and was out-competed by an excess of unlabeled LDL. The LDL did not bind to the 95 kDa protein (Senault *et al.*, 1994). Kozyraki *et al.* have demonstrated by plasmon resonance and cell uptake studies a high-affinity binding of human ^{125}I-HDL to cubilin, a 460 kDa receptor purified from the human as well as the rabbit renal cortex. The interaction was Ca^{2+} ion dependent, apoE independent and required apoA-I, as anti-apoA-I antibodies strongly inhibited HDL uptake (Kozyraki *et al.*, 1999). Furthermore, cubilin was localized exclusively in the apical membranes of the renal cortex (Sahali *et al.*, 1992). Cellular uptake studies of fluorescent phospholipid-labeled HDL or ^{125}I-HDL showed that HDL underwent cubilin-mediated endocytosis, leading to its delivery to lysosomes (Hammad

et al., 1999; Kozyraki *et al.*, 1999). The saturable and high specific binding of ^{125}I-HDL (at a low concentration of 100 nM) to HKC-8 cells observed in our competitive assay cannot be attributed to one particular receptor, and may be the result of any of the higher-affinity specific interactions described in the above-mentioned studies. There is a strong possibility that our specific HDL association may be the result of its binding to cubilin, as the binding was saturable and the HDL was localized in endocytic-like vesicles upon internalization by the HKC-8 cells. The studies by van Tol *et al.* and Senault *et al.* did not provide any evidence for endocytic-like HDL processing. The possibility that HDL undergoes endocytic processing after the interactions described in their studies still remains open. Furthermore, the results of our HDL processing studies in polarized HKC-8 cells (discussed later) suggest that more than one pathway may be responsible for HDL trafficking in the PCT cells of the renal cortex.

In our laboratory we have previously demonstrated that the lipid composition of HDL can greatly affect the charge and conformation of apoA-I, which along with the lipoprotein surface lipid composition can determine the overall surface charge of HDL (Sparks *et al.*, 1995; Braschi *et al.*, 1999). In conjunction with the previously described effect of the HDL surface charge on the plasma clearance of this lipoprotein (Braschi *et al.*, 1999), and with the importance of the kidneys in the HDL clearance *in vivo* (Braschi *et al.*, 2000), the data suggest that HDL composition may regulate the renal handling of this lipoprotein. In order to evaluate the effects of lipid composition of HDL on its association with HKC-8 cells, the association of reconstituted HDL particles with a varied lipid composition was evaluated in these cells. Poor association of lipid-free ^{125}I-apoA-I in comparison with that of the ^{125}I- native HDL was observed in our experiments.

Pure ^{125}I-apoA-I has also been shown to compete less effectively for HDL binding sites than ^{125}I-HDL$_3$ in human enterocytes (Sviridov *et al.*, 1988). Enterocytes are small intestine epithelial cells that display numerous structural and functional similarities to renal epithelia (Shaw, 1996). The addition of phospholipids to apoA-I (rHDL) also did not have a marked effect on the association with the HKC-8 cells, in fact its association with the cells was somewhat less efficient in comparison with lipid-free ^{125}I-apoA-I. These findings suggest that the factors required to promote the high specific binding and uptake by the cells seen with ^{125}I- native HDL are absent with the apoA-I alone or the rHDL particle. The factors may represent other apolipoprotein- or lipid- constituents of HDL which are missing in these particles. In order to determine if it is the lipid or the protein moiety that could enhance the HDL particle association with the HKC-8 cells, native HDL was subjected to an organic extraction to separate the HDL apolipoproteins from the HDL lipids, followed by a reconstitution with pure POPC and apoA-I respectively. The native HDL lipid containing particle displayed an enhanced specific cell-association comparable to that of the ^{125}I- native HDL, while the native HDL apolipoprotein containing particle displayed a 5-fold lower cell-association in comparison with the ^{125}I- native HDL. These results demonstrate that the HDL lipid composition plays an important role in the association of this lipoprotein with the HKC-8 renal PCT cells.

While apoA-I may be important for the initial association of HDL with the HDL receptors (Fidge, 1999), the HDL lipid composition may be important in determining the affinity of this interaction by markedly affecting the apoA-I conformation. Numerous studies show that HDL lipid composition has major effects on the conformation of apoA-

I and the stability and charge of the apoA-I containing HDL particle (Bergeron *et al.*, 1995; Sparks *et al.*, 1992a; Sparks *et al.*, 1992b; Calabresi *et al.*, 1993). Reconstitution of rHDL particles with specific lipids; DG, TG, SM, PI and FC did not enhance ^{125}I-rHDL association with the cells. These particles associated poorly, at levels comparable to the control ^{125}I-rHDL (POPC). In contrast, half of the specific binding obtained with the ^{125}I-native HDL was recovered by the addition of CE into the core of the rHDL particle. CE has been shown to exert major effects on HDL particles by increasing the content of α-helical structures in apoA-I resulting in an increase in the stability and negative surface charge of HDL (Braschi *et al.*, 1999). The increased stability of HDL has been shown to be associated with a decreased plasma clearance of this lipoprotein (Braschi *et al.*, 1999). *In vivo*, HDL_2 and HDL_3 represent CE-enriched HDL subfractions (Table 2). If the plasma levels of CE-enriched HDL holoparticles such as HDL_2 and HDL_3 do not significantly decrease upon their renal clearance, this suggests either that the amount of HDL_2 and HDL_3 taken-up by the kidneys is not large enough to affect their plasma levels or that the kidneys may possess mechanisms for returning such particles or their precursors back into the circulation. The exact fate of HDL holoparticles or CE-enriched rHDL particles after their association with the PCT cells is unknown. The possibility exists that such particles could traverse the PCT cells intact in transcytotic vesicles and could be delivered to the peritubular capillaries for their return into the systemic circulation. It is also possible that after internalization, the intact HDL particles may be depleted of CE, followed by a re-secretion of the lipid-depleted particle in a process similar to retroendocytosis. In our cell experiments we have not been able to follow the exact fate of the neutral lipid-components of HDL, as both HDL-labeling techniques

used; Cy_3- and ^{125}I- are protein-specific labeling procedures. While Hammad *et al.* have demonstrated a significant catabolism of HDL/HDL apolipoproteins in the PCT cells following cubilin-mediated endocytosis, they have also shown that chloroquine treatment, which inhibited ^{125}I-HDL degradation did not lead to an intracellular accumulation of internalized ^{125}I-HDL. This suggested the existence of a second alternative pathway for trafficking of HDL/HDL apolipoproteins which escape degradation in the PCT cells (Hammad *et al.*, 1999).

After their association with the HKC-8 cells, the ^{125}I-HDL, ^{125}I-apoA-I and ^{125}I-rHDL particles appear to undergo only minimal degradation during incubation on conventional plates. Less than 2% of protein degradation, comparable to the background values was detected in the cell media by TCA soluble radioactivity over the two hour incubation. This result is surprising, since it opposes findings shown by others. Peterson *et al.* have demonstrated by TCA precipitation the catabolism of ^{125}I-HDL_3, as the consequence of its renal clearance in nephron microperfusion studies performed in rabbits (Peterson *et al.*, 1984). Similarly, Kozyraki *et al.* have detected degradation of ^{125}I-HDL after its cubilin-mediated endocytosis in rat yolk sac epithelial cells *in vitro* over the three hour incubation (Kozyraki *et al.*, 1999). Finally, Hammad *et al.* have shown significant levels of lysosomal hydrolysis of ^{125}I-HDL in mouse yolk sac endoderm-like cells expressing cubilin (Hammad *et al.*, 1999). Also in contrast, our *in vitro* studies performed in the polarized HKC-8 cells (discussed later) did show significant degradation. While these incubations were done over a much longer time period (9 hours), the degradation of the ligands was already detectable after the first two hours of their incubation with the cells. The fact that no HDL degradation products are

detected in cell media of HKC-8 cells grown by conventional (solid surface) *in vitro* techniques but significant HDL degradation is detected in the media when the same cells are grown in a polarized setting suggests that the HKC-8 cells may display impaired HDL catabolism when grown on solid surface culture plates. Furthermore, because we have measured HDL degradation in cell media only, the possibility that the HKC-8 cells grown on solid surface culture plates may degrade HDL normally but accumulate the degradation products intra-cellularly still remains open. This would point towards a defect in secretion of the degraded products, rather than degradation itself when the cells are grown on solid surface culture plates. In addition, epithelial cells can undergo extensive morphological and biochemical re-modeling as a result of a decrease in the proliferation and an increase in the differentiation of the cells when grown in a setting enabling cell polarity in comparison to the solid surface cell culture (Shaw, 1996). This suggests, that while epithelial cell culture by solid surface *in vitro* techniques is invaluable for studying the cellular mechanisms of this cell type, culture enabling polarity may be more useful for studies of more specialized epithelial cell behaviour.

As shown previously in our *in vivo* EM experiment, a substantial apoA-I and rHDL enrichment in the basal lamina of renal proximal tubule cells was observed when the perfused ligands were localized with the 4H1 mAb. The basal lamina is a specialized extracellular matrix that provides a flexible attachment surface for epithelial cells, as well as regulates the passage of macromolecules to and from the epithelial cells (Shaw, 1996). To corroborate the *in vivo* findings, we have analyzed the interaction of the HKC-8 cell ECM with the HDL particles *in vitro*, using a cell matrix association assay.

In agreement with the *in vivo* accumulation of the HDL ligands in the tubular basement membrane, ^{125}I-apoA-I and ^{125}I-rHDL particles were found in the HKC-8 cell ECM as well. ^{125}I-rHDL displayed highest ECM association, followed by ^{125}I-apoA-I and ^{125}I-HDL. This trend is opposite to the observed cell-association of these ligands to the HKC-8 cells. In addition, from the total amount of ligands that associated with the HKC-8 cells, the largest proportion of ^{125}I-rHDL, followed by ^{125}I-apoA-I and ^{125}I-HDL accumulated in the ECM of the HKC-8 cells. Therefore more of lipid-free apoA-I or lipid-poor apoA-I complexed with phospholipid, than of native HDL, may be targeted towards the ECM in these cells. This suggests that in the HKC-8 cells, the lipid composition of the particles may play a role in their matrix association as well.

In summary, the *in vitro* data clearly demonstrate that the human HKC-8 proximal tubule cell line is capable of binding and internalization of HDL particles. In addition, the cells are capable of a saturable, specific binding of ^{125}I-HDL, suggestive of a receptor-mediated association. The lipid composition of the HDL particles appears to play a major role in this specific association, as some components of the HDL-lipid fraction markedly enhance the association, particularly the CE enrichment of HDL. The HKC-8 cells grown on conventional culture plates appear to have an impaired catabolic or secretory pathway as witnessed by the total absence of HDL degradation products in the cell media after incubation. The impairment seems to result from the mode of culture of the HKC-8 cells, as a high degree of HDL degradation is observed in the same cells when cultured in a polar setting (discussed later). Finally, the HDL lipid composition also seems to play a role in the association of the HDL particles with the cell matrix, as lipid-

free apoA-I and lipid poor-rHDL accumulate at higher levels in the HKC-8 cell ECM compared to native HDL.

III. *In vitro* Studies with Polarized Cells

When cultured under the appropriate conditions, epithelial cells display a structural and functional polarity which makes them more comparable to their counterparts *in vivo*. For this reason, we have decided to evaluate HDL processing in polarized HKC-8 cells grown on permeable filters. In this setting, the cells possess distinct apical and basolateral regions with a different morphology, function and biochemical composition.

An important feature of epithelial cells grown in a polarized setting is their ability to limit paracellular diffusion. Such paracellular leakage could interfere with the interpretation of the data representing active HDL processing by the cells. Our data shows that the HKC-8 cells cultured on fibronectin-coated permeable filters provide a considerable diffusion barrier to [^{14}C]inulin, a marker of passive paracellular diffusion.

Our ^{125}I-HDL cell association assay provides evidence for polarized processing of HDL by the HKC-8 cells. The ligand associates with both cell surfaces. The association of ^{125}I-HDL with the basolateral cell surface is 2.5 fold higher than with the apical cell surface. The HDL association increases over the first four hours of incubation, levels off thereafter and is maintained at this level over the entire twelve hour incubation. Remaley and colleagues have also shown a 3-fold increased association of ^{125}I-HDL with the basolateral membrane compared to the apical membrane of MDCK, canine renal cortex cells. (Remaley *et al.*, 1998). Similarly, Rabkin and coworkers have reported that the association of ^{125}I-insulin with the OK cells was two-fold higher with the basolateral cell

surface than with the apical (Rabkin *et al.*, 1996). These observations could reflect the greatly enlarged basolateral membrane of renal epithelial cells which comprises of extensive plasma membrane infoldings. With the finding of basolateral receptors capable of HDL binding, such membrane infoldings could provide more surface area to accommodate a great number of receptors. For example, MDCK cells have a 4 to 7 times greater basolateral than apical cell surface (von Bonsdorff *et al.*, 1985).

We have also performed HDL processing studies in these cells to examine the polarity of HDL transport and degradation in the HKC-8 cells. HKC-8 cells are capable of transporting about 2.5-fold more HDL from the basolateral cell surface to the apical cell surface, than in the opposite direction. This number parallels the previously observed levels of ^{125}I-HDL association with the two membrane surfaces. In addition, the basolateral to apical transport was increasing over the nine hour incubation while the apical to basolateral HDL transport was highest after six hours and decreased afterwards.

In these experiments, we have detected marked degradation of the ^{125}I-HDL, as observed by the appearance of TCA soluble protein fragments in the cell media over time. The amount of degradation was comparable to the amount transported across the cells, suggesting that the cells degraded most of the ligand encountered. The degradation appeared complete over all time points along the basolateral pathway, in comparison to the apical pathway, during which more than half of the HDL transported was in the degraded form during the first six hours of incubation. At nine hours, degradation paralleled HDL transport. As discussed previously, the presence of marked HDL degradation in these cells is in conflict with the previous observation of minimal HDL degradation in non-polarized HKC-8 cells, suggesting that the polarized expression of

these cells can reveal significant structural and functional differences in comparison to their non-polarized counterparts. These experiments however, do not allow us to determine the exact mechanisms responsible for intracellular processing of the HDL added to the opposing regions of the cells. While high levels of degradation detected on both sides do suggest an endocytic pathway resulting in lysosomal degradation of HDL, the degree of contribution of other processes (transcytosis of intact HDL, retroendocytosis) to the overall HDL processing by polarized HKC-8 cells cannot be assessed in these experiments. For future studies for example, the contribution of transcytosis could be assesed by inhibiting specific steps of the endocytic processing and monitoring the appearance of double-labeled (lipid and protein) HDL in the cell media on the side opposite to the side of ligand addition. Retroendocytosis could be detected by performing a pulse and chase assay with radiolabeled HDL and monitoring the appearance of the radiolabel on the side of the ligand addition.

As discussed previously, several studies have identified renal receptors capable of high- affinity HDL endocytosis (Hammad *et al.*, 1999; Kozyraki *et al.*, 1999), or putative HDL-binding proteins with either low-capacity, high-affinity or high-capacity, low affinity binding characteristics (Senault *et al.*; 1994; van Tol *et al.*, 1986). From our experiments in polarized HKC-8 cells, we cannot specifically assign the observed ligand-cell surface interactions to a specific receptor, however the HDL association observed at both, apical and basolateral cell membranes appear to be of a high capacity. A conclusive proof for an involvement of a particular HDL receptor would be to isolate it and block its physiological function using antibodies specific against an epitope on the receptor.

To determine the effect of the HDL particle composition on the processing of the HDL by polarized HKC-8 cells, we have performed HDL processing and degradation assays using a variety of particles; ^{125}I-apoA-I, ^{125}I-rHDL enriched in CE (rHDL–CE) and ^{125}I-rHDL reconstituted with HDL lipid and pure apoA-I (rHDL-lipid) in comparison with ^{125}I-HDL. We have described the nine hour time-point only, as the other time-points displayed similar trends.

The amounts of ^{125}I-rHDL-lipid and ^{125}I-rHDL-CE particles transported from the apical to the basolateral side are comparable to that of ^{125}I-HDL, with slightly more ^{125}I-rHDL-CE transported. The amount of ^{125}I-apoA-I particles transported in the same direction is about 3-fold lower, in comparison to ^{125}I-HDL transport. The amount of degradation of the three particles is considerably lower (20–35% of the total transported), in comparison to complete ^{125}I-HDL degradation after apical to basolateral transport. An assessment of the basolateral to apical transport revealed different observations. Lesser amounts of particles were transported in comparison with ^{125}I-HDL, with ^{125}I-apoA-I transported most efficiently, followed by ^{125}I-rHDL-CE and ^{125}I-rHDL-lipid. The levels of degradation of the particles were higher (40 – 70% of the total transported) in comparison to the particles during the opposite transport, but were still less in comparison to the complete degradation of ^{125}I-HDL. Together, the data show that there are significant composition-dependent differences in HDL particle processing when cell polarity is taken into account.

As observed from the results on ligand degradation in polarized HKC-8 cells, ^{125}I-HDL appears to be degraded completely during transport in both directions, while ^{125}I-apoA-I and the rHDL particles are only partially degraded. In addition, ^{125}I-apoA-I and

^{125}I-HDL degradation in the basolateral to apical direction of transport was consistently higher than that in the opposite direction. While CE and HDL lipid incorporation directly affected rHDL transport through the cells, these lipids had little effect on particle degradation. Thus, HDL apolipoprotein composition appears to govern the degradation of HDL in these cells. Therefore, to reveal the roles of specific apolipoproteins in this process, ligand association and degradation experiments in polarized HKC-8 cells could be conducted, utilizing rHDL particles varying in apolipoprotein composition. In support of the role of different HDL apolipoproteins in degradation of HDL, Braschi *et al.* have shown that inclusion of an apoA-II molecule into an apoA-I-containing rHDL particle resulted in its increased rate of clearance from rabbit plasma, compared to an rHDL particle containing apoA-I only. Furthermore, apoA-II appeared to induce changes in the charge of the rHDL particle and its apoA-I conformation (Braschi *et al.*, 1999). In addition, there are also some studies suggesting, that apoA-II in HDL particles is capable of associating with HDL binding proteins in a number of cell types (Fidge, 1999).

The observations of the particle processing after apical uptake appear somewhat similar to the observations obtained from the cell association studies in non-polar HKC-8 cells, where some HDL-lipid fraction components (with CE identified) were shown to have marked effects on the HDL particle association with the cells. This raises the possibility that the apical to basolateral HDL processing that we have observed in these experiments with polarized HKC-8 cells may be the consequence of HDL cell-association equivalent to that observed in the non-polar HKC-8 cells. The marked differences observed when comparing the apical to basolateral and basolateral to apical processing of HDL particles of various lipid compositions and apoA-I indicate that these

processes are most likely due to different mechanisms. As discussed previously, cubilin, the 460 kDa high-affinity HDL receptor is solely found at the apical membranes of the proximal tubule cells (Sahali *et al.*, 1992), while the basolateral membranes of renal tubule were found to display a two-component HDL-membrane association and were also enriched in a 95 kDa putative HDL-binding receptor (Senault *et al.*, 1994).

Numerous studies show, that while the apical processing of a variety of plasma proteins by the renal tubule cells plays an important role in the maintenance of homeostasis of these proteins *in vivo*, the basolateral membrane of the renal tubule cells, besides its physiologically important processing of hormones and growth factors is also involved in processing proteins for their own metabolic requirements (Christensen and Nielsen, 1991). Therefore, the possibility that a proportion of the lipid-rich HDL particles encountered by the PCT cells basolaterally is used to fulfill their metabolic needs cannot be ruled out. In accordance with this view, *in vitro,* HDL has been shown to sustain the growth of the MDCK and LLC-PK1 kidney cell lines with equal potency to FBS (Gospodarowicz *et al.*, 1983; Streather *et al.*, 1996).

In summary, the *in vitro* studies with polarized HKC-8 cells provide evidence for polarized processing of HDL, with both, apical and basolateral membrane-HDL association. The association is saturable and of high capacity, with higher basolateral than apical membrane-HDL association. The HDL processing and degradation assays show that polarized HKC-8 cells are also capable of a higher basolateral to apical HDL transport compared to one in the opposite direction, and that all transported HDL appears to be degraded over the 9 hour incubation. Furthermore, experiments show that there are significant composition-dependent differences in HDL particle processing, when cell

polarity is taken into account. Neutral lipid-rich rHDL particles were transported more efficiently, but degraded less readily in the apical to basolateral direction than in the opposite direction, where their transport was exceeded by that of apoA-I. Together, the transport and degradation of all particles and apoA-I were lower than those of native HDL. The data show that the two poles of the HKC-8 cells differ in their HDL processing, suggesting an involvement of different mechanisms which could consequently result in different physiological roles for the apical and basolateral regions of the renal tubule cells in HDL processing (Fig. 20).

IV. Physiological Relevance

Patients with clinical disorders such as hyperlipidemia, or LCAT deficiency display reduced levels of HDL in their plasma, resulting in a higher risk of atherosclerosis. In hyperlipidemia, the TG content of HDL is increased while the CE content is reduced (Brinton *et al.*, 1994; Horowitz *et al.*, 1993). Such HDL is the preferred substrate for LPL, resulting in its lipolysis, reducing its size (Brinton *et al.*, 1991). The process results in an increased plasma clearance of these lipid-poor HDL particles. LCAT deficiency in patients results in a reduction of CE content of HDL and an abnormal accumulation of lipid-poor nascent type HDL which are rapidly cleared from plasma (Castro and Fielding, 1988; Kuivenhoven *et al.*, 1997). Finally, CETP overexpression results in an exchange of CE in HDL for TG in LDL, resulting in a decreased CE/TG ratio (Fielding and Fielding, 1996). Such HDL particles can then undergo LPL-mediated hydrolysis, consequently resulting in their increased clearance from plasma.

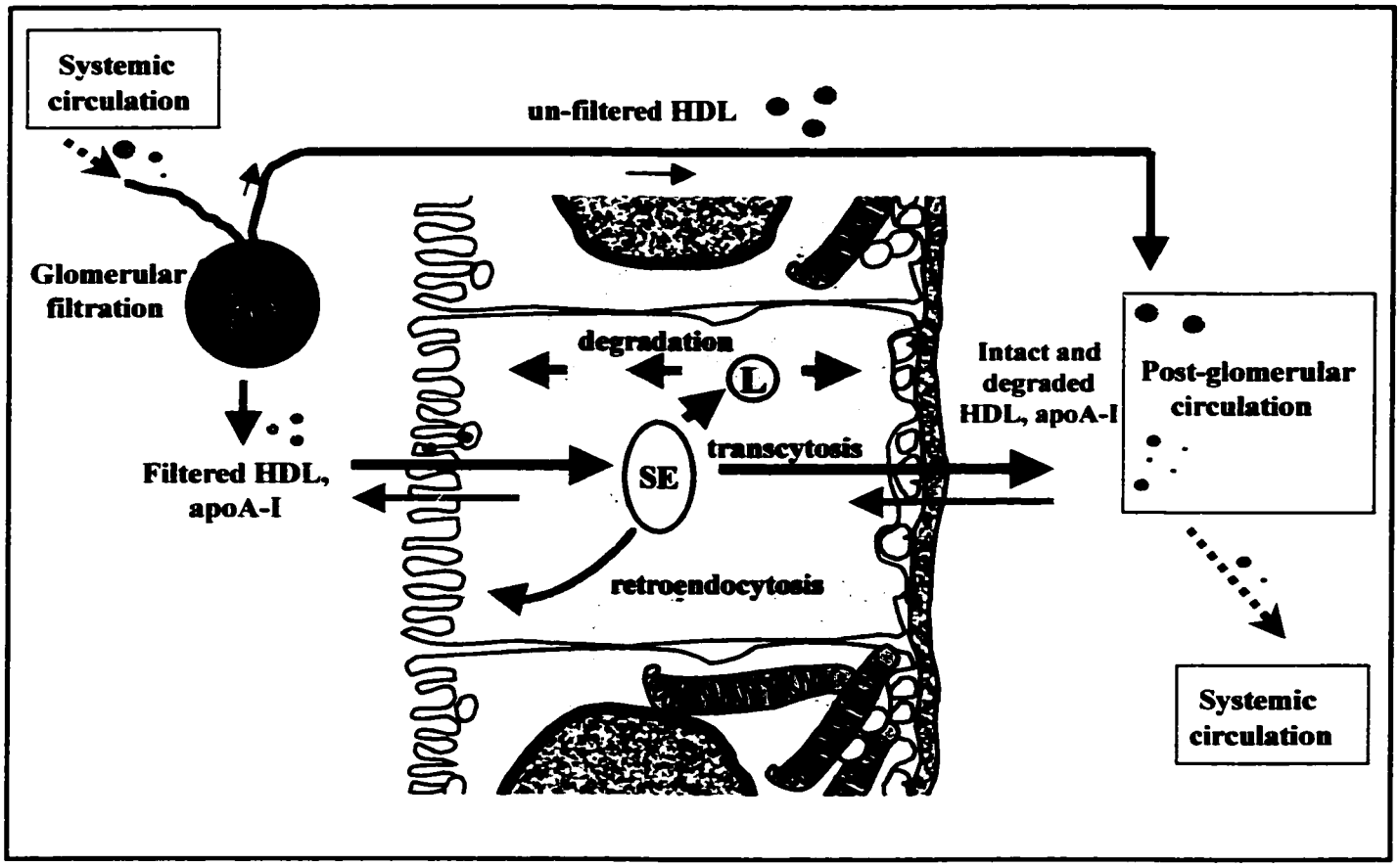
Systemic circulation
un-filtered HDL
Glomerular filtration
degradation
L
Intact and degraded HDL, apoA-I
Post-glomerular circulation
Filtered HDL, apoA-I
SE
transcytosis
retroendocytosis
Systemic circulation

Figure 20: Potential mechanisms of HDL metabolism in proximal tubule cells (PT) of the renal cortex.

Small HDL particles (<10nm) and apoA-I filtered by the glomerulus are available for luminal uptake by the PT cells. The HDL and apoA-I may undergo receptor-mediated endocytosis, with most of the ligands degraded in the lysosomes. Some of the HDL and apoA-I may also undergo transcytosis and appear intact on the opposite side of the cell. The degraded and intact HDL can then return to the systemic circulation through the peritubular network of capillaries. Luminal retroendocytosis of small HDL and apoA-I may also occur, releasing the ligands back into the tubular lumen. Larger HDL particles (>10nm) that fail to undergo glomerular filtration are carried away towards the basolateral poles of PT cells through the peritubular circulation. At the basolateral pole of the PT cells, the ligands may undergo receptor-mediated endocytosis and transcytosis to be degraded intra-cellularly and released degraded or intact into the tubular lumen. Upon apical secretion, the ligands could be taken up by the downstream PT cells for degradation. Lysosome (**L**), Sorting Endosome (**SE**).

Our findings show that the CE content of HDL particles can enhance their interaction with receptors in proximal tubule cells, possibly through affecting the apoA-I conformation. Such process may result in a preferential re-absorption of these particles by the kidney and their return to the circulation in intact, or partially degraded form. This process could decrease pernicious plasma clearance of HDL, and therefore be anti-atherogenic. The exact metabolic fate of intact HDL particles in proximal tubule cells still remains unknown. Therefore metabolic studies monitoring co-localization of double-labeled HDL particles and specific transport markers in proximal tubule cells need to be performed.

Our data further suggests, that the differences observed in HDL processing across the apical and basolateral regions of the HKC-8 cells may result in different physiological roles of these cellular regions in HDL processing. While the apical to basolateral transport could serve to deliver both, intact and degraded HDL/apoA-I to the tubular basement membrane, and consequently back to the circulation in accordance with the proposed role of the kidney in HDL metabolism, the physiological relevance of HDL transport in the basolateral to apical direction remains unknown. Such transport would result in the delivery and release of HDL back into the tubular lumen. We posit, that *in vivo*, HDL released into the tubular lumen upon apical secretion would most likely be taken up and degraded by the downstream tubular cells (Fig. 20). Taken this view then, the identification and isolation of regulators of intracellular traffic that could enhance basolateral delivery and secretion in renal tubule cells may possibly have some therapeutic effects in HDL-deficient states, as their administration could serve to prolong HDL half-life in the blood plasma.

Dalibor Breznan

29 Sovereign Avenue,
Nepean, K2G 4W8
Ontario, Canada
(613) 224-6753
dalbreznan@rogers.com

Education

1999 - present	Master of Science candidate in Biochemistry University of Ottawa, Heart Institute Ottawa, Ontario, Canada Supervisor: Dr. D.L. Sparks Thesis Title: The High Density Lipoprotein Metabolism by the Kidney
1998 – 1999	Master of Science in Biology 1st year, (transfer to University of Ottawa) Carleton University, Ottawa Supervisor: Dr. N. Chaly
1993 - 1998	Bachelor of Science in Biology / Biotechnology (Magna Cum Laude) Carleton University Ottawa, Ontario, Canada Supervisor: Dr. N. Chaly Thesis Title: An Analysis of Apoptotic Nuclear Events in Heat-treated M Mouse Splenocytes and in Differentiating Rat L6E9 Muscle Cells.

Employment

Sept 1998 - May 1999	Teaching Assistant in the Department of Biology, Carleton University for a second year biochemistry course and a third year cell biology course.
Sept 1996 - May 1997	Laboratory Assistant in the Department of Biology, Carleton University, cell biology laboratory.
May 1995 - present	Avian Care Technician at the Wild Bird Care Centre, Ottawa

Awards and Memberships

- Best M.Sc. student research presentation of the Department of Biochemistry, Microbiology and Immunology, University of Ottawa (2000)
- JIAS academic scholarship (1998)
- Deans' Honour list (1997)
- member of the Carleton University Biology Society (CUBS)
- treasurer of the Heart Institute Graduate Students Association (HIGSA), 2000-2001

Presentations (oral and poster)

- M.Sc. Graduate Students Research Presentation, University of Ottawa (2001)
- Annual Research Day of the Department of Pathology and Laboratory Medicine, University of Ottawa (2000)
- Canadian Lipoprotein Conference, White Rock, BC (2000)
- Second Annual Celebration of Excellence research presentation of the Faculty of Medicine, University of Ottawa (2000)
- Annual Research Day of the Department of Pathology and Laboratory Medicine, University of Ottawa (2000)
- University of Ottawa Heart Institute Research Day, University of Ottawa (2000)
- Annual Research Presentation of the Department of Biochemistry, Microbiology and Immunology, University of Ottawa (2000)
- Graduate Students Research Presentation, Carleton University (1998)

Publications

Stamler, C.J., **Breznan, D.**, Neville, T.A., Viau, F.J., Camlioglu, E., and D.L. Sparks. 2000. Phosphatidylinositol promotes cholesterol transport *in vivo*. *J. Lipid Res.* **41:** 1214-21.

Bibliography

Acton, S., Rigotti, A., Landsculz, K.T., Xu, S., Hobbs, H.H. and M. Krieger. 1996. Identification of scavenger receptor SR-BI as a high density lipoprotein receptor. *Science.* **271:** 518-20.

Acton, S., Kozarsky, K.F., and A. Rigotti. 1999. The HDL receptor SR-BI: A new therapeutic target for atherosclerosis? *Mol. Med. Today.* **5:** 518-24.

Babitt J., Trigatti B., Rigotti A., Smart E.J., Anderson R.G., Xu S., and M. Krieger. 1997. Murine SR-BI, a high density lipoprotein receptor that mediates selective lipid uptake, is N-glycosylated and fatty acylated and colocalizes with plasma membrane caveolae. *J. Biol. Chem.* **272:** 13242-9.

Batuman V., Verroust P.J., Navar G.L., Kaysen J.H., Goda F.O., Campbell W.C., Simon E., Pontillon F., Lyles M., Bruno J., and T.G. Hammond. 1998. Myeloma light chains are ligands for cubilin (gp280). *Am. J. Physiol.* **275:** F246-54.

Bergeron, J., Frank, P.G., Scales, D., Meng, Q.H., Castro, G., and Y.L. Marcel. 1995. Apolipoprotein A-I conformation in recombinant discoidal lipoproteins varying in phospholipid and cholesterol content. *J. Biol. Chem.* **270:** 27429-38.

Birn H., Verroust P.J., Nexo E., Hager H., Jacobsen C., Christensen E.I., and S.K. Moestrup. 1997. Characterization of an epithelial approximately 460-kDa protein that facilitates endocytosis of intrinsic factor-vitamin B12 and binds receptor-associated protein. *J. Biol. Chem.* **272:** 26497-504.

Birn H., Fyfe J.C., Jacobsen C., Mounier F., Verroust P.J., Orskov H., Willnow T.E., Moestrup S.K., and E.I. Christensen. 2000. Cubilin is an albumin binding protein important for renal tubular albumin reabsorption. 2000. *J. Clin. Invest.* **105:** 1353-61.

Bodzioch, M., Orzo, E., Klucken, J., Langmann, T., Bottcher, A., Diederich, W., Drobnik, W., Barlage, S., Buchler, C., Porsch-Ozcurumez, M., Kaminski, W.E., Hahmann, H.W., Oette, K., Rothe, G., Aslanidis, C., Lackner, K.J., and G. Schmitz. 1999. The gene encoding ATP-binding cassette transporter 1 is mutated in Tangier disease. *Nat. Genet.* **22:** 347-51.

Braschi, S., Neville, A.M., Vohl, M.C., and D.L. Sparks. 1999. Apolipoprotein A-I charge and conformation regulate the clearance of reconstituted high density lipoprotein in vivo. *J. Lipid Res.* **40:** 522-32.

Braschi, S., Neville, A.M., Maugeais, C., Ramsamy, T.A., Seymour, R., and D.L. Sparks. 2000. Role of the kidney in regulating the metabolism of HDL in rabbits: evidence that iodination alters the catabolism of apolipoprotein A-I by the kidney. *Biochemistry.* **39:**

5441-9.

Breslow, J.L. 2000. Genetics of lipoprotein abnormalities associated with coronary artery disease susceptibility. *Annu. Rev. Genet.* **34:** 233-54.

Brewer, H.B. Jr, Ronan, R., Meng, M., and C. Bishop. 1986. Isolation and characterization of apolipoproteins A-I, A-II, and A-IV. *Methods Enzymol.* **128:** 223-46.

Brinton, E.A., Eisenberg, S., Windmueller, H.G., and J.L. Breslow. 1991. Increased apo A-I and apo A-II fractional catabolic rate in patients with low high density lipoprotein-cholesterol levels with or without hypertriglyceridemia. *J. Clin. Invest.* **87:** 536-44.

Brinton, E.A., Eisenberg, S., and J.L. Breslow. 1994. Human HDL cholesterol levels are determined by apoA-I fractional catabolic rate, which correlates inversely with estimates of HDL particle size. Effects of gender, hepatic and lipoprotein lipases, triglyceride and insulin levels, and body fat distribution. *Arterioscler. Thromb.* **14:** 707-20.

Brown, M.S., and J.L. Goldstein, J. 1986. A receptor-mediated pathway for cholesterol homeostasis. *Science.* **232:** 34-47.

Brown, M.S., and J.L. Goldstein, J. 1987. *In* Garrett, R.H., and C.M. Grisham, eds., 1995. *Biochemistry,* Saunders College Publishing, Orlando, FL, pp. 793.

Calabresi, L., Meng, Q.H., Castro, G.R., and Y.L. Marcel. 1993. Apolipoprotein A-I conformation in discoidal: Evidence for alternate structures. *Biochemistry.* **32:** 6477-84.

Castro, G.R. and C.J. Fielding. 1988. Early incorporation of cell-derived cholesterol into pre-beta-migrating high-density lipoprotein. *Biochemistry.* **27:** 25-9.

Chiu D.S., Oram J.F., LeBoeuf R.C., Alpers C.E., and K.D. O'Brien. 1997. High-density lipoprotein-binding protein (HBP)/vigilin is expressed in human atherosclerotic lesions and colocalizes with apolipoprotein E. *Arterioscler. Thromb. Vasc. Biol.* **17:** 2350-8.

Christensen, E.I. 1982. Rapid membrane recycling in renal proximal tubule cells. *Eur. J. Cell Biol.* **29:** 43-9.

Christensen, E.I. and S. Nielsen. 1991. Structural and functional features of protein handling in the kidney proximal tubule. *Semin. Nephrol.* **11:** 414-39.

Christensen E.I., Nielsen S., Moestrup S.K., Borre C., Maunsbach A.B., de Heer E., Ronco P., Hammond T.G., and P. Verroust. 1995. Segmental distribution of the endocytosis receptor gp330 in renal proximal tubules. *Eur. J. Cell Biol.* **66:** 349-64.

Collet X., Perret B., Simard G., Raffai E., and Y.L. Marcel. 1991. Differential effects of lecithin and cholesterol on the immunoreactivity and conformation of apolipoprotein A-I in high density lipoproteins. *J. Biol. Chem.* **266:** 9145-52.

Coudrier, E., Kerjaschki, D., and D. Louvard. 1988. Cytoskeleton organization and submembranous interactions in intestinal and renal brush borders. *Kidney Int.* **34(3):** 309-20.

Cui, S. and E.I. Christensen. 1993. Three-dimensional organization of the vacuolar apparatus involved in endocytosis and membrane recycling of rat kidney proximal tubule cells. An electron-microscopic study of serial sections. *Exp. Nephrol.* **1:** 175-84.

Davis, R.A. and J.E. Vance. 1996. Structure, assembly and secretion of lipoproteins. *In* Vance, D.E. and J.E. Vance, eds., *Biochemistry of lipids, lipoproteins and membranes,* Elsevier Science B.V., New York, NY, pp. 473-93.

DeLamatre, J.G., Sarphie, T.G., Archibold, R.C., and C.A. Hornick. 1990 Metabolism of apoE-free high density lipoproteins in rat hepatoma cells: evidence for a retroendocytic pathway. *J. Lipid Res.* **31:** 191-202.

Dworkin, L.D., Sun, A.M., and B.M. Brenner. 2000. The renal circulations. *In* Brenner, B.M, ed., *The Kidney*, volume 1, 6th edition, W.B. Saunders Company, Philadelphia, PA., pp. 277-290.

Fidge, N.H. 1986. Partial purification of a high density lipoprotein-binding protein from rat liver and kidney membranes. *FEBS Lett.* **199:** 265-8.

Fidge, N.H. 1999. High density lipoprotein receptors, binding proteins, and ligands. *J. Lipid Res.* **40:** 187-201.

Fielding, P.E. and C.J. Fielding. 1996. Dynamics of lipoprotein transport in the human circulatory system. *In* Vance, D.E. and J.E. Vance, eds., *Biochemistry of lipids, lipoproteins and membranes,* Elsevier Science B.V., New York, NY, pp. 495-516.

Garrett, R.H. and C.M. Grisham. 1995. Lipid biosynthesis. *In* Garrett, R.H. and C.M. Grisham, eds., *Biochemistry,* Saunders College Publishing, Orlando, FL., pp. 757-802.

Ginsberg, H.N. 1998. Lipoprotein physiology. *Endocrinol. Metab. Clin. North Am.* **27:** 503-19.

Glass, C.K., Pittman, R.C., Keller, G.A., and D. Steinberg. 1983. Tissue sites of degradation of apoprotein A-I in the rat. *J. Biol. Chem.* **258:** 7161-7.

Glass, C., Pittman, R.C., Civen, M., and D. Steinberg. 1985. Uptake of high-density lipoprotein-associated apoprotein A-I and cholesterol esters by 16 tissues of the rat in vivo and by adrenal cells and hepatocytes in vitro. *J Biol. Chem.* **260:** 744-50.

Glass, C.K. and J.L. Witztum. 2001. Atherosclerosis: The road ahead. *Cell.* **104:** 503-16.

Gliemann, J. 1998. Receptors of the low density lipoprotein (LDL) receptor family in man. Multiple functions of the large family members via interaction with complex ligands. *Biol. Chem.* **379:** 951-64.

Goldberg, I.J., Le, N.A., Ginsberg, H.N., Krauss, R.M., and F.T. Lindgren. 1988. Lipoprotein metabolism during acute inhibition of lipoprotein lipase in the cynomolgus monkey. *J. Clin. Invest.* **81:** 561-8.

Goligorsky, M.S. and K.A. Hruska. 1986. Transcytosis in cultured proximal tubular cells. *J. Membr. Biol.* **93:** 237-47.

Gomo, Z.A.R. and L. O. Henderson. 1988. High-density lipoprotein apolipoproteins in urine: II. Enzyme-linked immunoassay of apolipoprotein A-I. *Clin. Chem.* **34:** 1781-86.

Gordon, D.J. and B.M. Rifkind. 1989. High-density lipoprotein -- The clinical implications of recent studies. *N. Engl. J. Med.* **321:** 1311-6.

Gospodarowicz, D., Cohen, D.C., and S.L. Massoglia. 1983. Stimulation of the proliferation of the Madin-Darby canine kidney (MDCK) epithelial cell line by high-density lipoproteins and their induction of 3-hydroxy-3-methylglutaryl coenzyme A reductase activity. *J. Cell Physiol.* **117**: 76-90.

Graham, D.L. and J.F. Oram. 1987. Identification and characterization of a high density lipoprotein-binding protein in cell membranes by ligand blotting. *J. Biol. Chem.* **262:** 7439-42.

Gumbiner, B.M. 1993. Breaking through the tight junction barrier. *J. Cell Biol.* **123:** 1631-3.

Hammad, S.M., Stefansson, S., Twal, W.O., Drake, C.J., Fleming, P., Remaley, A., Brewer, H.B. Jr., and W.S. Argraves. 1999. Cubilin, the endocytic receptor for intrinsic factor-vitamin B(12) complex, mediates high-density lipoprotein holoparticle endocytosis. *Proc. Natl. Acad. Sci. U S A.* **96:** 10158-63.

Hammad, S.M., Barth, J.L., Knaak, C., and W.S. Argraves. 2000. Megalin acts in concert with cubilin to mediate endocytosis of high density lipoproteins. *J. Biol. Chem.* **275:** 12003-8.

Havel, R.J., Eder, H.A., and J.H., Bragdon. 1955. The distribution and chemical composition of ultracentrifugally separated lipoproteins in human serum. *J. Clin. Invest.* **34:** 1345-53.

Hidaka, H. and N.H. Fidge. 1992. Affinity purification of the hepatic high-density lipoprotein receptor identifies two acidic glycoproteins and enables further characterization of their binding properties. *Biochem. J.* **284:** 161-7.

Hobbs, H.H. and D.H. Rader. 1999. ABC1: connecting yellow tonsils, neuropathy, and very low HDL. *J. Clin. Invest.* **104:** 1015-7.

Horowitz, B.S., Goldberg, I.J., Merab, J., Vanni, T.M., and R. Ramakrishnan. 1993. Increased plasma and renal clearance of an exchangeable pool of apolipoprotein A-I in subjects with low levels of high density lipoprotein cholesterol. *J. Clin. Invest.* **91:** 1743-52.

Ikewaki K., Zech L.A., Kindt M., Brewer H.B. Jr, and D.J. Rader. 1995. Apolipoprotein A-II production rate is a major factor regulating the distribution of apolipoprotein A-I among HDL subclasses LpA-I and LpA-I:A-II in normolipidemic humans. *Arterioscler. Thromb. Vasc. Biol.* **15:** 306-12.

Junqueira, L.C., Carneiro, J., and R.O. Kelley.1998. The urinary system. *In* Junqueira, L.C., Carneiro, J., and R.O. Kelley, *Basic Histology*, 9th edition, Appleton & Lange, Stamford, CT., pp. 360-377.

Kates, M., ed., 1972. *Techniques of lipidology*, Elsevier Publishing Co., New York, NY., pp. 347-53.

Kaysen, G.A., Hoye, E., and H.J. Jones. 1995. Apolipoprotein AI levels are increased in part as a consequence of reduced catabolism in nephrotic rats. *Am J Physiol.* **268:** F532-40.

Kozyraki, R., Fyfe, J., Kristiansen, M., Gerdes, C., Jacobsen, C., Cui, S., Christensen, E.I., Aminoff, M., de la Chapelle, A., Krahe, R., Verroust, P.J., and S.K. Moestrup. 1999. The intrinsic factor-vitamin B12 receptor, cubilin, is a high-affinity apolipoprotein A-I receptor facilitating endocytosis of high-density lipoprotein. *Nat. Med.* **5:** 656-61.

Kristiansen M., Kozyraki R., Jacobsen C., Nexo E., Verroust P.J., and S.K. Moestrup. 1999. Molecular dissection of the intrinsic factor-vitamin B12 receptor, cubilin, discloses regions important for membrane association and ligand binding. *J. Biol. Chem.* **274:** 20540-4.

Kuivenhoven, J.A., Pritchard, H., Hill, J., Frohlich, J., Assmann, G., and J. Kastelein. The molecular pathology of lecithin:cholesterol acyltransferase (LCAT) deficiency syndromes. *J. Lipid Res.* **38:** 191-205.

Lambert G., Chase M.B., Dugi K., Bensadoun A., Brewer H.B. Jr, and S. Santamarina-Fojo. 1999. Hepatic lipase promotes the selective uptake of high density lipoprotein-cholesteryl esters via the scavenger receptor B1. *J. Lipid Res.* **40:** 1294-303.

Lindstrom, K.E., Johnsson, E., and B. Haraldsson. 1998. Glomerular charge selectivity for proteins larger than serum albumin as revealed by lactate dehydrogenase isoforms. *Acta Physiol. Scand.* **162:** 481-8.

Luke, R.L. 1984. Glomerular permselection: shape and flow. *J. Theor. Biol.* **106:** 141-56.

Lusis, A.J. 2000. Atherosclerosis. *Nature.* **407:** 233-241.

Marcel, Y.L., Provost, P.R., Koa, H., Raffai, E., Dac, N.V., Fruchart, J.C., and E. Rassart. 1991. The epitopes of apolipoprotein A-I define distinct structural domains including a mobile middle region. *J. Biol. Chem.* **266:** 3644-53.

Lutton, C. and N. Fidge. 1994. Distribution of high density lipoprotein binding proteins among various tissues in the rat. *C. R. Acad. Sci. III.* **317:** 731-5.

Maunsbach, A.B. 1966. Observations on the ultrastructure and acid phosphatase activity of the cytoplasmic bodies in rat kidney proximal tubule cells. With a comment on their classification. *J. Ultrastruct. Res.* **16:** 197-238.

Markwell M.A., Haas S.M., Bieber L.L., and N.E. Tolbert. 1978. A modification of the Lowry procedure to simplify protein determination in membrane and lipoprotein samples. *Anal Biochem.* **87:** 206-10.

Matsumoto, A., Mitchell., A., Kurata, A., Pyle, L., Kondo, K., Itakura, H., and N. Fidge. 1997. Cloning and characterization of HB_2, a candidate high density lipoprotein receptor. *J. Biol. Chem.* **272:** 16778-82.

McKnight G.L., Reasoner J., Gilbert T., Sundquist K.O., Hokland B., McKernan P.A., Champagne J., Johnson C.J., Bailey M.C., Holly R., et al. 1992. Cloning and expression of a cellular high density lipoprotein-binding protein that is up-regulated by cholesterol loading of cells. *J. Biol. Chem.* **267:** 12131-41.

Moestrup S.K., Kozyraki R., Kristiansen M., Kaysen J.H., Rasmussen H.H., Brault D., Pontillon F., Goda F.O., Christensen E.I., Hammond T.G., and P.J. Verroust. 1998. The intrinsic factor-vitamin B12 receptor and target of teratogenic antibodies is a megalin-binding peripheral membrane protein with homology to developmental proteins. *J. Biol. Chem.* **273:** 5235-42.

Moestrup, S.K. and R. Kozyraki. 2000. Cubilin, a high-density lipoprotein receptor. *Curr. Opin. Lipidol.* **11:** 133-40.

Myers, B.D. 1989. Determinants of the glomerular filtration of macromolecules. *In* Massry, S.G. and R.J. Glassock, eds., *Textbook of Nephrology*, volume 1, 2nd edition, Williams & Wilkins, Baltimore, MD., pp. 60-64.

Nelson, W.J. 1992. Regulation of cell surface polarity from bacteria to mammals. *Science* **258:** 948-954.

Nielsen, J.T. and E.I. Christensen. 1985. Basolateral endocytosis of protein in isolated perfused proximal tubules. *Kidney Int.* **27:** 39-45.

Nielsen J.T., Nielsen S., and E.I. Christensen. 1985. Transtubular transport of proteins in rabbit proximal tubules. *J. Ultrastruct. Res.* **92:** 133-45.

Nielsen S., Nielsen J.T., and E.I. Christensen. 1987. Luminal and basolateral uptake of insulin in isolated, perfused, proximal tubules. *Am. J. Physiol.* **253:** F857-67.

Nielsen S., Nexo E., and E.I. Christensen. 1989. Absorption of epidermal growth factor and insulin in rabbit renal proximal tubules. *Am. J. Physiol.* **256:** E55-63.

Ottosen, P.D. 1978. Reversible peritubular binding of a cationic protein (lysozyme) to flounder kidney tubules. *Cell. Tissue Res.* **194:** 207-18.

Paszty, C., Maeda, N., Verstuyft, J., and E.M. Rubin. 1994. Apolipoprotein AI transgene corrects apolipoprotein E deficiency-induced atherosclerosis in mice. *J. Clin. Invest.* **94:** 899-903.

Peterson D.R., Carone F.A., Oparil S., and E.I. Christensen. 1982. Differences between renal tubular processing of glucagon and insulin. *Am. J. Physiol.* **242:** F112-8.

Peterson, D.R., Hjelle, J.T., Carone, F.A., and P.A. Moore. 1984. Renal handling of plasma high density lipoprotein. *Kidney Int.* **26:** 411-21.

Plump, A.S., Scott, C.J., and J.L. Breslow. 1994. Human apolipoprotein A-I gene expression increases high density lipoprotein and suppresses atherosclerosis in the apolipoprotein E-deficient mouse. *Proc. Natl. Acad. Sci. U S A.* **91:** 9607-11.

Racusen, L.C., Monteil, C., Sgrignoli, A., Lucskay, M., Marouillat, S., Rhim, J.G.S., and J.P. Morin. 1997. Cell lines with extended in vitro growth potential from human renal proximal tubule: characterization, response to inducers, and comparison with established cell lines. *J. Lab. Clin. Med.* **129:** 318-29.

Rabkin, R., Hamik, A., Yagil, C., Hamel, F.G., Duckworth, W.C., and J. Fawcett. 1996. Processing of 125I-insulin by polarized cultured kidney cells. *Exp. Cell. Res.* **224:**136-42.

Rader, D.J. and K. Ikewaki. 1996. Unravelling high density lipoprotein-apolipoprotein metabolism in human mutants and animal models. *Curr. Opin. Lipidol.* **7:** 117-23.

Rader, D.J. and D. Maugeais. 2000. Genes influencing HDL metabolism: new perspectives and implications for atherosclerosis prevention. *Mol. Med. Today.* 2000 **6:**170-5.

Remaley, A.T., Farsi, B.D., Shirali, A.C., Hoeg, J.M., and H.B. Brewer Jr. 1998. Differential rate of cholesterol efflux from the apical and basolateral membranes of MDCK cells. *J. Lipid Res.* **39:** 1231-8.

Rodman J.S., Kerjaschki D., Merisko E., and M.G. Farquhar. 1984. Presence of an extensive clathrin coat on the apical plasmalemma of the rat kidney proximal tubule cell. *J. Cell Biol.* **98:** 1630-6.

Ross, R. 1999. Atherosclerosis -- An inflammatory disease. *N. Engl. J. Med.* **340:** 115-26.

Sahali D., Mulliez N., Chatelet F., Dupuis R., Ronco P., and P. Verroust. 1988. Characterization of a 280-kD protein restricted to the coated pits of the renal brush border and the epithelial cells of the yolk sac. Teratogenic effect of the specific monoclonal antibodies. *J. Exp. Med.* **167:** 213-8.

Sahali D., Mulliez N., Chatelet F., Laurent-Winter C., Citadelle D., Roux C., Ronco P., and P. Verroust. 1992. Coexpression in humans by kidney and fetal envelopes of a 280 kDa-coated pit-restricted protein. Similarity with the murine target of teratogenic antibodies. *Am. J. Pathol.* **140:** 33-44.

Saku, K., Reddy, G.S., Hynd, B.A., and L. Kashyap. 1984. Renal handling of high density lipoproteins by isolated perfused kidneys. *Metabolism.* **33:** 432-8.

Santamarina-Fojo, S., Lambert, G., Hoeg, J.M., and H.B. Brewer Jr. 2000. Lecithin-cholesterol acyltransferase: role in lipoprotein metabolism, reverse cholesterol transport and atherosclerosis. *Curr. Opin. Lipidol.* **11:** 267-75.

Scanu, A.M. 1971. Human plasma high density lipoproteins. *Biochem. Soc. Symp.* **1:** 29-45.

Scanu, A.M. and C. Edelstein. 1971. Solubility in aqueous solutions of ethanol of the small molecular weight peptides of the serum very low density and high density lipoproteins: relevance to the recovery problem during delipidation of serum lipoproteins. *Anal. Biochem.* **44:** 576-88.

Scanu, A.M., Lagocki, P., and J. Chung. 1980. Effect of apolipoprotein A-II on the structure of high-density lipoproteins: relationship to the activity of lecithin:cholesterol acyl transferase in vitro. *Ann N Y Acad Sci.* **348:** 160-73.

Seetharam B., Christensen E.I., Moestrup S.K., Hammond T.G., and P.J. Verroust. 1997. Identification of rat yolk sac target protein of teratogenic antibodies, gp280, as intrinsic factor-cobalamin receptor. *J. Clin. Invest.* **99:** 2317-22.

Seetharam B., Bose, S., and N. Li. 1999. Cellular import of cobalamin (Vitamin B-12). *J. Nutr.* **129:** 1761-4.

Segal, P., Gidez, L.I., Vega, G.L., Edelstein, D., Eder, H.A., and P.S. Roheim. 1979 Apoproteins of high density lipoproteins in the urine of normal subjects. *J. Lipid Res.* **20:** 772-83.

Segrest J.P., Jones M.K., De Loof H., Brouillette C.G., Venkatachalapathi Y.V., and G.M. Anantharamaiah. 1992. The amphipathic helix in the exchangeable apolipoproteins: a review of secondary structure and function. *J. Lipid Res.* **33:** 141-66.

Senault, C., Vacher, D., Sakr, S., and A.G. Globa. 1994. Binding of HDL to basolateral membranes of the renal cortex. Evidence for two components in the HDL-membrane association. *Biochim. Biophys. Acta.* **1189:** 168-74.

Shamburek, R.D., Nong, Z., Fyfe, J.C., Hoyt, R.F. Jr., and H.B. Brewer Jr. 2000. Renal HDL catabolism: Roles of cubilin and megalin receptors in apoA-I catabolism in the canine cubilin dysfunctional animal model. *American Heart Association Abstracts*: # **47223**.

Shaw, A.J. 1996. Modelling epithelial tissues *in vitro*. *In* Shaw, A.J., ed., *Epithelial cell culture: A practical approach*, IRL Press, Oxford, England., pp. 1-16.

Shepherd, J. 1994. Lipoprotein metabolism. An overview. *Drugs*. **47 Suppl 2**: 1-10.

Spady, D.K., Woollett, L.A., Meidell, R.S., and H.H. Hobbs. 1998. Kinetic characteristics and regulation of HDL cholesteryl ester and apolipoprotein transport in the apoA-I-/- mouse. *J. Lipid Res.* **39(7):** 1483-92.

Sparks, D.L., Lund-Katz, S., and M.C. Phillips. 1992. The charge and structural stability of apolipoprotein A-I in discoidal and spherical recombinant high density lipoprotein particles. *J. Biol. Chem.* **267:** 25839-47.

Sparks, D.L. and M.C. Phillips. 1992. Quantitative measurements of lipoprotein surface charge by agarose gel electrophoresis. *J. Lipid Res.* **33:** 123-30.

Sparks, D.L., Davidson, W.S., Lund-Katz, S., and M.C. Phillips. 1995. Effects of the neutral lipid content of high density lipoprotein on apolipoprotein A-I structure and particle stability. *J. Biol. Chem.* **270:** 26910-7.

Sparks, D.L., Frank, P.G., Braschi, S., Neville, A.M., and Y.L. Marcel. 1999. Effect of apolipoprotein A-I lipidation on the formation and function of pre-beta and alpha-migrating LpA-I particles. *Biochemistry*.**38:** 1727-35.

Streather, C.P., Owen, J.S., Hendry, B.M., and J.E. Soble. 1996. Incubation of porcine high-density lipoprotein with the apical surface of LLC-PK1 renal tubular cells sustains the properties of orientated monolayers. *Nephrol. Dial. Transplant.* **11:** 431-7.

Sviridov, D.D., Misharin, A.Y., Safonova, I.G., Bushmakina, N.G., Repin, V.S., and V.N. Smirnov. 1988. Binding of partially reassembled high-density lipoprotein to isolated human small intestine epithelial cells. Effect of lipid composition. *Biochim. Biophys. Acta.* **963:** 119-25.

Swaney, J.B. 1980. Properties of lipid-apolipoprotein association products. Complexes of human apo AI and binary phospholipid mixtures. *J. Biol. Chem.* **255:** 8798-803.

Tall, A.R., Jiang, X.C., Luo, Y., and D. Silver. 2000. 1999 George Lyman Duff memorial lecture: Lipid transfer proteins, HDL metabolism, and atherogenesis. *Arterioscler. Thromb. Vasc. Biol.* **20:** 1185-88.

Tangirala, R.K., Tsukamoto, K., Chun, S.H., Usher, D., Pure, E., and D.J. Rader. 1999. Regression of atherosclerosis induced by liver-directed gene transfer of apolipoprotein A-I in mice. *Circulation.* **100:** 1816-22.

Tisher, C.C. and J.P. Kokko. 1974. Relationship between peritubular oncotic pressure gradients and morphology in isolated proximal tubules. *Kidney Int.* **6:** 146-56.

Tisher, C.C and K.M. Madsen. 2000. Anatomy of the kidney. *In* Brenner, B.M., ed., *The Kidney*, volume 1, 6th edition, W.B. Saunders Company, Philadelphia, PA., pp. 3-67.

van Tol, A. 1984. Organ specific metabolism of low density lipoprotein and high density lipoprotein. *Agents Actions Suppl.* **16:** 69-85.

van Tol, A., Dallinga-Thie, G.M., van Gent, T., and F.M. van 't Hooft. 1986. Specific saturable binding of rat high-density lipoproteins to rat kidney membranes. *Biochim. Biophys. Acta.* **876:** 340-51.

Verroust, P.J. and R. Kozyraki. 2001. The roles of cubilin and megalin, two multiligand receptors, in proximal tubule function: possible implication in the progression of renal disease. *Curr. Opin. Nephrol. Hypertens.* **10:** 33-8.

von Bonsdorff C.H., Fuller SD, and K. Simons. 1985. Apical and basolateral endocytosis in Madin-Darby canine kidney (MDCK) cells grown on nitrocellulose filters. *EMBO J.* **4:** 2781-92.

von Eckardstein, A. and G. Assmann. 2000. Prevention of coronary heart disease by raising high-density lipoprotein cholesterol ? *Curr. Opin. Lipidol.* **11:** 627-37.

von Eckardstein, A., Nofer, J.R., and G. Assmann. 2001. High density lipoproteins and arteriosclerosis: Role of cholesterol efflux and reverse cholesterol transport. *Arterioscler. Thromb. Vasc. Biol.* **21:** 13-27.

Wang, N., Arai, T., Ji, Y., Rinninger, F., and A.R. Tall. 1998. Liver-specific overexpression of scavenger receptor BI decreases levels of very low density lipoprotein ApoB, low density lipoprotein ApoB, and high density lipoprotein in transgenic mice. *J. Biol. Chem.* **273:** 32920-6.

Willnow, T.E., Nykjaer, A., and J. Herz. 1999. Lipoprotein receptors: new roles for ancient proteins. *Nat. Cell Biol.* **1:** E157-62.

Woollett, L.A. and D.K. Spady. 1997. Kinetic parameters for high density lipoprotein apoprotein AI and cholesteryl ester transport in the hamster. *J. Clin. Invest.* **99:** 1704-13.

Zamboni, L. 1989. Morphology and embryology. *In* Massry, S.G. and R.J. Glassock, eds., *Textbook of Nephrology*, volume 1, 2nd edition, Williams & Wilkins, Baltimore, MD., pp. 3-29.